NEW CONSTRAINTS ON THE SOCORRO MAGMA BODY BASED ON IMPROVED HYPOCENTERS

by

Robert S. Balch

Submitted in Partial Fulfillment of
the Requirements for the Degree of
Master of Science in
Geophysics

New Mexico Insitute of Mining and Technology
Socorro, New Mexico, 87801

December, 1992

Abstract

Two models for the lateral extent of the Socorro Magama Body have been proposed, one by *Rinehart et al.* [1979] and the other by *Hartse* [1991]. These models, which are based on data from different networks and time periods, are markedly different; particularily along the southern and southeastern margins. In addition, neither model constrains the northern margin. Both of these problems were addressed by relocating events for the time period 1975-78 using stations from both the Socorro portable network and the Albuquerque Seismological Laboratory (USGS) network and inverting arrival times for a crustal model using all Socorro phases (P, S, P_zP, S_zP, and S_zS).

I inverted for a single layer crustal model using the generalized least squares algorithm SEISMOS [*Hartse*, 1991]. The data were comprised of 84 events with an average of almost seven stations per event and over seven reflections per event. The total number of arrival times for each phase was; 579 P, 489 S, 85 P_zP, 183 S_zP, and 352 S_zS arrivals, for a total of 1068 direct arrivals and 620 reflected arrivals. The 84 events produced 336 unknown hypocenter parameters, one velocity, one Poisson's ratio, and one reflector depth; a total of 339 unknowns. The model inversion converged to a unique solution with all eigenvalues kept. The results were $V_p = 5.861 \pm 0.032$ km/s, $\nu = 0.243 \pm 0.002$, and reflector depth z=19.255 ± 0.111 km. Station corrections were found in a previous inversion holding the best average velocity model constant.

Maps of observed reflection points were compared with maps of all possible theoretical reflection points to determine the lateral extent of the SMB. The reflection points for the 42 events which were common between my study and that of *Rinehart et al.* [1979] produced a map very similiar to their results. The addition of the other 42 events produced a map which is similiar to that of *Hartse* [1991]. In addition on the map based on the total data set, the northern boundary of the SMB was well constrained decreasing the northern extent proposed by *Hartse* by over five kilometers.

Acknowledgments

Several individuals have contributed to the success of this study. First, my advisor, Allan Sanford. His extensive knowledge, and constructive conversations were indispensible. I thank Hans Hartse for the use of his inversion package SEISMOS, without which this study could not have been completed in a timely manner. The scope of this study was increased due to the use of data from the Albuquerque Seismological Laboratory, courtesy of Larry Jaksha. I also thank Mike Skov for converting the digital data to XPick format. Finally, I thank my wife Darlene for her continuing support of this course of study.

This study was partially funded by a generous fellowship from AMOCO.

Table of Contents

List of Figures

List of Tables

1. Introduction

Background and Purpose

The Socorro area of the Rio Grande rift has long been recognized as a region of unusually high seismic activity [*Sanford et al.*, 1991]. The Socorro area has experienced numerous earthquake swarms, and has been described as the most active area of the Rio Grande rift [*Bagg*, 1904; *Reid*, 1911; *Northrop*, 1945, 1947; *Sanford et al.*, 1991]. The largest recent swarm was centered approximately 35 km north of Socorro (near Bernardo, NM), and had 45 magnitude 2.0 or greater events between November of 1989 and May of 1992. There were four events above magnitude 4.0, and sporadic activity continues until the present in the swarm area [*Sanford*, 1992].

A characteristic of seismograms for earthquakes in the Socorro area are sharp clear reflections from a mid-crustal magma body. Two prominent studies have mapped the lateral extent of the Socorro Magma Body (SMB); *Rinehart* [1979], and *Hartse* [1991]. Rinehart's study employed the inversion of S to S reflections (S_zS), while Hartse's study used all three of the observed reflected phases from the SMB (P_zP, S_zP, and S_zS). Both studies inverted arrival time data from Socorro area seismograms for crustal velocity models above the magma body, then used the calculated velocity models to generate maps of reflection points from which the outline of the magma body was determined. Both maps coincide with an area of surface uplift (Figures 1.1 and 1.2) thought to be related to inflation of the SMB [*Larsen et al.*, 1986]. *Ouichi* [1983] gives geomorphic evidence suggesting uplift of about 0.18 cm/yr for the last 20,000 years over the same region.

Two networks have operated in the Socorro area. The first was a portable

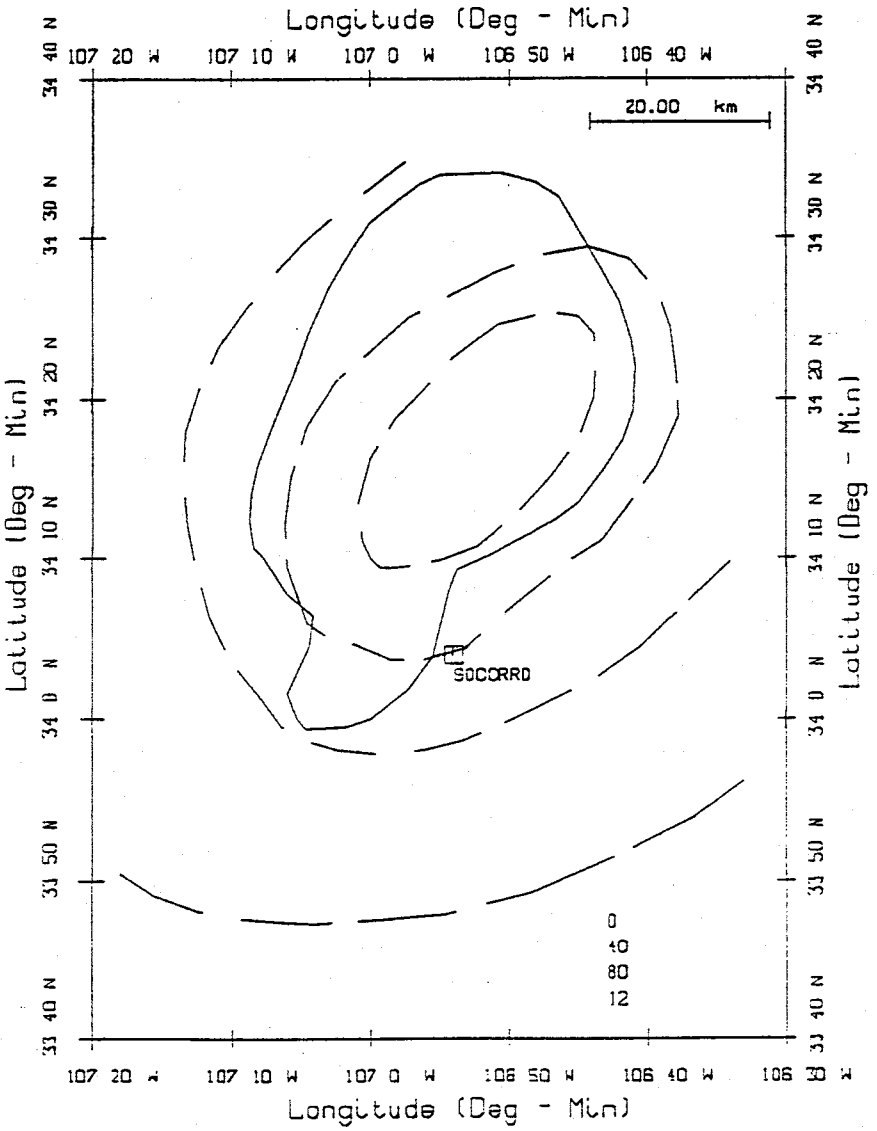

Figure 1.1. *Rinehart et al.* [1979] estimate of Socorro Magma Body lateral extent superimposed on uplift contours (dashed) from *Larsen et al.* [1986].

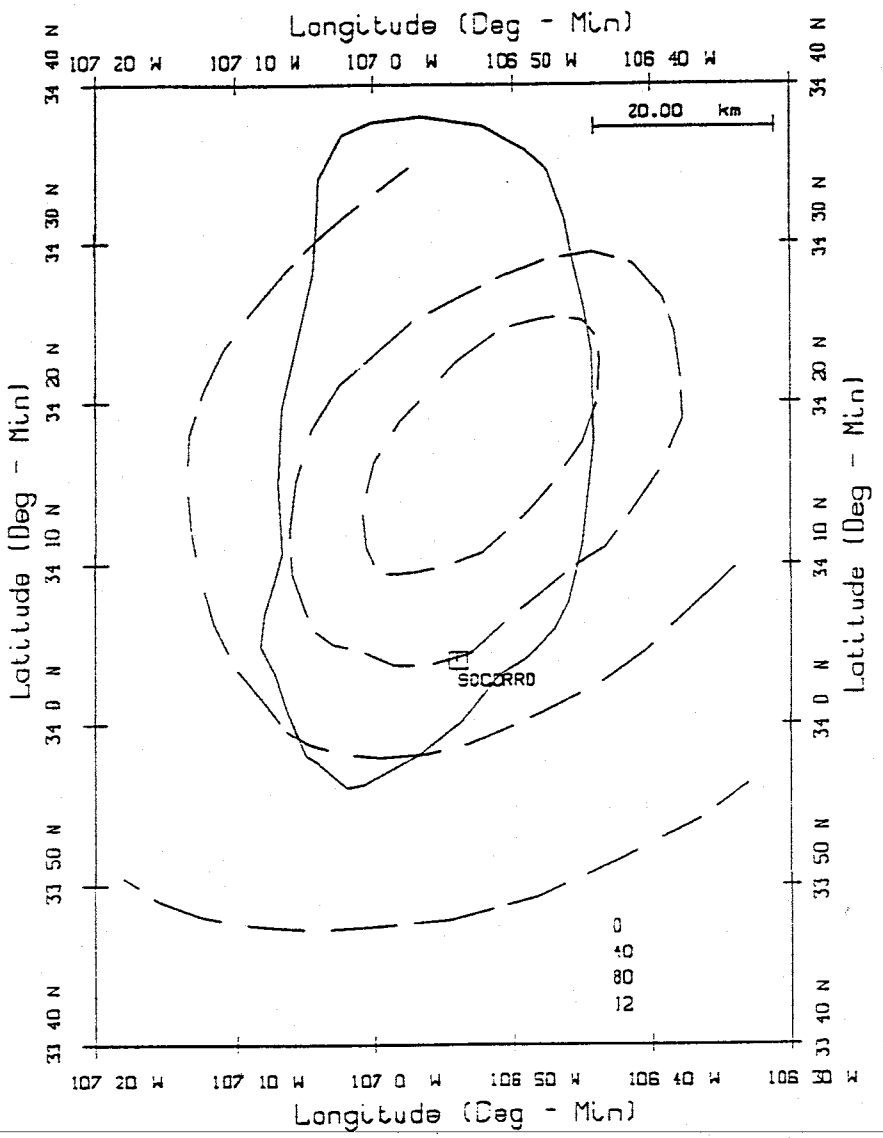

Figure 1.2. *Hartse* [1991] estimate of Socorro Magma Body lateral extent superimposed on uplift contours (dashed) from *Larsen et al.* [1986].

network operated between May of 1975 and January of 1978. The network was composed of up to six Sprengnether MEQ-800 seismic recording systems, two Sprengnether DR-100 digital recording systems (after May of 1977), and starting in 1977, real time telemetry of stations LAD and LPM from the Albuquerque Seismological Laboratory. This is the network *Rinehart* [1979] based his reflection study upon (Figure 1.3). The second network is a permanent telemetered seismic network, which has operated since the fall of 1982 until the present (Figure 1.4). *Hartse* [1991] used data from this network.

The initial purpose of my study was to address the differences between two estimates of the lateral extent of the SMB, that of *Rinehart* [1979] and of *Hartse* [1991]. The purpose has been expanded to include better constraint on the position of the northern end of the magma body, and inversion for a crustal velocity model. Examination of Figures 1.3 and 1.4 shows that the estimates of lateral extent as found by *Hartse* [1991], and by *Rinehart* [1979], differ significantly. The largest differences occur along the south and southeastern margins of the magma body, and may indicate inadequacies in Rinehart's data set, or lateral extension of the magma body between the time periods covered by the two studies. Good constraint on the northern end of the magma body was not found by either study.

The Albuquerque Seismological Laboratory ran a telemetered network in the Albuquerque area from 1975 through 1979. Addition of two of the southern stations (MLM and ALQ) and data for stations LAD and LPM beginning in 1975, enhances the portable network data used by Rinehart. I used this combined data set to address the differences in the mapped southern margins of the magma body, and also to better constrain the lateral extent of the northern end of the magma body.

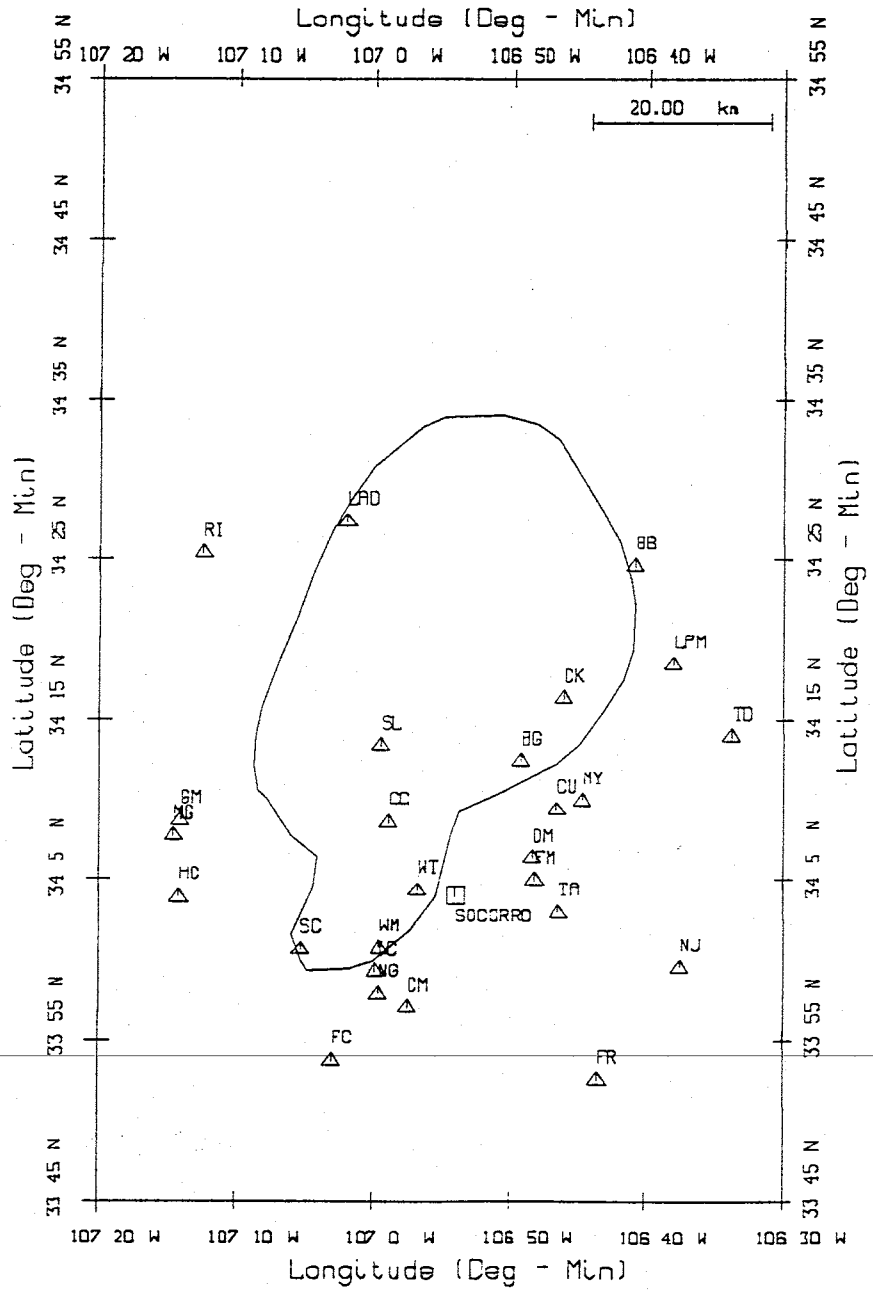

Figure 1.3. *Rinehart et al.* [1979] estimate of Socorro Magma Body lateral extent with stations used to collect data for their study.

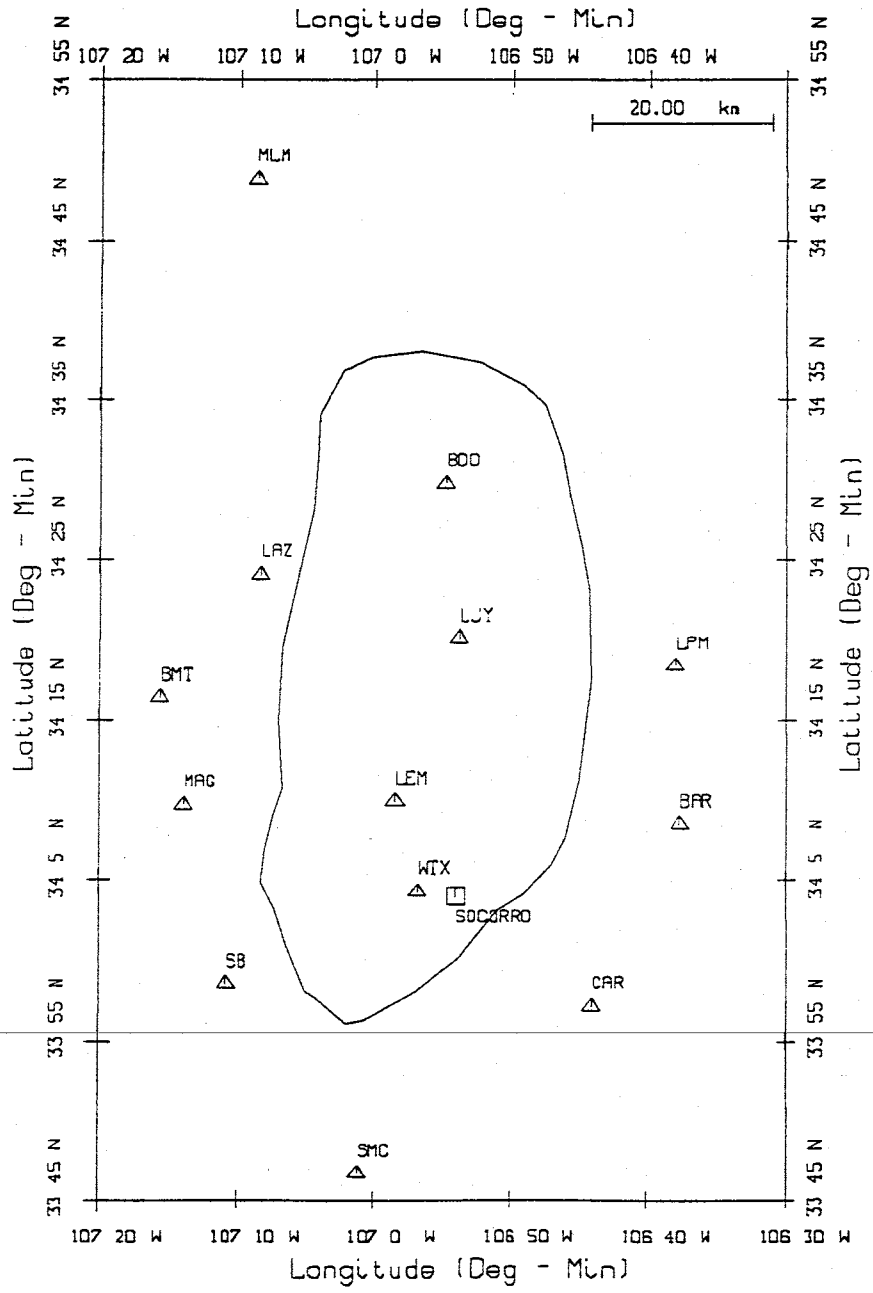

Figure 1.4. *Hartse* [1991] estimate of Socorro Magma Body Lateral extent with stations used to collect data for his study.

Overview of Method

I combined the Socorro and Albuquerque data for the period May 1975 to January 1978. Most of the Socorro network temporary station locations were reconfirmed by visits to the sites and replotted on newer and higher resolution 7.5 minute topographic maps. Events for the study were selected based on previous HYPO71 (revised) [*Lee and Lahr*, 1975] locations using only direct arrivals. The events were picked on the basis of azimuthal gap, number of stations, and geographical locations; the latter to obtain a good distribution of hypocenters over the magma body.

The program **SEISMOS** (**S**eismic **E**vent **I**nversion by **S**imultaneously using **M**ultiple phases for **O**ptimum **S**olutions) [*Hartse*, 1991] was used to incorporate magma body reflections into the event location process. **SEISMOS** revolutionized earthquake location in the Socorro area by allowing the use of reflected phases in event location and thus improving hypocenter estimates.

I inverted 84 hypocenters for a crustal model using the location algorithm **SEISMOS**. Using the final hypocenter estimates, maps were generated showing observed and theoretical reflection points. These maps were used in constraining the magma body outline, and in resolving differences between the *Rinehart* [1979] and the *Hartse* [1991] estimates of lateral extent of the magma body. Observed vs. theoretical reflection points for the two most northern stations (MLM and ALQ) helped constrain the limits of the northern end of the magma body. Improved hypocenter depth estimates allowed the refinement of the bounds of the seismogenic zone over the SMB, and possibly indicated the existence of lateral variation in average hypocenter depth. The existence of large residuals for good quality arrival time picks that did not fit an average flat layer crustal model may indicate that the vertical component seismic data

can delineate lateral heterogeneities in the upper crust in the study area.

In summary the primary objectives of my study were as follows:

1) Determine the reason(s) for the differences between the *Rinehart* [1979], and the *Hartse* [1991] estimates of the lateral extent of the SMB.

2) Constrain the northern boundary of the SMB, by addition of data from the Albuquerque Seismological Laboratory network.

The secondary objectives were as follows:

1) Examine the characteristics of the seismogenic zone above the SMB using improved hypocenter depth estimates.

2) Interpret crustal model inversion results in context of previous studies.

Organization of the Study

This section describes the organization and contents of the remainder of this Independent Study. First in **Geophysical Setting** I discuss the geology and geophysics of the Rio Grande rift - in particular the SMB and earthquake swarms. In **Previous Studies** I discuss relevant previous work. Then, in **Data** I detail the networks used in this study, event selection, and observations about the data set used. Also, I compare my data set to those used in other studies. In the **Analysis and Results** chapter, I discuss the inversion technique used, the inversion results, stability of the portable network data, hypocenters, and crustal models determined. In the **Discussion** chapter, I consider the results in the context of my primary and secondary objectives. I finish with **Conclusions**.

2. Geophysical Setting.

The Rio Grande Rift

The Rio Grande rift began forming about 32 my ago as a result of extensional reactivation of the southern Rocky Mountains [*Chapin*, 1979]; a major north trending zone of weakness formed during the late Paleozoic Ouchita-Marathon orogeny [*Kluth and Coney*, 1981]. The Rio Grande rift can be divided into three main segments; El Paso, Texas to Socorro, New Mexico, Socorro to Alamosa, Colorado, and Alamosa to Leadville, Colorado.

Rifting began in the southern segment (Socorro to El Paso) about 32 Ma and this section has experienced the most extension as evidenced by the width of associated basins (Figure 2.1). The southern Rio Grande rift is characterized as a series of north trending parallel basins. The central Rio Grande rift has north-northeast trending en echelon basins separated by northeast trending lineaments such as the Jemez and Morenci lineaments (Figure 2.2). The northern segment began rifting about 27 m.y. ago, and is characterized by a north-northwest trend dominated by the late Paleozoic and Laramide structural grain [*Chapin*, 1979].

Bimodal volcanism occurred early in the rifting of the southern segment with basaltic-andesitic lavas interbedded with high silicic ash flow sheets dated 32 to 26 m.y. old. Andesitic volcanism continued until a middle Miocene hiatus between 20 and 13 m.y. ago. After the hiatus the volcanism was basalt-rhyolitic [*Chapin*, 1979]. Deep mantle upwelling is a suggested mechanism for rifting based upon comparison of radiogenic lead found in the rift basalts, with radiogenic lead in oceanic basalts of Pliocene and Pleistocene age [*Everson and Silver*, 1978]. The lack of systematic chemical changes between late-rift and

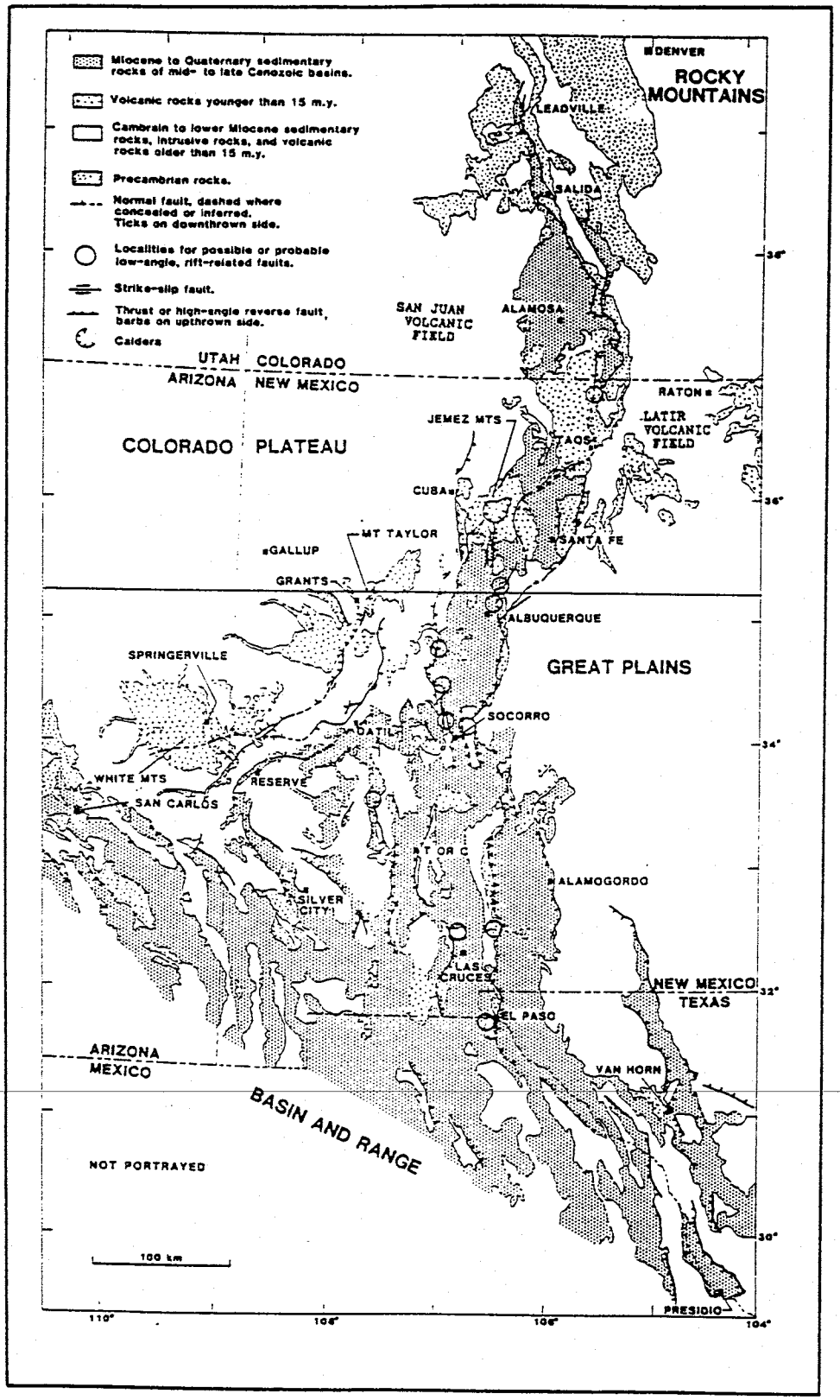

Figure 2.1. Generalized structural map of the Rio Grande rift (modified from *Baldridge et al.* [1984]).

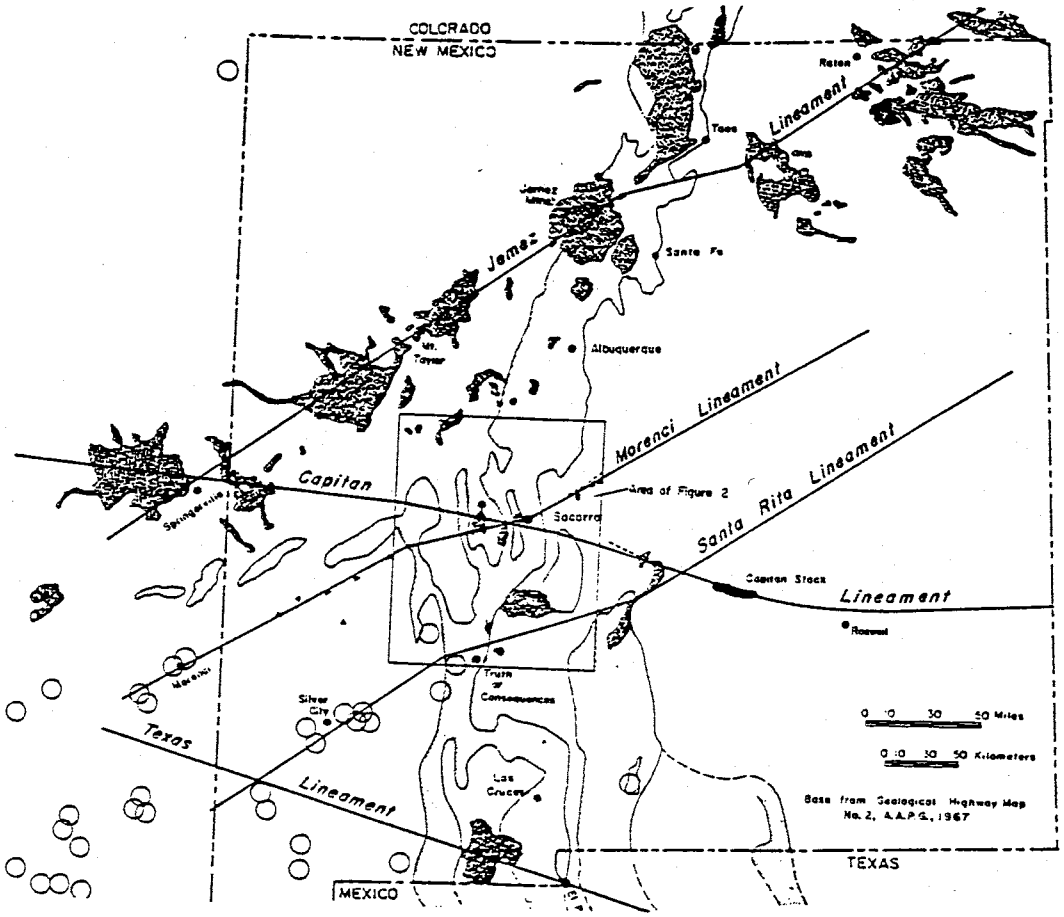

Figure 2.2. Rio Grande Rift in New Mexico. Note the prominent northeast trending structures of the Jemez and Morenci lineaments (modified from *Chapin et al.* [1978]).

early-rift rocks of the central and northern segments of the rift indicates that the magma sources stayed in the lithosphere throughout rifting [*Baldridge*, 1979]. It is possible that differences in age and composition of the Precambrian basement in the southern segment may have enabled more silicic rocks to form during or before early rifting.

Volcanism slowly increased after the Miocene hiatus, predominantly in the Socorro area and the Jemez mountains. Uplift of the southern Rocky Mountains between 7 and 4 m.y. ago, accompanied by block faulting disrupted earlier rift structures and resulted in the narrower, more sharply defined basins of the modern Rio Grande rift. A sharp increase in basaltic volcanism about 5 m.y. ago combined with erosion associated with the lowering of the base level of the Rio Grande, has left basalt capped mesas and dissected basins along the river drainage [*Chapin* ,1979].

The boundaries of the Rio Grande rift in New Mexico has been the object considerable debate [*Sanford et al.*, 1991]. Early estimates of the rift boundaries [*Bryan* 1938, *Kelley* 1952] include only the narrow chain of prominent structural basins which form the Rio Grande river valley. *Chapin* [1971] proposed including adjacent structural basins, more than doubling the earlier estimates of areal extent. Figure 2.3 shows boundaries of the Rio Grande rift in New Mexico, as well as the positions of other physiographic provinces in the state.

The Socorro Area

The Socorro area is bounded by the Great Plains to the east, the Colorado Plateau to the northwest, and the Datil-Mogollon volcanic field to the southwest (Figure 2.3). Rifting of the central Rio Grande rift in the Socorro area

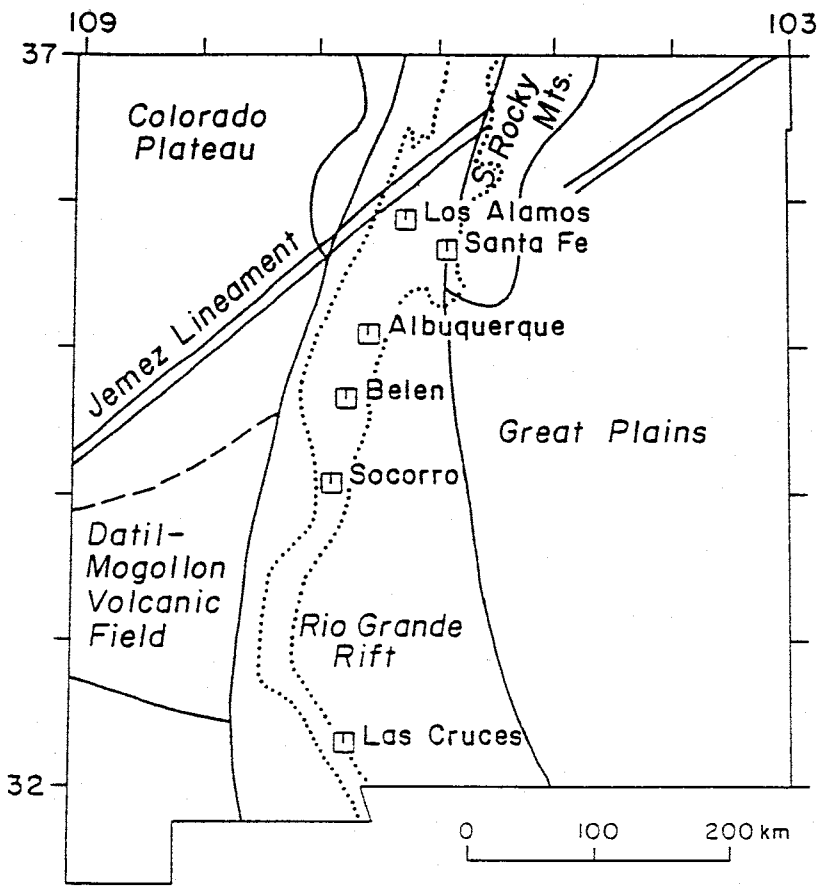

Figure 2.3. Boundaries proposed for the Rio Grande rift. Dotted lines include only the narrow chain of prominent structural depressions through which the Rio Grande flows (*Bryan*, 1938; *Kelley*, 1952). Solid lines show the approximate boundaries of the rift proposed by *Chapin* [1971] in relation to other physiographic provinces in New Mexico. Chapins boundaries includes structural basins adjacent to those through which the Rio Grande flows. Figure from *Sanford et al.* [1991].

began about 29 m.y. ago [*Chapin*, 1979]. Features of the study area include the Morenci lineament, Tertiary calderas, observed crustal doming, and the SMB. The Socorro area also has the greatest amount of seismic activity of any area (Figure 2.4) within the Rio Grande rift [*Bagg*, 1904; *Reid*, 1911; *Northrop*, 1945, 1947; *Sanford et al.*, 1991], both in numbers and strengths. Most of the earthquakes in the Socorro area occur on normal faults with north-south strikes [*Sanford et al.*, 1991].

The Morenci lineament is a major transverse shear zone trending southwest-northeast from Arizona to the Socorro area of the Rio Grande rift. The lineament has not been correlated with seismicity in the Socorro area, perhaps due to weakness in the crust induced by the shear zone [*Sanford et al.*, 1991].

Figure 1.1 shows the contours of crustal deformation in the Socorro area [*Larsen et al.*, 1986], as determined by releveling bench marks between 1911 and 1980 (uplift of over 120 mm was observed). *Ouichi* [1983] presented geomorphic evidence for 1.8 mm/yr of uplift for the last 20,000 years in the area of maximum deformation that agrees well with the rate from the releveling measurements. Based on the tilt of Rio Grande river sand deposits [*Bachman and Mehnert*, 1978] and assuming the ancestral Rio Grande had the same gradient as the present river, *Sanford et al.* [1991] calculated that uplift in the Socorro area may have begun about 40,000 years ago. Sanford's calculation assumed the magma body had a minimum areal extent of 1700 km^2 [*Rinehart et al*, 1979] and a thickness of about 130 to 190 m [*Brocher*, 1981; *Ake and Sanford*, 1988].

Analysis of the SMB relies primarily on seismic data recorded during Socorro area earthquake swarms. These swarms, which account for most of the

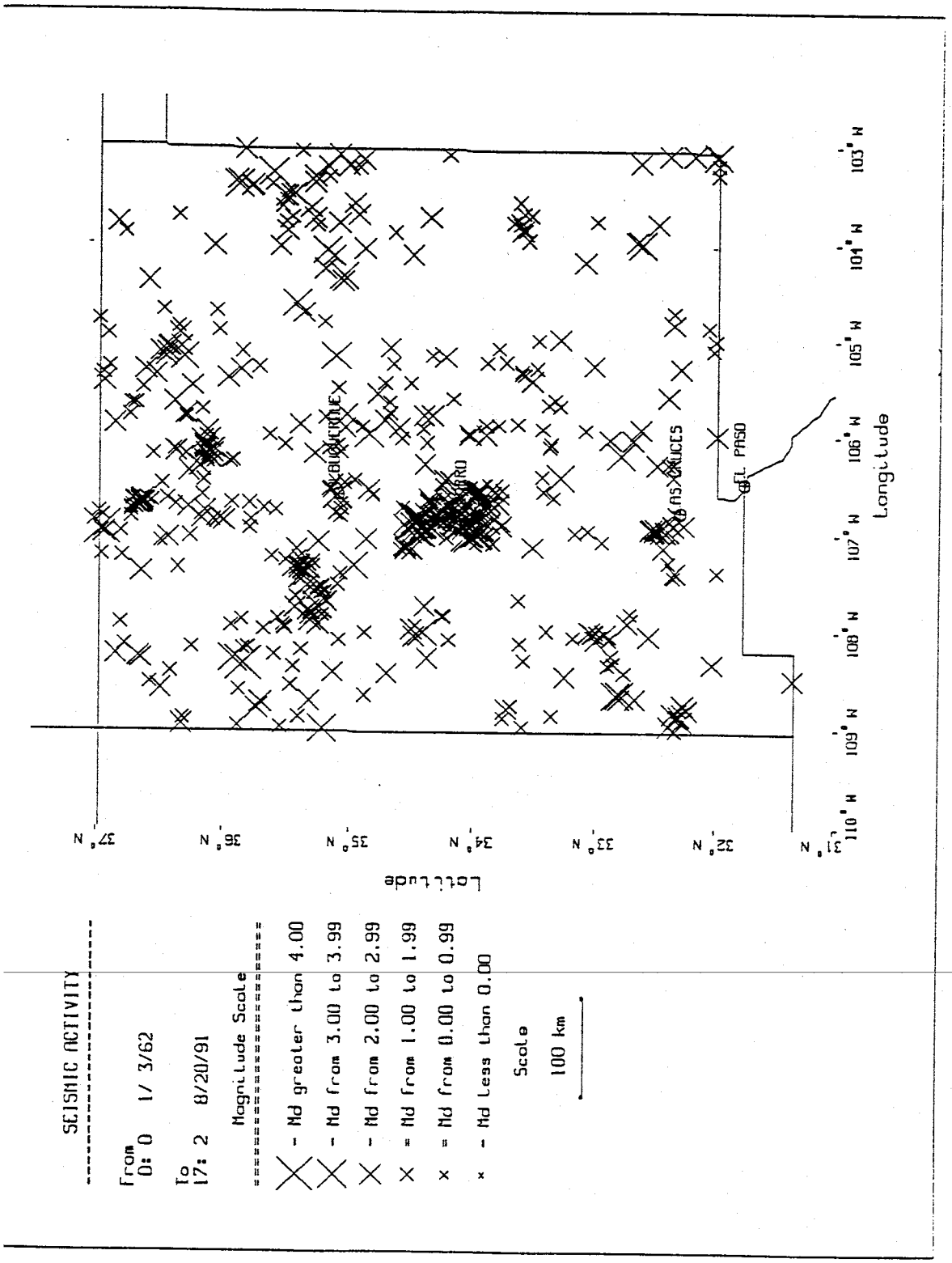

Figure 2.4. New Mexico Seismicity $m_d > 1.5$. Note Jemez lineament and the aseismic halo around the Socorro seismic anomaly.

Socorro area earthquakes, may be related to the injection of small amounts of magma into the upper crust [*Sanford and Einarson*, 1982]. The seismicity, like the crustal uplift, is centered over the magma body. This suggests a relationship between the seismicity and the localized uplift which may be the result of inflation of the SMB. Socorro area earthquakes may also be occurring on faults reactivated by the stretching of the crust above the inflating body [*Sanford* , 1991]. This crustal bulging could also help explain the observed aseismic halo surrounding the Socorro seismic anomaly (Figure 2.4).

Earthquake swarms have often struck the Socorro area. The earliest report is that of a U.S. Army surgeon who reported 22 felt shocks during a swarm that lasted from December 11, 1849 to February 8, 1850 [*Hammond*, 1966]. Earlier records may exist in Spanish and Mexican archives. Other notable swarms have occurred near Socorro including a vigorous swarm between July of 1906 and January of 1907 which produced felt events nearly daily, sometimes within hours of each other. The most recent strong earthquake swarm in the Socorro area was centered near the village of Bernardo, New Mexico, and had 45 magnitude 2.0 or greater events between November of 1989 and May of 1992. Four earthquakes of magnitude 4.0 or greater were recorded during the same time period. Activity continues to the present at a much reduced level.

3. Previous Studies

Organization

In this chapter I review the previous work on the SMB which is most relevant to my study. I begin by covering the early work and the identification of anomalous phases on Socorro area seismograms. I continue with more recent reflection studies, in particular those which examine the lateral extent of the SMB, such as the Vibroseis reflection data acquired by COCORP near Socorro. Next, I cover the direct arrival studies utilizing data from Socorro area seismograms. Last, I discuss refraction studies related to the study area. A summary of previous work is presented at the end of this chapter in table form (Table 3.4).

Early Reflection Studies

As early as 1960, anomalous phases were identified on Socorro area seismograms [*Sanford and Holmes*, 1960]. Two of these phases identified as P_xP? and S_xS? were determined to be matched phases like direct P and S, and it was suggested that they might be P and S reflections from a crustal discontinuity. In 1965 *Sanford and Long* [1965] used amplitude vs. offset (AVO) analysis for the S_zP and S_zS phases to determine that the amplitudes of these phases were far greater than theoretical values for reflection from a solid-solid interface. In 1973 [*Sanford et al.*, 1973] analyzed arrival times and amplitudes of the S_zP and S_zS phases to determine that the reflector was at about 18 km depth and that the discontinuity was sharp and could be underlain by material of low rigidity. Finally in 1977 (*Sanford et al.*, 1977), the extent of the magma body was mapped using reflection points (S_zS). In the same study, it was was con-

cluded that the reflector was magma on the basis of observed vs. theoretical ratios of amplitudes for the S_zP and S_zS phases. Minimum lateral extent was estimated at 1200 km^2.

These early papers served to identify the anomalous reflected phases in the Socorro area; related the reflections to the mid-crustal discontinuity; determined that the reflector was composed of a low rigidity material (magma); and established that the magma body had considerable lateral extent beneath the Socorro area. Both the early and more recent reflection studies are summarized in Table 3.1.

More Recent Reflection Studies

In the late 1970's the Consortium for Continental Reflection Profiling (COCORP) carried out seismic reflection surveys in the Rio Grande rift near Socorro [*Brown et al.*, 1980]. Data was collected using the standard VIBROSEIS (trademark Continental Oil Co.)technique. The reflection surveys covered 155 km and detected two strong P-wave reflectors, one at about 20 km depth. By far the most distinctive set of deep reflections observed in the rift, the high amplitude reflections (averaging 6 db above background) at 6 to 8 seconds (18 to 24 km), correspond well in depth to the shear wave reflector depth from microearthquake data. Early interpretations of the data are found in [*Brown et al.*, 1980 and *Brocher*, 1981]. Reinterpretation of the upper P-wave reflector, originally thought to be the interface between Phanerozoic and Precambrian rock, can be found in *de Voogd et al.* [1988].

More detailed mapping of the magma body was completed by *Rinehart et al.* [1979]. The lateral extent was revised to 1700 km^2 by the use of 220 S_zS reflection points from the upper surface of the magma body. The surface

Table 3.1 Reflected Phase Studies

Investigators	Method	Data	Results
Sanford and Holmes (1960)	Phase comparison	P_zP and S_zS	Identified anomalous phases
Sanford and Long (1965)	Amplitude vs. offset and travel-time modeling	S_zP and S_zS	Identified S_zP and S_zS phases
Sanford et al. (1973)	Arrival time modeling	S_zP and S_zS	Reflector depth approximately 18 km
Sanford et al. (1977)	Reflection point mapping	S_zP and S_zS	Reflector is magma, lateral extent mapped
Rinehart et al. (1979)	Reflection point mapping	S_zS	Areal extent of magma body at least 1700 km^2
Rinehart and Sanford (1981)	Travel-time inversion	S_zS	Vs = 3.41 ± 0.03 km/s Depth = 19.2 ± 0.6 km
Ake and Sanford (1988)	Digital signal processing and forward modeling	P_zP and S_zS	Magma body internal structure examined
Hartse (1991)	Travel-time inversion	P, S, P_zP, S_zP, and S_zS	Vp = 5.91 km/s depth = 18.48 ± 0.223 ν = 0.255

relief on the magma body surface was interpreted to be minimal based on calculated reflector depths at different stations for well recorded earthquakes. This study also used data from the COCORP study to constrain lateral extent of portions of the magma body. Rinehart's map was extended [*Gridley*, 1989], to both the southwest and southeast. *Gridley* used reflections found on earthquakes recorded between 1982 and 1988 on the Socorro network, and hypocenters determined by the location algorithm HYPO71. Since Gridley's mapping used data from a later time period than Rinehart's study, it was possible to speculate that the magma body had physically changed in lateral extent.

S_zS reflections from 163 microearthquakes were inverted for reflector depth and S-wave velocity above the magma body by *Rinehart and Sanford* [1981], the first study to use inversion of the reflected phases. Using hypocenter estimates obtained from the location algorithm of *Ward* [1980], several models of the crust were found to fit the data. Though unable to simultaneously solve for reflector depth and S-wave velocity, a best fit model was found. Constraining the depth to 19.2 km $\pm$0.6 km resulted in a V_s of 3.41 km/s averaged from the surface to the reflector. Between 10 km and 19.2 km, V_s was determined to be 3.44 km/s.

The internal structure of a small portion of the magma body was determined by *Ake and Sanford* [1988] using P_zP and S_zS reflected phases. Ake and Sanford found that the S and S_zS phases correlated well (average correlation coefficient, +0.79), while the P and P_zP phases did not (average correlation coefficient, +0.45). The study was based on digital recordings of an earthquake swarm near station SC (South Canyon) that sampled about a 500 m length of the magma body surface. For this swarm the S and S_zS phases left the focal

region 180° out of phase and because the correlation coefficient between these two phases was positive, the magma body surface must have produced a 180° phase shift. A very high correlation coefficient between the S and S_zS phases for different swarm events demonstrated that the reflecting surface had little topographic variation over the study area. On the other hand, variability in the P_zP phase (as indicated by low cross correlation coefficients) implied that the internal structure of the magma body was not uniform. An average two layer magma body was proposed, a layer of full melt over a layer of partial melt. Comparisons between theoretical and observed spectra indicated a best fit for a 70 m layer of full melt over a 60 m thick layer of partial melt.

Hartse [1991] produced a new hypocenter location program **SEISMOS**, capable of utilizing all of the observed reflections in the location process, and in inversions for crustal models. *Hartse et al.* [1992] found that the use of reflected phases improved hypocenter locations, in particular the depth estimate which was improved by about a factor of three. Hartse inverted jointly for 75 hypocenters, and a one dimensional velocity model using over 1000 direct arrivals and over 400 reflected arrivals. Important results of this undamped inversion were that the Socorro magma body appears to have no perceptible dip and is located at about 18.50 km depth ($\pm 0.23 km$). In addition, it was found that Poissons ratio may be unusually low beneath the seismogenic zone (about 10 km depth). Hartse also analyzed the distribution of reflection points to place the lateral extent of the magma body at 2000 km^2. The results of Hartse's study will be discussed in more detail in the **Discussion** section of this paper.

Direct Phase Studies

Routine location of microearthquakes in the Socorro area depended on direct arrivals only until the advent of **SEISMOS** [*Hartse*, 1991]. Numerous studies have employed these direct arrivals. *Ward et al.* [1981] used 262 direct P arrivals to obtain a three-dimensional velocity model for the uppermost upper crust. Initial half-space inversion gave $V_p = 5.85 \pm 0.02$ km/s, and subdivision of blocks detected a low velocity cell ($V_p = 5.17 \pm 0.11$ km/s) about 15 km southwest of Socorro. Other blocks had less significant but noticeable anomalies.

Poisson's ratio has been studied several times in the immediate Socorro area. Two studies used direct P and S phases only, thus restricting the Poisson's ratio estimates to the seismogenic zone. *Caravella* [1976] found $\nu = 0.262 \pm 0.034$ using 50 events; and *Fender* [1978] found $\nu = 0.251 \pm 0.052$ using 294 events. *Hartse et al* [1992] found Poisson's ratio for the whole crust above the magma body to be ($\nu = 0.255 \pm 0.002$). For Hartse's two layer case $\nu = 0.256 \pm 0.002$ for the upper 10 km layer, and $\nu = 0.228 \pm 0.007$ for the lower 8.75 km layer.

Two relatively detailed studies of the seismogenic zone in the Socorro area have been completed. *King* [1986] found the limits of the seismogenic zone to be between 4 km and 12 km. King used direct arrivals only in his hypocenter locations, thus the error margins were large on his depth estimates. *Hartse* [1991] studied the seismogenic zone using 75 hypocenters located with **SEISMOS**. Since he included reflections, the focal depth estimates were much better constrained than King's. Hartse found that the upper limit of the seismogenic zone was not as well defined as the lower limit, with some events as shallow as two km depth. Most events occur between 4 km and 10 km

depth (89.33 percent), with a greater percentage of events less than 6 km than found in King's study. The direct phase studies are summarized in Table 3.2.

Refraction Studies

Only two refraction studies have been conducted which concern the crust directly beneath the Socorro area. *Carlson* [1983] found an average V_p of 5.76 km/s for depths of 2.5 - 6.0 km, a velocity of 6.25 km/s for depths of 6.0 - 19.0 km, and a velocity of 6.48 km/s below a discontinuity at about 19.0 km depth. *Singer* [1989] found a velocity of 5.95 km/s ($\pm$0.03 km/s) between 2.5 and 10.00 km depth, and a velocity of 6.40 km/s ($\pm$0.16 km/s) below a discontinuity at about 19.4 km depth. Both of these studies used time-term analysis of earthquake and explosion data recorded on Socorro networks. The results of the refraction studies are summarized in Table 3.3.

Table 3.2 Direct Phase Studies

Investigator	Method	Data	Results
Ward et al. (1981)	Arrival-time inversion	P	Vp = 5.85 km/s
Caravella (1976)	Wadati diagrams (50 events)	P and S	$\nu = 0.262 \pm 0.034$
Fender (1978)	Wadati diagrams (294 events)	P and S	$\nu = 0.251 \pm 0.052$
King (1986)	Hypocenter cross-sections and histograms	P and S	Seismogenic zone 4 - 12 km

Table 3.3 Refracted Phase Studies

Investigator	Method	Data	Results
Carlson (1983)	Time-term analysis	P_g, P^*, and P_n	V_p=5.76 (2.5-6.0) V_p=6.25 (6.0-19.0) V_p=6.48 (19.-32.5) V_p=8.08 (mantle)
Singer (1989)	Time-term analysis	P_g, P^*, and P_n	V_p=5.95 (2.5-10.0) V_p=6.40 (19.4-33.5) V_p=8.14 (mantle)

Table 3.4 Socorro Area Velocity Models - Previous Study Summary

Parameter	Previous Investigator	Model Value
V_{p1} (km/s	Ward (1980)	5.85 ± 0.02
	Singer (1989)	5.95 ± 0.03
	Hartse (1991) 1-Layer	5.91 ± 0.05
	Hartse (1991) 2-Layer	5.95 ± 0.05
ν_1	Caravella (1976)	0.262 ± 0.034
	Fender (1978)	0.251 ± 0.052
	Hartse (1991) 1-Layer	0.255 ± 0.002
	Hartse (1991) 2-Layer	0.256 ± 0.002
V_{s1} (km/s)	Hartse (1991) 1-Layer	3.39 ± 0.04
	Hartse (1991) 2-Layer	3.41 ± 0.04
V_{p2} (km/s)	Hartse (1991) 2-Layer	5.80 ± 0.08
ν_2	Hartse (1991) 2-Layer	0.228 ± 0.007
V_{s2} (km/s)	Rinehart and Sanford (1981)	3.44 ± 0.03
	Hartse (1991) 2-Layer	3.44 ± 0.07
Z (km)	Rinehart and Sanford (1981)	19.20 ± 0.60
	Hartse (1991) 1-Layer	18.50 ± 0.23*
	Hartse (1991) 2-Layer	18.75 ± 0.28*

Hartse's Two-Layer model has an upper layer with a base at 10 km depth, roughly corresponding with the base of the seismogenic zone where a compositional change may occur. Hartse's Single Layer model treats the entire upper crust from the surface to the magma body as a single layer.

4. Data

Overview

In this chapter the seismic network used in this study is discussed. The discussion includes the Albuquerque Seismological Laboratory (U.S.G.S.) network, and the Socorro portable network with both analog and digital stations. I also detail the event selection process, and the constraints used in obtaining the best hypocenters. In addition I make observations about the final data set, including anomalies and the statistics of the set. In summary I make comparisons with other data sets, particularly with the data set of *Hartse* [1991]. The data used in this study is comprised of arrival times of direct phases (P and S) and SMB reflected phases (P_zP, S_zP, and S_zS).

Network Information

A majority of the data for this study was recorded on a movable array of five to six Sprengthener MEQ-800 seismic recording systems operated between July of 1975 and January of 1978. The network was deployed at a number of locations about the Socorro area, primarily in caves and mines, and other sheltered sites in order to reduce background noise. The MEQ-800 seismic stations recorded an analog signal onto a smoked paper drum revolving at 2 mm/s. Self contained quartz crystal chronometers were synchronized at the beginning of each recording week with WWV, and again at the end of the recording week in order to correct for clock drift. Mark Products vertical L4-C geophones (1.0 Hz natural frequency) were used as sensors for the stations. A magnification response curve for average field settings is shown in Figure 4.1.

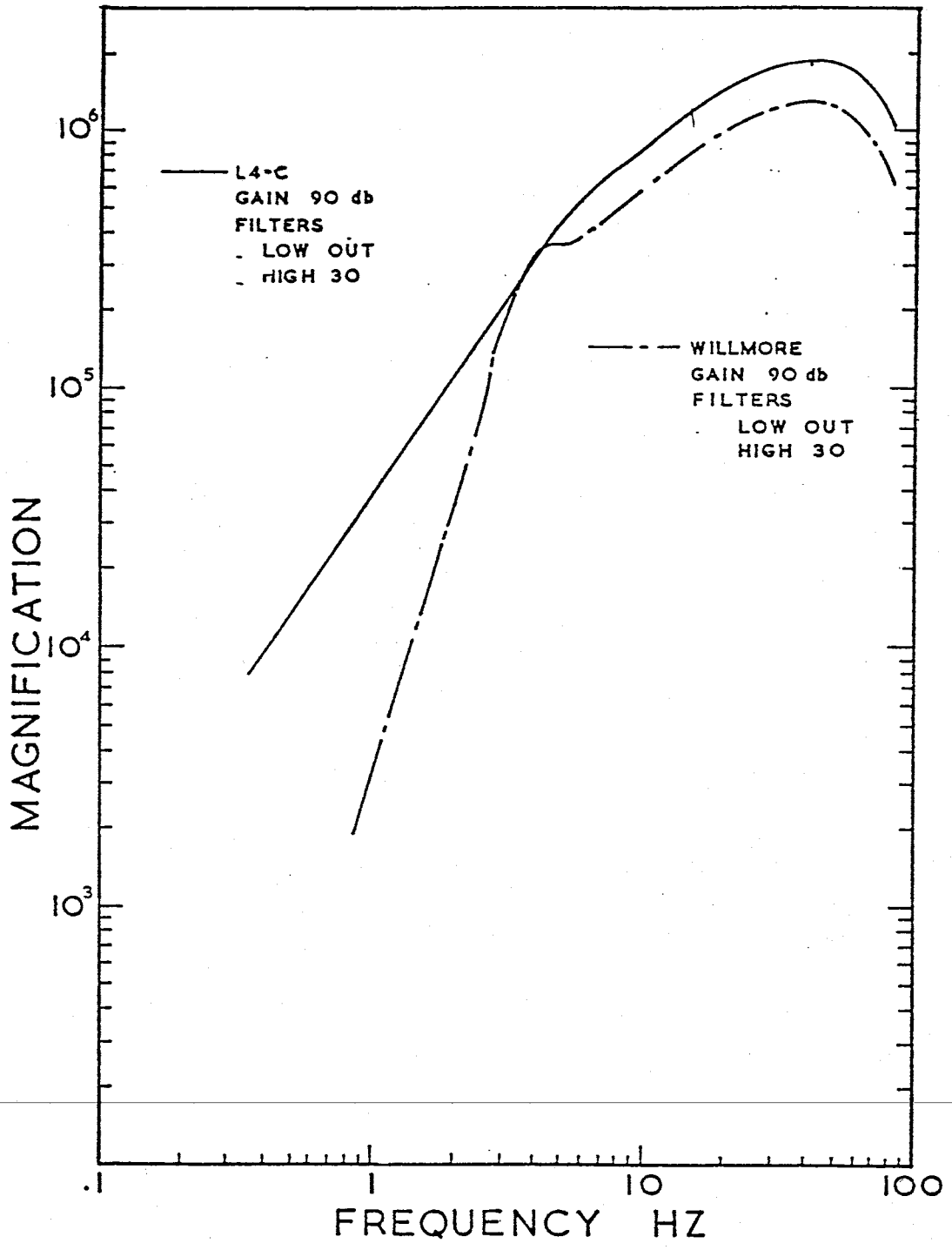

Figure 4.1 Magnification response curves for the MEQ-800 seismographs using either an L4-C or Willmore geophone. Curves are for the usual field settings (from *Rinehart* [1979]).

Between April of 1977 and January of 1978, the portable network was supplemented by two DR-100 portable 12-bit digital seismic recorders. The DR-100 continuously samples the seismic signal until triggered by an event with a larger short-term average (by a set amount) than the long-term average. The triggering signal is recorded on magnetic tape at 100 samples per second. Mark Products vertical L4-C geophones were used with these systems also.

The portable array was used to occupy any of the 24 station sites shown in Figure 4.2 and listed in Table 4.1 (excluding MLM and ALQ). Prior to the fall of 1977, stations in the south were occupied more frequently than those to the north, and after that time, the reverse was the case. The MEQ-800's were deployed on Mondays and retrieved on Fridays, while the DR-100's could be left in the field for up to four weeks at a time.

In order to increase coverage in the northern portion of the network, and increase the aperture and stability of the network, I added four stations (ALQ, MLM, LAD, and LPM) from the USGS Albuquerque Seismological Laboratory network which was operated north of the Socorro network, primarily from January of 1976 to November of 1981. The network was a permanent radio telemetered network operated into the Albuquerque Seismological Laboratory. Key field components were a vertical component seismometer (ALQ also had horizontal component seismometers) operating at either 0.8 Hz or 1.0 Hz natural frequency. Also in the field were a preamplifier-VCO and a transmitter. The components for each station in the observatory were a reciever and a discriminator. The analog signals from the discriminators were recorded continuously on film using a Geotech Develocorder. Sometimes individual stations were recorded on heliocorders using a hot-wire stylus on heat sensitive paper. The timing was controlled at the observatory with a quartz-controlled clock

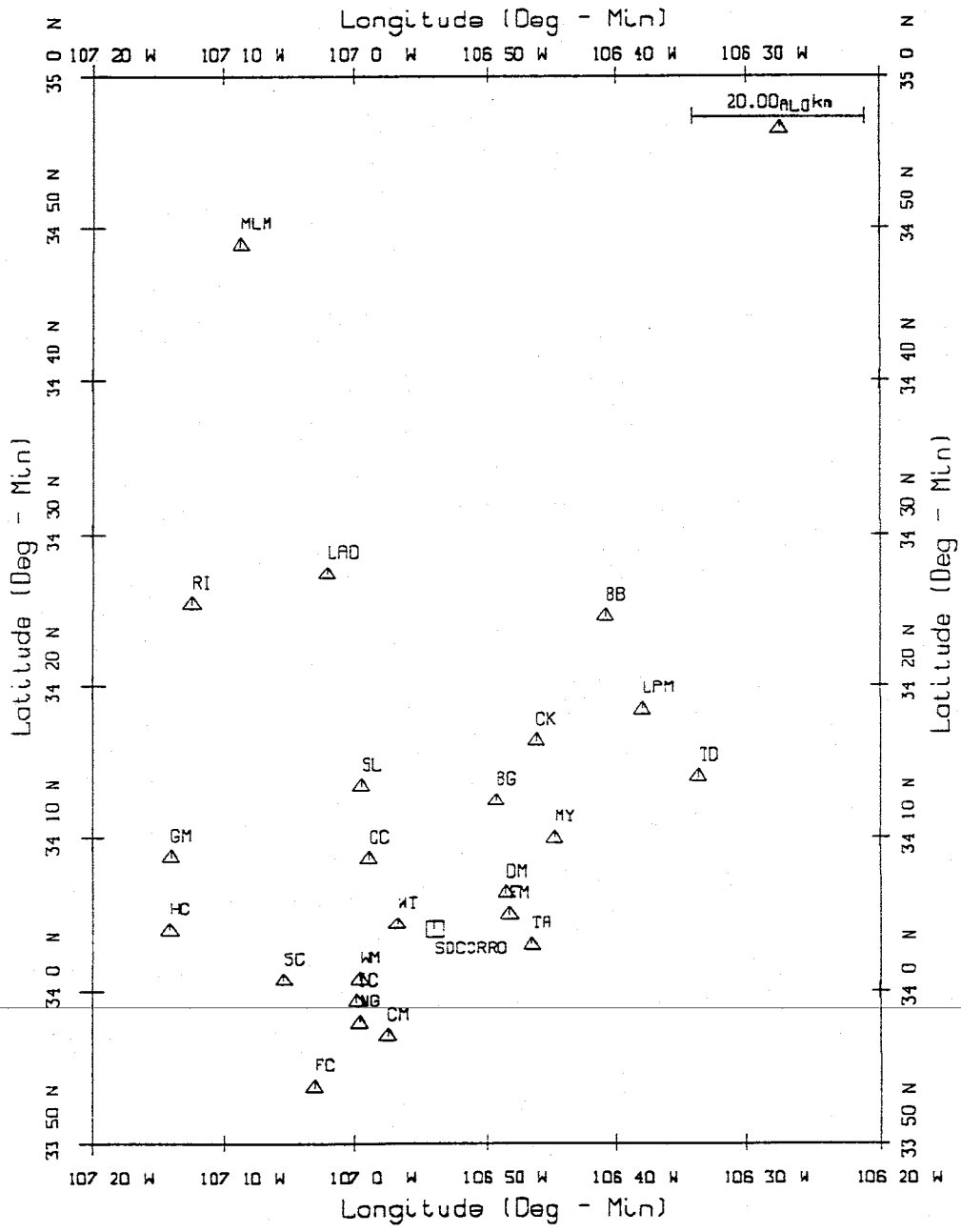

Figure 4.2. Stations used to collect data for this study.

Table 4.1 Station Locations and Surface Geology

Station	Latitude	Longitude	Elevation	Surface Geology
ALQ	34.9417	106.4583	1853	Precambrian
BB	34.4099	106.6813	1612	Tertiary Volcanics
BG	34.2070	106.8220	1512	Tertiary Volcanics
CC	34.1445	106.9814	1646	Precambrian
CK	34.2725	106.7702	1578	Cretaceous Dakota S.S.
CM	33.9501	106.9582	1640	Tertiary Volcanics
DM	34.1067	106.8085	1545	Pennsylvanian Limestone
FC	33.8950	107.0504	1850	Tertiary Volcanics
FM	34.0825	106.8050	1536	Precambrian
GM	34.1457	107.2344	1945	Tertiary Intrusive
HC	34.0658	107.2356	2231	Tertiary Volcanics
IC	33.9874	106.9967	1725	Tertiary Volcanics
LAD	34.4565	107.0338	1768	Precambrian Metasediments
LPM	34.3076	106.6336	2088	Precambrian
MLM	34.8142	107.1450	1707	Quaternary Extrusive Basalt
MY	34.1667	106.7459	1645	Permian Sedimentary Rocks
NG	33.9648	106.9933	1722	Tertiary Volcanics
RI	34.4231	107.2076	1853	Permian Yeso
SC	34.0108	107.0892	2103	Tertiary Volcanics
SL	34.2234	106.9910	1615	Tertiary Sedimentary Rocks
TA	34.0500	106.7757	1554	Permian Abo S.S.
TD	34.2335	106.5623	1823	Permian Sedimentary Rocks
WM	34.0120	106.9929	1670	Tertiary Volcanics
WT	34.0722	106.9459	1555	Precambrian

Surface geology should not be taken as representative of local geology to great depth. Latitude is in degrees north, longitude is in degrees west, and elevation is in meters.

synchronized with WWV. The theoretical system response based on manufacturer specifications is plotted in Figure 4.3.

Station Locations

At the beginning of the study, station locations were field checked and their positions replotted on 7.5 minute quadrangles. Many of the stations were originally located on 15 minute quadrangles, because those were the maps available for the Socorro area during the middle 1970's. The field check had three purposes; first, to check the location of stations sites with respect to early photographs; second, to refine station locations based on the greater detail of the 7.5 minute maps; and third, to familiarize myself with the geology of the individual station sites. Most station locations changed by less than 100 meters and some changed not at all. However, station TD changed location by more than 1400 meters. The station locations both past and as relocated are presented in Table 4.2 along with the offset between location estimates.

Event Selection

Initial solutions for all events used in my study were found by *Weider* [1981] using HYPO71. For the Socorro portable array, 534 events were located between mid-1975 and January of 1978. I used Weider's solutions to search for a wide geographical distribution of hypocenters in the Socorro area, attempting to maximize number of stations and minimize azimuthal gap. I selected possible events on the basis of number and quality of reflections, noisiness of record, and magnitude (large magnitude events obscure the reflected phases in the P and S codas). Also I looked for events which could benefit from the addition of the four northern stations, ALQ, MLM, LAD, and LPM. In total

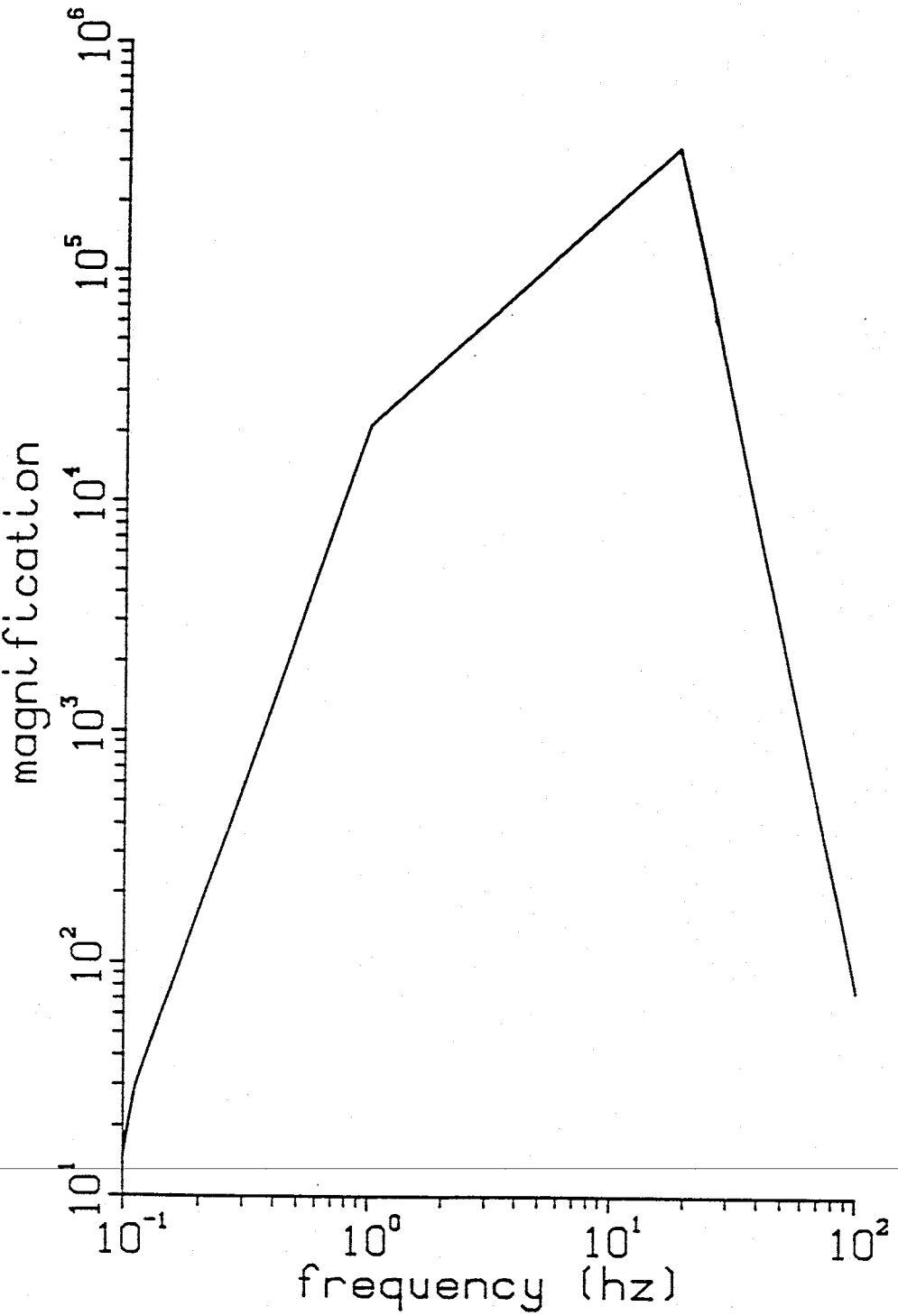

Figure 4.3. System response of a typical telemetered network station (from *Hartse* [1991]).

Table 4.2 Station Relocations

Station	Original Latitude	Original Longitude	Relocated Latitude	Relocated Longitude	Difference in meters
ALQ	34.9417	106.4583	34.9417	106.4583	*
BB	34.4090	106.6818	34.4099	106.6813	**108**
BG	34.2068	106.8205	34.2070	106.8220	**132**
CC	34.1442	106.9819	34.1445	106.9814	**50**
CK	34.2725	106.7702	34.2725	106.7702	*
CM	33.9501	106.9576	33.9501	106.9582	**60**
DM	34.1075	106.8079	34.1067	106.8085	**103**
FC	33.8950	107.0504	33.8950	107.0504	*
FM	34.0829	106.8047	34.0825	106.8050	**58**
GM	34.1454	107.2345	34.1457	107.2344	**32**
HC	34.0658	107.2361	34.0658	107.2356	**40**
IC	33.9870	106.9967	33.9874	106.9967	**50**
LAD	34.4583	107.0375	34.4565	107.0338	**396**
LPM	34.3076	106.6336	34.3076	106.6336	*
MLM	34.8142	107.1450	34.8142	107.1450	*
MY	34.1667	106.7459	34.1667	106.7459	*
NG	33.9648	106.9933	33.9648	106.9933	**0**
RI	34.4234	107.2075	34.4231	107.2076	**41**
SC	34.0100	107.0894	34.0108	107.0892	**91**
SL	34.2234	106.9910	34.2234	106.9910	**0**
TA	34.0498	106.7751	34.0500	106.7757	**60**
TD	34.2339	106.5778	34.2335	106.5623	**1431**
WM	34.0120	106.9929	34.0120	106.9929	**0**
WT	34.0722	106.9459	34.0722	106.9459	*

The *'s indicate stations which were already well located on 7.5 minute maps. The difference between stations is the straight line measurement of horizontal separation. Latitude is in degrees north and longitude is in degrees west.

I found 130 events, including some without any reflections or with only one reflection. These 130 events had azimuthal gaps of less than 180° and at least four recording stations.

A subset of 84 events was established by requiring that each event be recorded by at least five stations and have 12 picked arrival times. The most common number of stations was six with the average nearly seven (Table 4.3), while the most common number of picks per event was 18, with an average of about 20 (Table 4.4). At least two stations were required to have reflections for each event, as long as one station had a reflection pair, and if no reflection pairs were found, at least three stations needed to record a reflection (with one exception). Thirty-five events had three or more reflection pairs; 60 events had two or more reflection pairs; 21 events observed only one reflection pair; and only three events had no reflection pairs. The number of reflections per event (Table 4.5) ranged from two to fourteen, with the most common number being six, and an average of more than seven. Differences between the statistics of this set and that of *Hartse* [1991] are summarized in Table 4.6. The 84 event subset was used to invert for a crustal velocity model. Epicenters for this data set are shown in Figure 4.4.

Identification, Timing, and Weighting of Arrival Times

The identification of reflected phases has been routine for some time in Socorro area microearthquake studies. Often theoretical arrival time curves based on the best known crustal model (e.g. Figure 4.5) are used in the identification of phases. The travel time curves are generated for 1 km intervals of focal depth covering the seismogenic zone (2-12 km). The curves I used in this study were based on the crustal model of *Hartse* [1991]. Many of the events

Table 4.3 Stations Per Event	
Number of stations	Number of events
5	13
6	23
7	18
8	16
9	12
10	2

Table 4.4 Picks Per Event	
Number of Picks	Number of events
12	1
13	1
14	6
15	5
16	5
17	7
18	12
19	4
20	7
21	4
22	6
23	5
24	7
25	4
26	4
27	2
28	1
29	2
30	1

Table 4.5 Reflections Per Event	
Number of reflections	Number of events
2	1
3	3
4	7
5	9
6	16
7	10
8	8
9	13
10	6
11	6
12	3
13	1
14	1

Table 4.6 Summary of Statistics: This Study and Hartse [1991]

Statistic	Hartse [1991]	This study
Number of epicenters	75	84
Minimum number of stations per event	6	5
Average number of stations	8.32	6.96
Average number of picks per event	19.40	20.10
Average number of reflections per event	5.41	7.38
Number of P arrivals	564	579
Number of S arrivals	485	489
Total number of direct arrivals	**1049**	**1068**
Number of PzP arrivals	77	85
Number of SzP arrivals	160	183
Number of SzS arrivals	169	352
Total number of reflected arrivals	**406**	**620**
Total number of arrivals	**1455**	**1688**

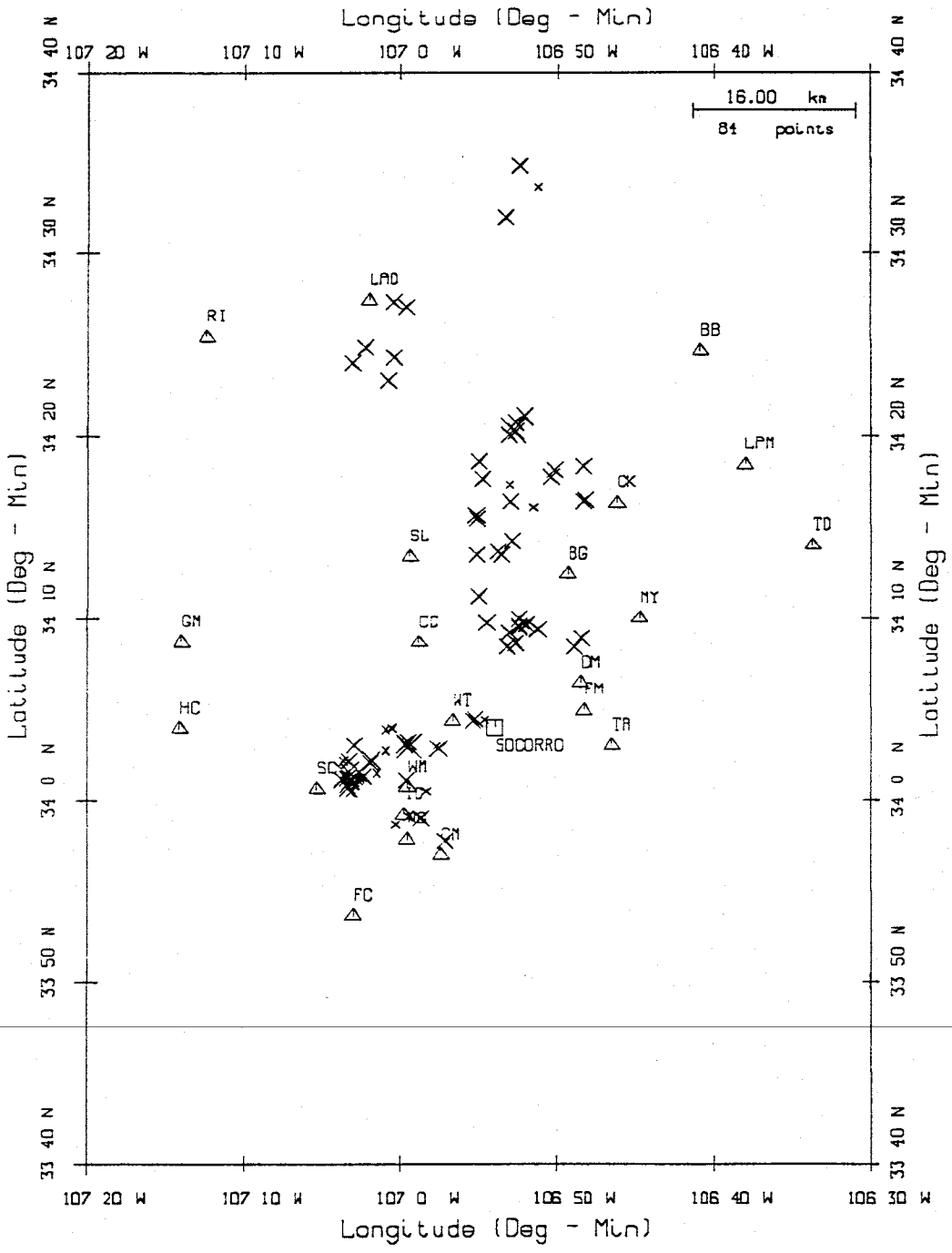

Figure 4.4. Epicenters (X's) of the 84 events used in my study. Also shown are the stations used to collect the data (△'s).

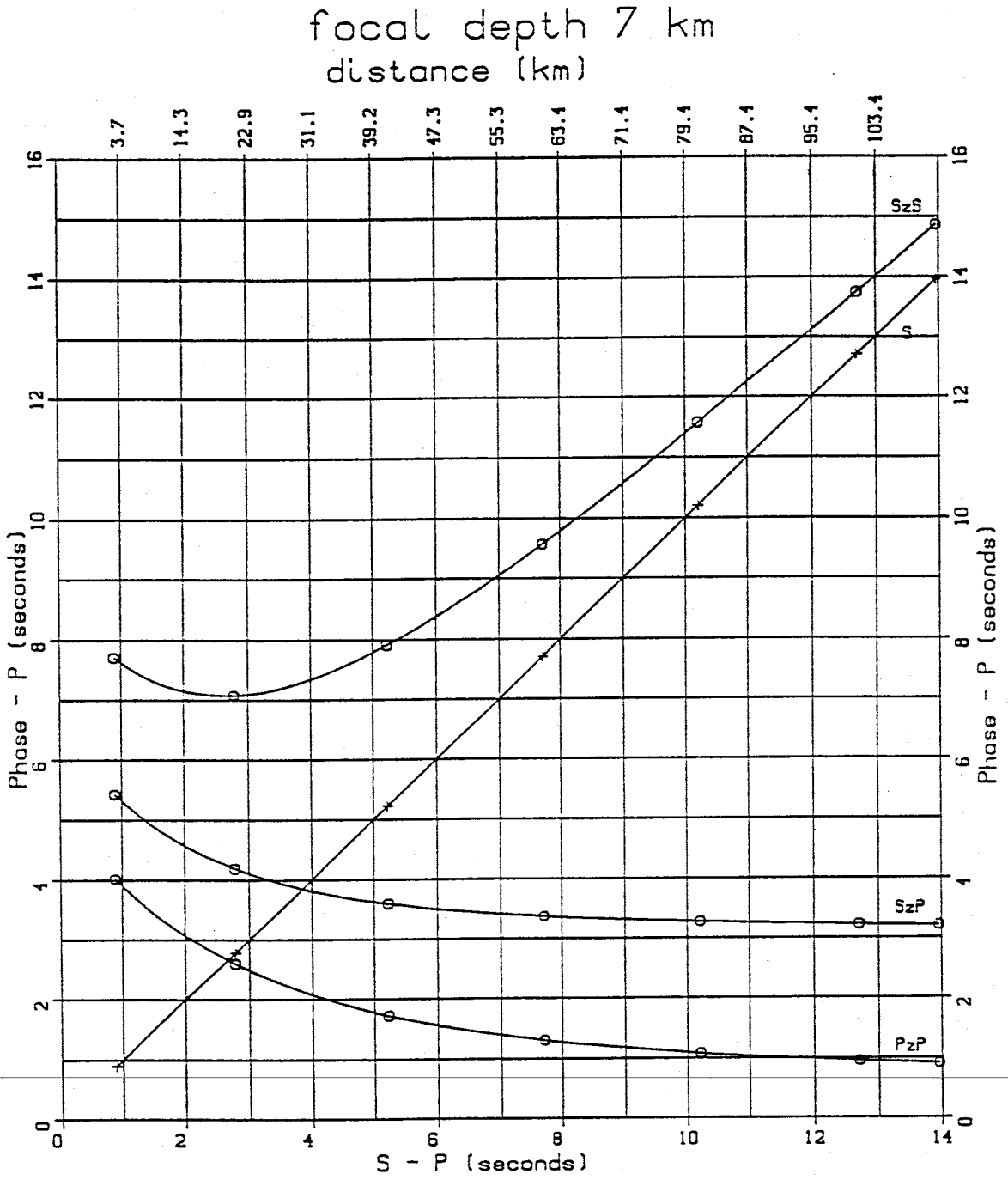

Figure 4.5. Sample travel-time curve used to identify phases used in this study (from *Hartse* [1991]).

in my study had a number of stations near to the epicenter, and thus P_zP and S_zP reflections could be obscured in the P or S codas or arrive shortly before the direct S. This required that a preliminary location be found using only direct arrivals and unambiguous reflected phases in order to constrain focal depth well enough to determine if the other observed phases were reflected or direct.

Three different methods of obtaining arrival times were employed in this study, corresponding to the three types of data used: The analog data recorded on smoked paper using the MEQ-800 portable seismic systems; the digital data recorded at 100 samples per second on the DR-100 portable digital recorders; and the analog data recorded on film by the telemetered USGS network near Albuquerque. In all three cases arrival times were carefully picked, and always double checked.

Timing of the smoked paper records was done on a light table using a magnifying eyepiece which contained a graticle with 0.1 millimeter gradations. Since the smoked paper drums revolve at 2 mm/s, 0.1 millimeters corresponds to 0.05 seconds. Picks were measured to within 0.05 millimeters, giving an idealized picking error of 0.025 seconds maximum. I accepted *Weider's* [1981] P picks since they were already corrected for clock drift, and only picked the later phases. Overall, a standard error for a clear, impulsive P pick was assumed to be 0.075 seconds, corresponding to a weight of 0. Weights of 1 through 4 were also applied by adding 0.075 s for each additional weight factor. A weight of 1 was applied if the arrival was impulsive without a recognizable direction of first motion - including secondary arrivals such as very high quality direct S, P_zP, S_zP, and S_zS picks. A weight of 2 was given for clear picks, a

weight of 3 for good picks, and a weight of 4 for poor picks.

The digital data recorded by the DR-100 portable recorders was picked using XPICK (University of Alaska) to extremely high accuracy. In keeping with the prior weighting scheme used for the smoked paper records I elected to use the same error estimates. An MEQ-800 was usually operated concurrently at the same station site as the DR-100 and provided more accurate absolute timing than the digital system. As such the digital data was used as more of a supplement to the analog data. Examples of Earthquakes similar to those used in this study and recorded digitally are found in Figures 4.6 and 4.7, and demonstrate all observed phases. Digital seismograms of some events used in this study are found in Appendix 2.

The data acquired from the Albuquerque Seismological Laboratory was recorded continuously on 16mm film with time marks every 10 seconds. A film reader was used to examine earthquakes, and picks were made using a scale with 1 millimeters gradations. The magnification of the reader produced a recording rate of 1 centimeter per second. Picks were made to the nearest 0.5 mm, and therefore a very good impulsive first motion would have a picking error of 0.05 seconds. Considering clock drift, which was corrected once per day, I again used a weight factor of 0.075 seconds for a quality 0 pick.

An important concern about combining data from two networks operated by different groups is the possibility of clock differences leading to relative timing errors. Fortunately, station WT was periodically recorded on paper in Socorro and telemetered to Albuquerque and recorded on film. Comparison of seismograms and clock times between the two recordings indicated no discernible differences in absolute timing of first arrivals.

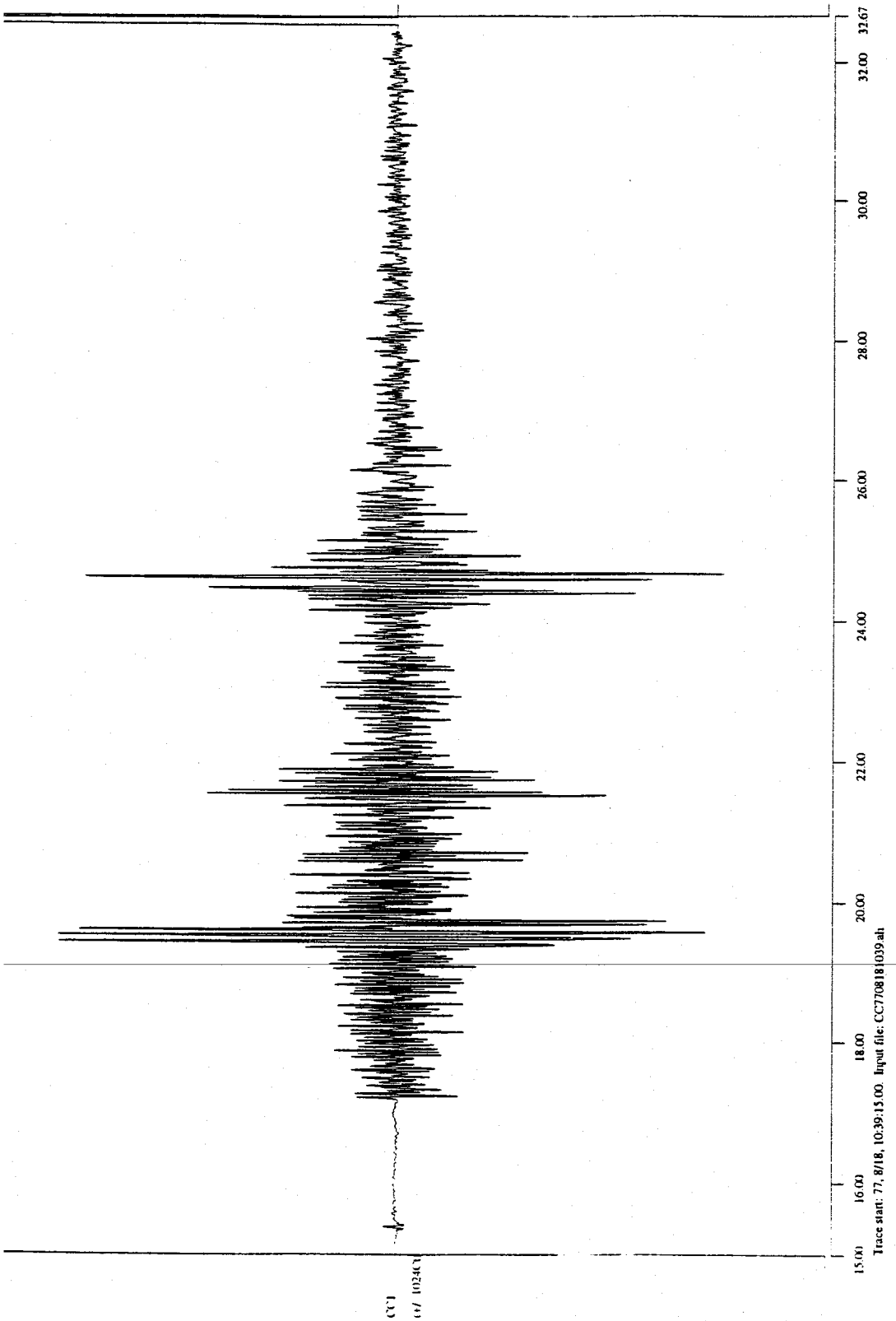

Figure 4.6. Digital seismogram showing Socorro reflected phases. This event was recorded at station CC (Corkscrew Canyon) at 10:39 (UT) on August 18, 1977. Phases in order of arrival are P, S, S_zP, and S_zS. Note the high amplitude of the reflected phases with respect to direct P and S.

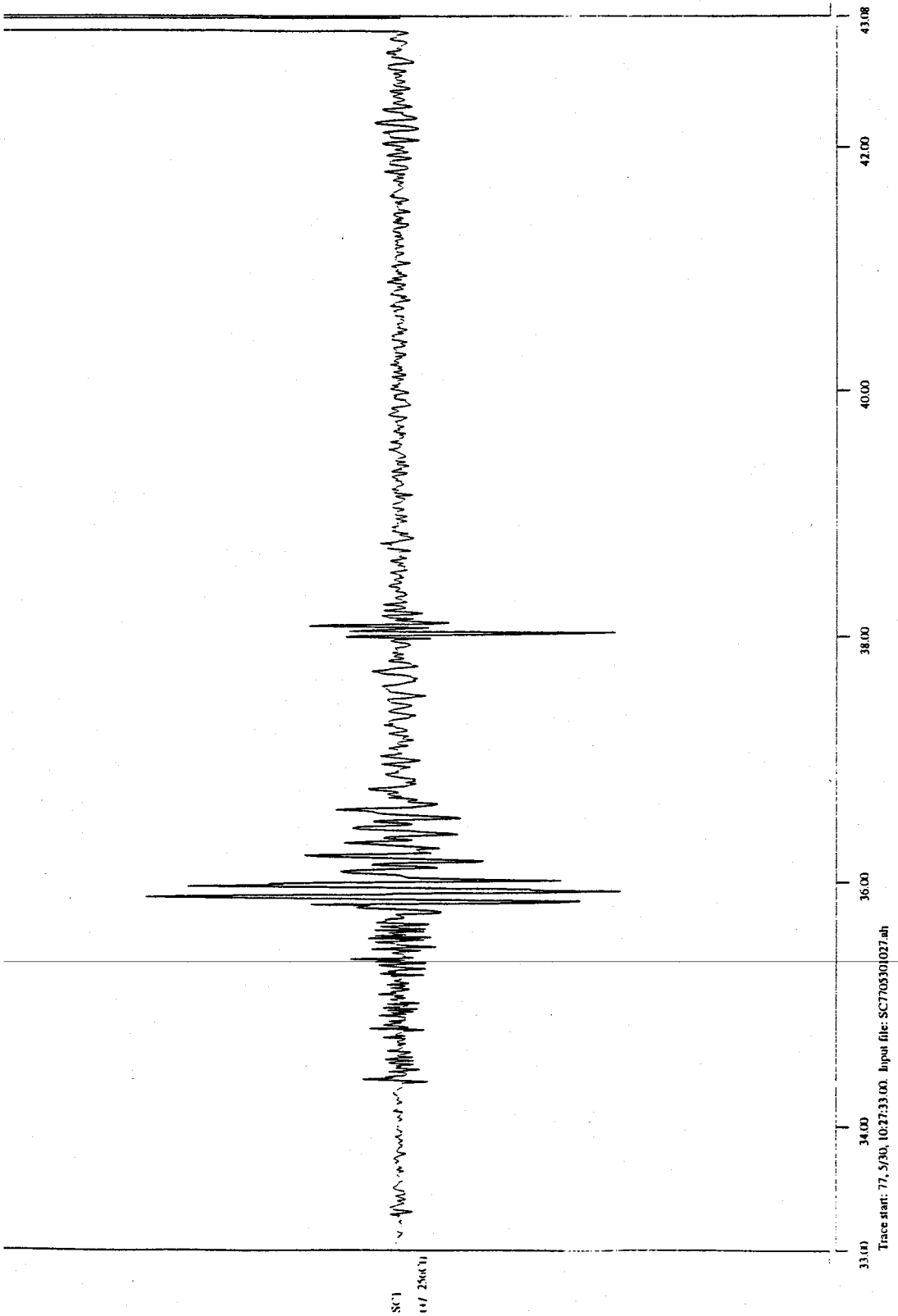

Figure 4.7. Digital seismogram showing Socorro reflected phases. This event was recorded at station SC (South Canyon) at 10:27 (UT) on May 30, 1977. Phases in order of arrival are P, S, P_zP, and S_zS.

Phases

Socorro area microearthquake seismograms typically exhibit five phases - direct P and S, and P_zP, S_zP, and S_zS phases reflected from the magma body surface, although not all phases are likely to be observed on the seismogram for a single station, particularly the reflected phases. A schematic diagram showing the crustal model of *Hartse* [1991] and sample raypaths of phases used in this study is given in Figure 4.8. The frequency of occurrence and characteristics of each phase is discussed in the next two sections.

Direct Phases

Microearthquakes recorded on the Socorro network generally have both direct P and S arrivals. The P arrival is usually very sharp with clear first motions. The direct P phase gives information on V_p from the base of the seismogenic zone to the surface and contributes to hypocenter estimation and Poissons ratio calculations. Since the direct P is the best recorded phase it also heavily influences station corrections. Out of a total of 579 P picks (Table 4.7) 466 were given a weight of 0 and 84 were given a weight of 1.

The direct S phase is often recognizable on Socorro area seismograms. The data taken from the smoked paper records had unusually clear S phases, due to the quiet station sites and 2 mm/s recording rate. The use of low magnitude events also contributes to the large number of S phases observed, since the P coda is relatively short. Of the 489 direct S phases used in this study (Table 4.7), 76 picks received a weight of 1, 287 picks were given a weight of 2, and 120 had a weight of 3. The direct S phase (with matching P) contributes to Poissons ratio and origin time estimates, as well as focal depth determination when a near station (within 1.5 times the

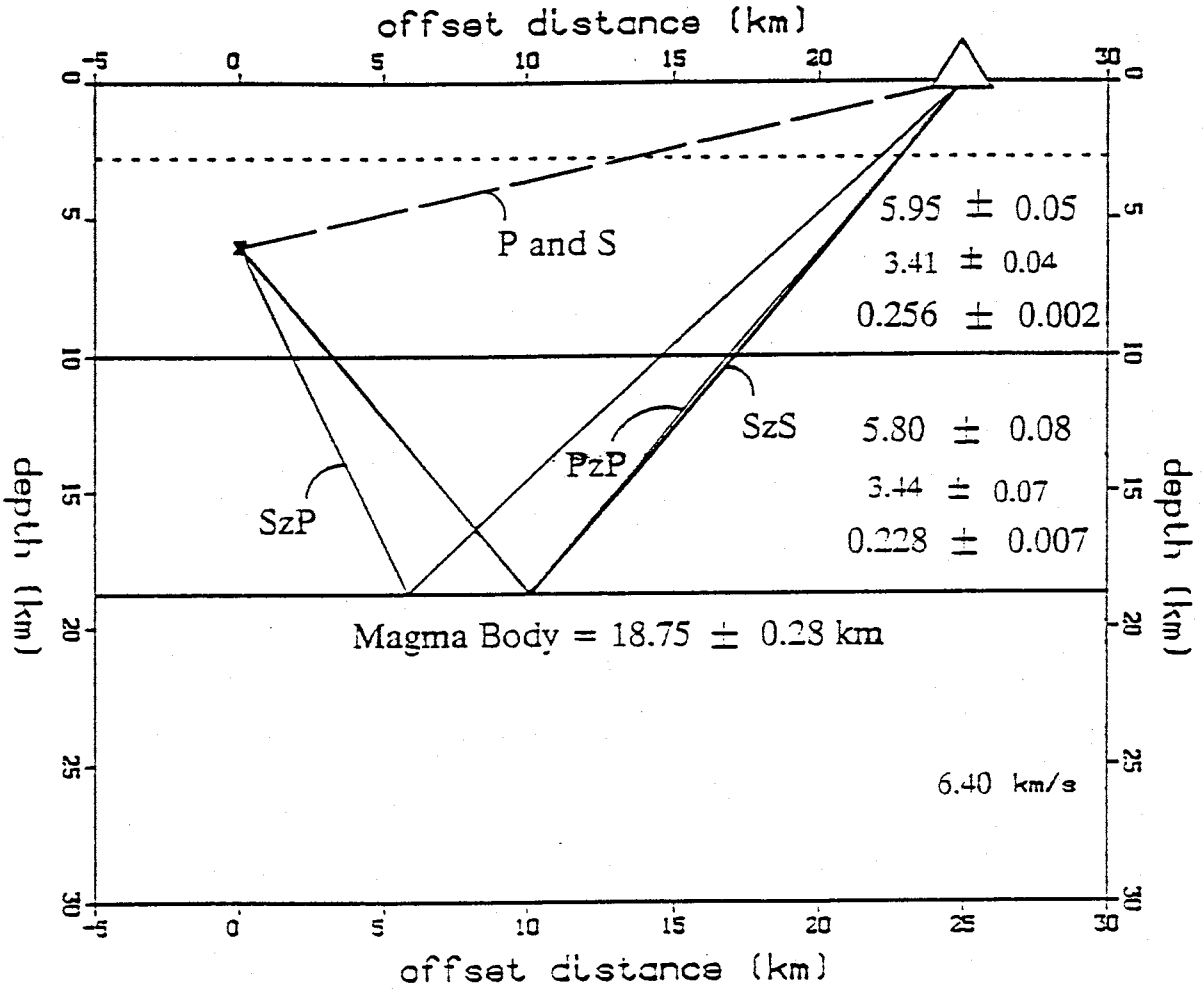

Figure 4.8. Sample raypaths for an event at 6km depth, recorded at a station 25 km from the epicenter. The crustal model is the two layer inversion result from *Hartse* [1991], the model parameters for each layer are in descending order V_p, V_s, and ν.

Table 4.7 Phase and Weight Summary					
Weight	P	S	P_zP	S_zP	S_zS
0	**466**	0	0	0	0
1	84	76	2	18	5
2	28	**287**	**63**	**102**	122
3	1	120	20	59	**202**
4	0	6	0	5	23
Totals	579	489	85	183	352

The weight factors are measured in units of 0.075 secs, with a weight of 0 being equal to 1 unit. Therefore a weight of 1 would be two units (0.150 seconds) and so on up to a weight of four (5 units).

focal depth) is used in the location process [*Gomberg et al*, 1989].

Reflected Phases

Information below the seismogenic zone down to the magma body is provided by the reflected phases (Figure 4.8). Information gained from these phases include estimates of Poissons ratio, reflector depth, hypocenter depths, and V_P beneath the seismogenic zone. As can be seen in Figures 4.5 and 4.6 the amplitude of reflected phases on vertical-component seismograms are often quite large with respect to direct P and S values. *Sanford et al.* [1973] concluded that this may require asymmetric radiation of energy from the foci, as well as magma at full melt at the upper surface of the magma body.

For the data set used by *Hartse* [1991] the S_zP and S_zS reflections were observed about equally as often. I found that S_zS reflections were observed almost twice as often as S_zP reflections (Table 4.7). I agreed with Hartse's observation that the quality of the S_zP reflection is generally greater than that of the S_zS. This is likely due to the vertical component instruments used in Socorro network stations. The S_zS phase always arrives last, which eases identification. The S_zP reflection is sometimes difficult to identify because the S phase coda can obscure it. The P_zP phase is the least often observed reflection from the magma body, and generally is of low amplitude. P wave reflections are weak because the P phase is much weaker than the S phase and the P energy can transmit through the magma body, or even set up destructive interference by reflecting off both the upper and lower surfaces of the magma body. The P_zP phase is thus difficult to pick in events with strong direct P and S codas.

Observations

The distribution of data for the various stations is found in Table 4.8. From examination of this table it is apparent that the largest numbers of arrivals are recorded at stations CC, WT, SC, GM, BG, LPM, LAD, DM, CM, and ALQ. Stations which were operated more or less continuously throughout the study period were CC, CM, WT, SC, and GM for the Socorro network, and LPM, LAD, MLM, and ALQ for the Albuquerque Seismological Laboratorynetwork.

All stations except ALQ had observed reflections, though the number and types varied greatly. Reflections have been observed at ALQ but not for any events used in this study. For the events selected for my study, stations CC, WT, BG, and SC nearly always had reflections, perhaps due to the central location of these stations over the magma body. Reflections recorded at station CM (located to the south) were generally not as clear as for the above stations.

The Albuquerque Seismological Laboratory (ASL) station MLM, was the farthest station to the northwest, and recorded few reflections - mainly because the earthquakes recorded at MLM tended to be very emergent. ASL station LAD recorded S_zS reflections on the majority of events and a respectable number of S_zP and P_zP reflections.

Comparison to Other Data Sets

The number of direct and reflected arrivals used in earlier studies in the Socorro area are listed in Table 4.9. The important data sets to compare with mine are those of *Rinehart* [1979, 1981] and *Hartse* [1991]. In my study I use the method, and inversion program **SEISMOS** written by Hartse, in order to make use of all Socorro reflected phases. The study done by Hartse was the first to use all of the reflected phases in inversions for crustal models.

Table 4.8 Station and Phase Data						
Station	P	S	P_zP	S_zP	S_zS	Total
ALQ	24	0	0	0	0	**24**
BB	5	4	0	2	2	**13**
BG	35	30	4	12	29	**110**
CC	64	60	20	38	56	**238**
CK	6	5	1	4	4	**20**
CM	46	39	4	18	11	**108**
DM	28	23	5	5	8	**69**
FC	6	6	1	0	3	**16**
FM	14	9	1	2	4	**30**
GM	43	41	5	5	22	**116**
HC	10	10	3	3	6	**32**
IC	11	10	2	7	10	**40**
LAD	51	44	10	17	34	**156**
LPM	41	37	1	7	19	**105**
MLM	17	15	0	3	3	**38**
MY	4	3	0	2	0	**9**
NG	17	17	3	7	14	**58**
RI	11	9	1	3	10	**34**
SC	61	54	11	20	52	**198**
SL	7	7	2	4	7	**27**
TA	6	4	0	1	3	**14**
TD	11	9	3	1	7	**31**
WM	6	5	3	4	5	**23**
WT	55	48	5	28	43	**179**

Table 4.9 Comparison of Data Sets

Investigator	Purpose	Data	Quantity
Rinehart et al. (1979)	Map the magma body	S_zS	200
Rinehart and Sanford (1981)	V_s to the magma body, magma body depth	S_zS	~250
Ward et al. (1981)	V_p in seismogenic zone, and hypocenters	P	262
Hartse (1991)	V_p, ν, depth to magma body, and hypocenters	P, S, P_zP, S_zP, and S_zS	564, 485, 77, 160, and 169 (1455 total)
Present study	V_p, ν, depth to magma body, and hypocenters	P, S, P_zP, S_zP, and S_zS	579, 489, 85, 183, and 352 (1688 total)

In comparing the three relevant data sets, both Hartse and I have better epicenter distribution than *Rinehart* [1979]. Hartse's study has better coverage of the southern end of the magma body than either Rinehart's or my study, primarily due to array geometry. Neither Hartse or Rinehart cover the northern end of the magma body very well. With the addition of data from the ASL network, mapping of the northern extent of the magma body was possible in my study.

In general I have nearly as wide a range of epicenters as *Hartse*, though the array geometries of the temporary network leaves less of an even distribution of reflected phases. Both of the data sets have a prominent seismic gap immediately northwest of Socorro. Figures 4.9 and 4.10 show the epicenters and reflection points used by *Rinehart* [1979, 1981]; Figures 4.11 and 4.12 are the epicenters and reflection points used by *Hartse* [1991]; Figures 4.4 and 4.13 are the epicenters and reflections used in my study.

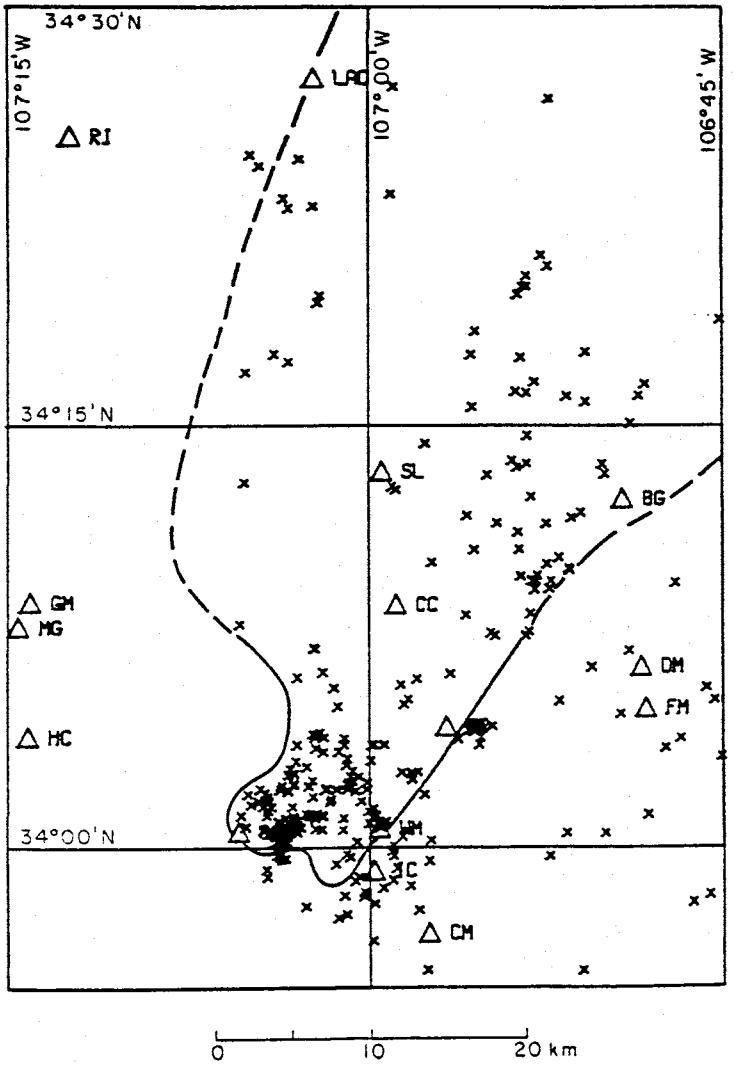

Figure 4.9. Microearthquake epicenters from *Rinehart* [1979]. Also plotted are Socorro portable network recording sites (△'s) and the magma body outline estimated by Rinehart.

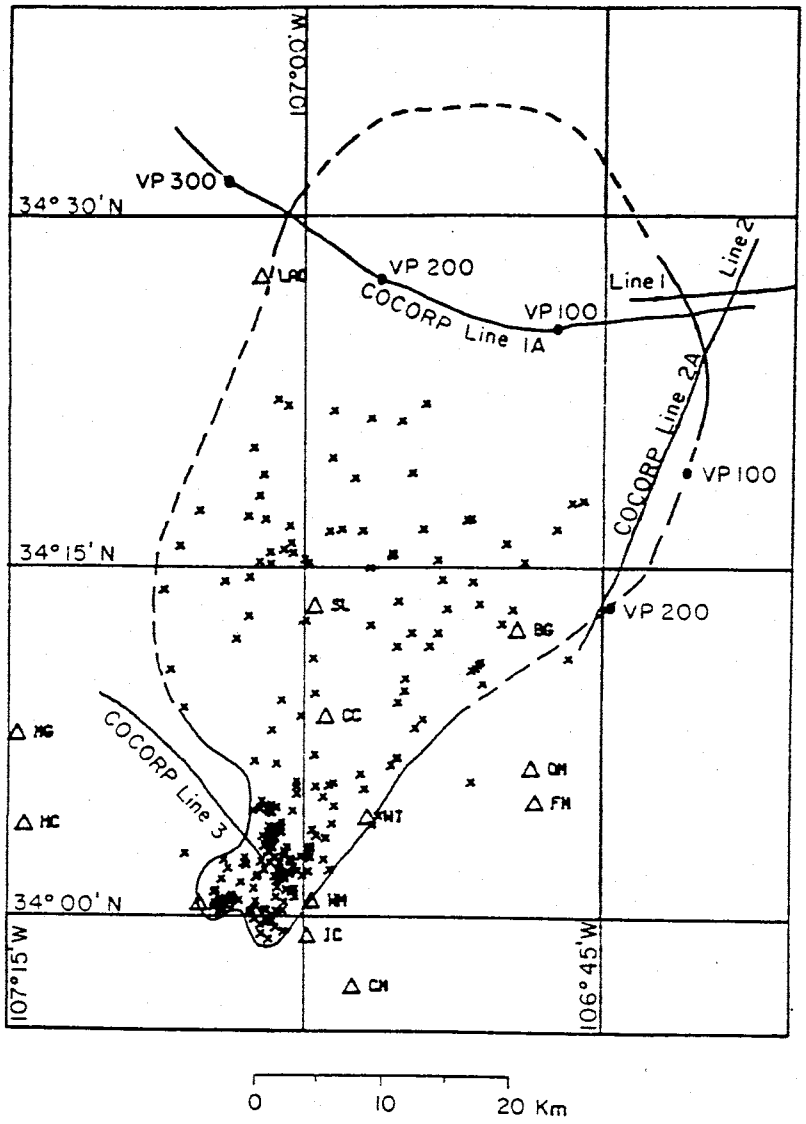

Figure 4.10. Observed reflection point map from *Rinehart et al.* [1979]. Also shown are the COCORP lines used to constrain portions of the magma body's extent. Solid boundaries indicate actual extent, dashed boundaries represent minimum extent.

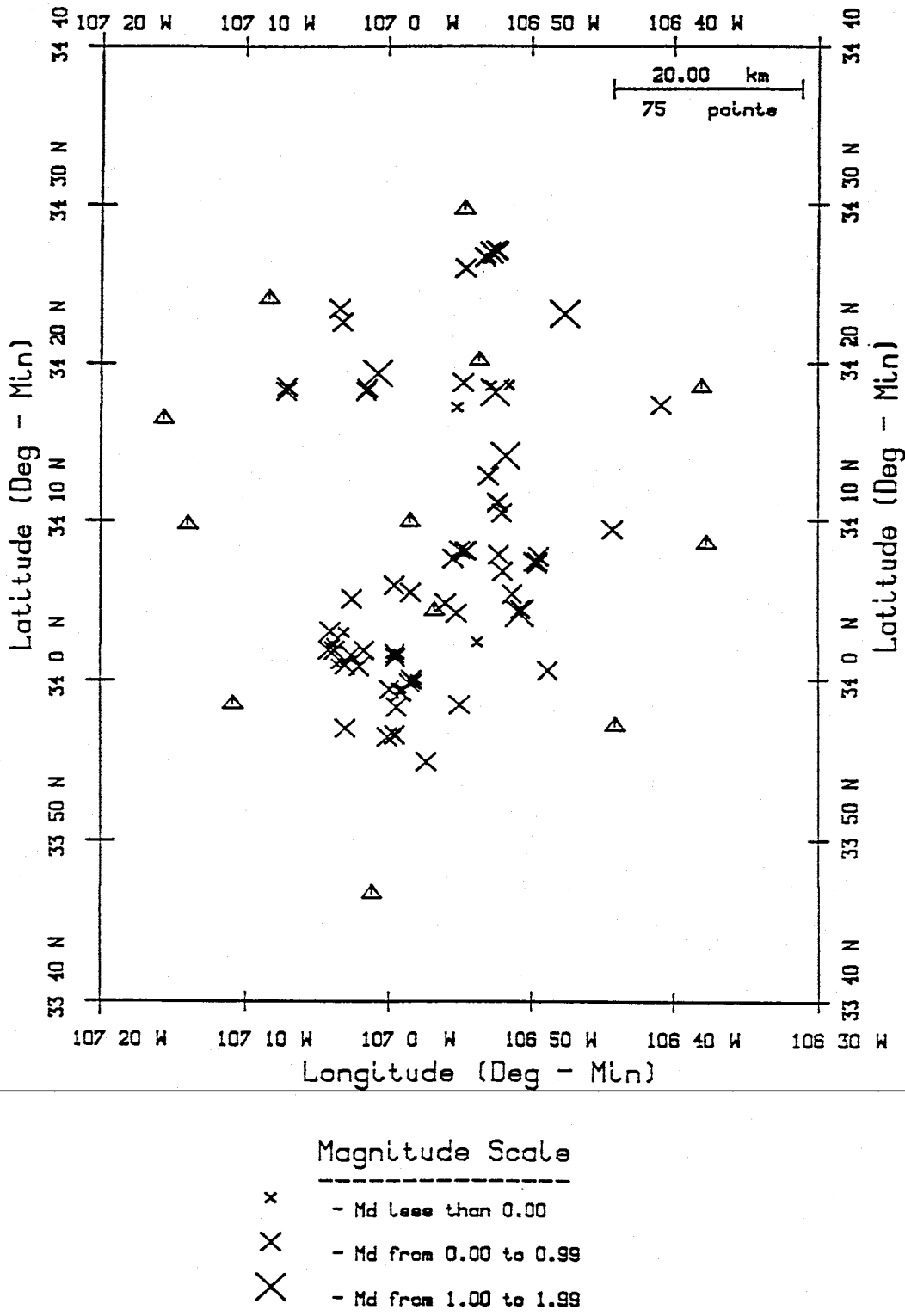

Figure 4.11. Epicenters of the 75 events (X's) used by *Hartse* [1991]. The stations used to collect the data are represented by $\triangle$'s.

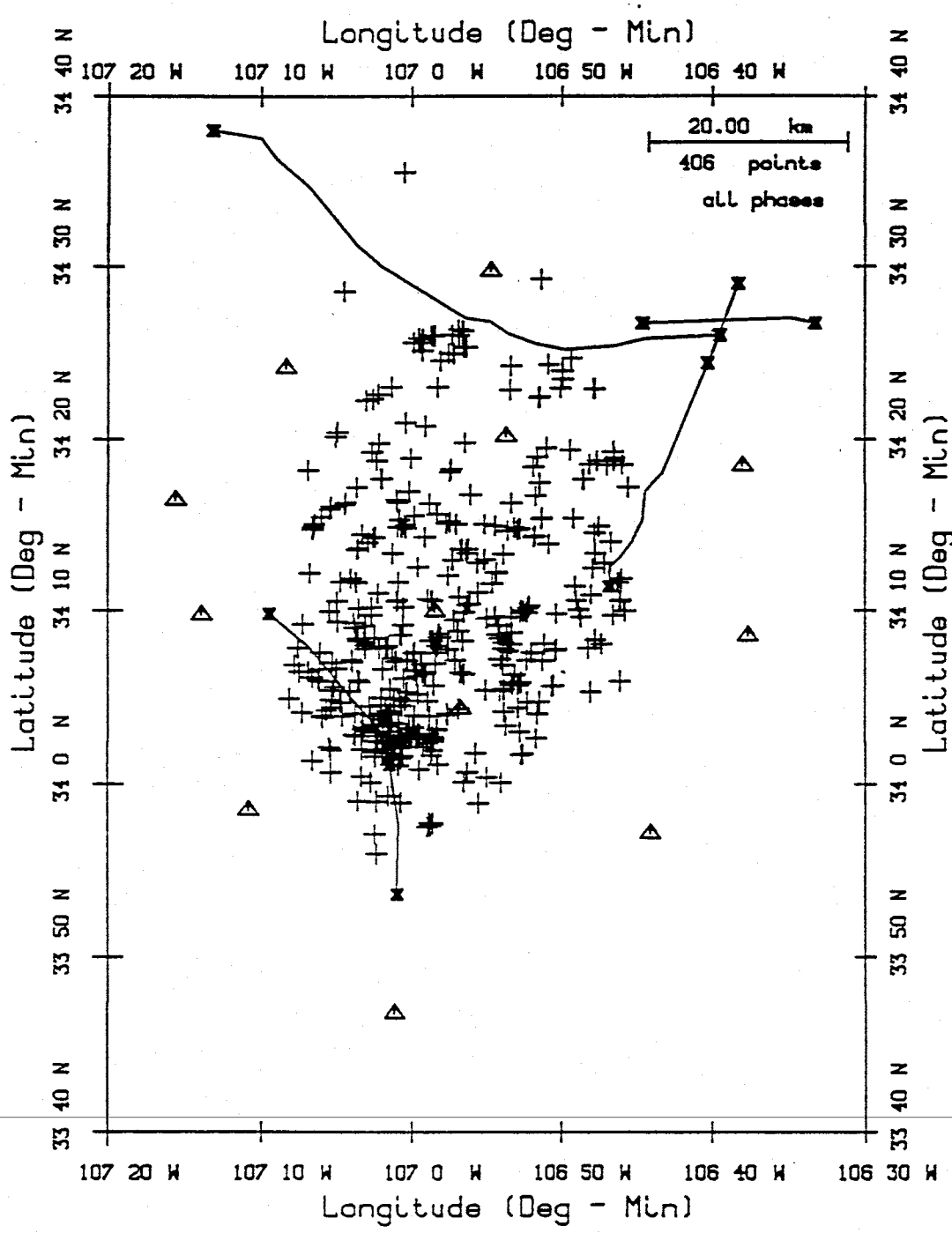

Figure 4.12. Observed reflection point map (from *Hartse* [1991]. Also shown are the COCORP lines in the Socorro area.

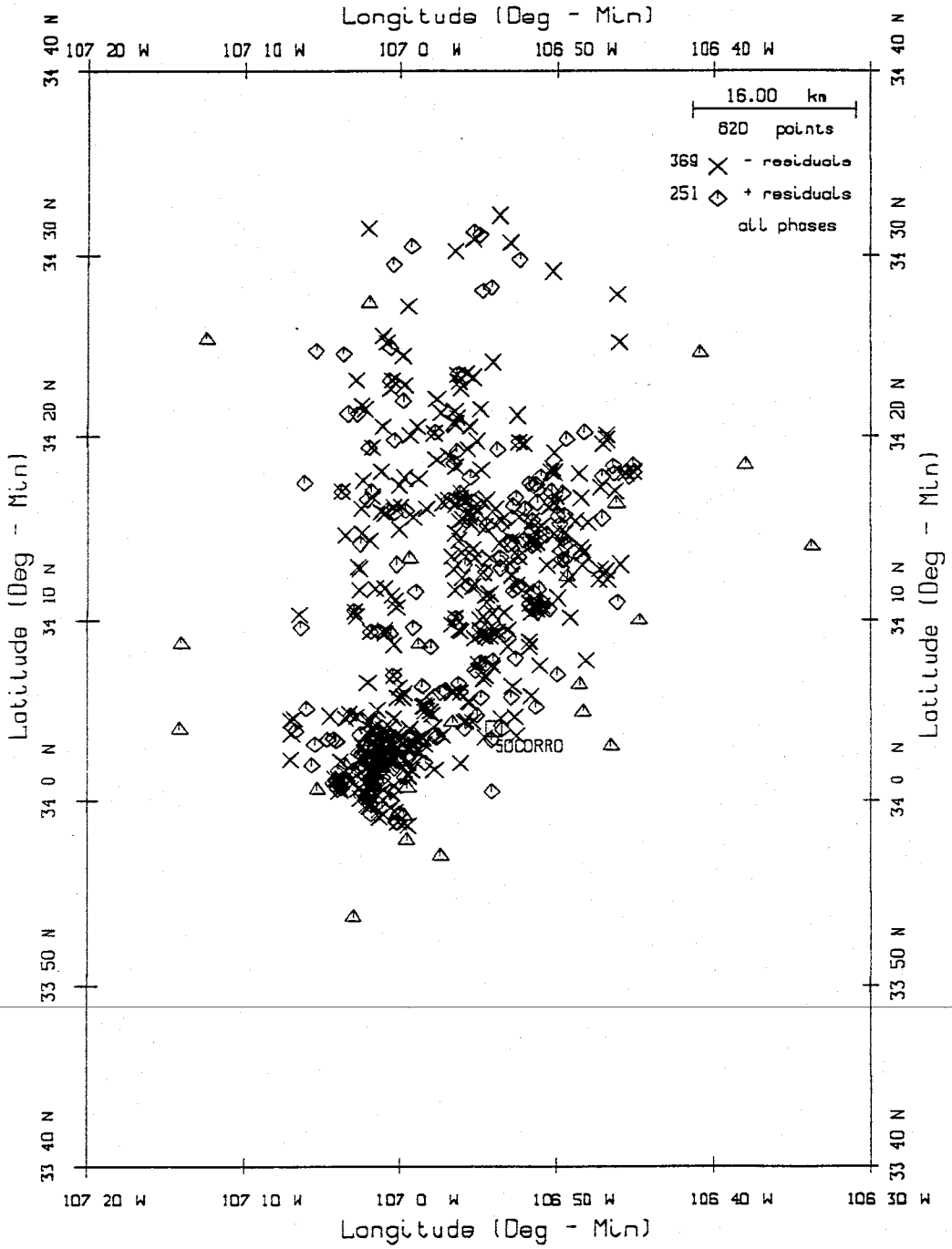

Figure 4.13. Observed reflection point map from the 84 events used in my study. The x's represent reflection points with negative residuals, ◇'s are reflection points with positive residuals. Also shown are the stations used to collect the data (△'s).

5. Analysis and Results

Overview

After selecting the 84 event data set, I inverted for a single layer crustal model. In the inversion, velocity and Poisson's ratio above the magma body, magma body depth, and the four hypocenter parameters (latitude, longitude, depth, and origin time) for each event were treated as unknowns. For the 84 events in this data set there were 336 unknown hypocenter parameters, one velocity, one Poisson's ratio, and one reflector depth; a total of 339 unknowns. The 84 events included 1688 arrival times; 579 direct P, 489 direct S, 85 P_zP, 183 S_zP, and 352 S_zS phases.

Station corrections were obtained by holding the best average model for the Socorro area constant, while jointly inverting for hypocenters and station corrections. The average model used was the single layer model of *Hartse* [1991]. The correction for station WT was held at -0.08 for the inversion, since this is considered the "standard" correction. WT had the same location as WTX used in Hartse's study, which was held at -0.08 during his crustal inversions. The use of this "standard" correction allowed direct comparison of station corrections between studies. The calculated station corrections are listed in Table 5.1.

I followed the method of *Hartse* [1991], in setting up the initial conditions for the inversion. Each station correction had an initial starting value of 0.0 seconds, V_p was set to 6.0 km/s, Poisson's ratio was set to 0.25, and the initial reflector depth was 20.0 km. Station corrections were calculated in a separate inversion in the manner described above. Then hypocenters were calculated holding the station corrections and initial velocity model constant. Last, I

Table 5.1: Final station corrections			
Station	Correction	Error (1 std)	r matrix diag
ALQ	-0.400	0.043	1.000
BB	+0.118	0.050	1.000
BG	+0.007	0.022	1.000
CC	-0.155	0.017	1.000
CK	+0.010	0.045	1.000
CM	+0.081	0.020	1.000
DM	+0.020	0.020	1.000
FC	+0.145	0.041	1.000
FM	-0.006	0.032	1.000
GM	-0.072	0.022	1.000
HC	+0.050	0.034	1.000
IC	+0.025	0.028	1.000
LAD	-0.202	0.026	1.000
LPM	-0.111	0.026	1.000
MLM	-0.136	0.047	1.000
MY	-0.096	0.051	1.000
NG	+0.015	0.025	1.000
RI	+0.090	0.040	1.000
SC	+0.144	0.019	1.000
SL	-0.123	0.040	1.000
TA	-0.013	0.039	1.000
TD	-0.209	0.037	1.000
WM	+0.121	0.037	1.000
WT	-0.080	*	*
General iteration results			
R = 0.956		rms = 0.209	

inverted simultaneously for the crustal model and hypocenters, with only the station corrections held constant.

The inversion produced reasonable values for all unknown parameters. All eigenvalues were kept, and the inversion solved for all parameters within three iterations. Attempts to include station corrections in the crustal inversions resulted in non-convergence, or convergence to unrealistic crustal models. The inversion used the algorithm **SEISMOS**, a complete description of the program can be found in *Hartse* [1991].

The One Layer Model

Using the method discussed, I inverted for a single layer crustal model. The model inversion converged to a unique solution, since all of the resolution matrix diagonal elements were 1.0, and no eigenvalues were lost. Therefore, each model parameter is independent of the initial model. The final model computed is presented in Table 5.2. Since the overall R value for the inversion is less than 1.0 (Table 5.3), the data is presumed to have been assigned accurate timing errors. Therefore the errors at one standard deviation are considered to be reliable estimates of the crustal model uncertainties.

Two layer velocity model inversions, such as those done by *Hartse* [1991], were attempted. In all cases, the inversion failed to converge, or converged to unrealistic values. Even when station corrections were held constant the crustal model inversions led to unrealistic solutions. It is beyond the scope of this study to diagnose the reason(s) for these results, though I will make two observations: 1) Often a trade off between station corrections and the magnitude of layer velocities, and/or depth to the reflector was observed; and 2) the ASL stations MLM and ALQ are located above a different crustal

Table 5.2 One Layer Crustal Model Inversion Results			
Parameter	Result	1 std.	r matrix diag.
V_p	5.861 km/s	0.032	1.000
ν	0.243	0.002	1.000
Depth	19.255 km	0.111	1.000

Table 5.3 Inversion Diagnostics		
Arrivals	R Value	rms Value
Direct	0.881	0.152
Reflected	1.017	0.267
Combined	0.933	0.202

structure than the Socorro network. In my study I used 38 picks from MLM and 24 picks from ALQ whereas Hartse used 12 arrival time picks for station MLM and did not use station ALQ.

Magma Body Dip

Since one of the primary assumptions of SEISMOS is flat-layers, it is necessary to check for dip on the reflector because it will affect the validity of inversion results and hypocenter estimates. *Hartse* [1991] performed such checks on his results, and I did also because of the importance of the question.

Several characteristics of my data set make a check for dip relatively conclusive. First, the epicenters (Figure 5.1) and the observed reflected phases (Figure 5.2) are well distributed over the study area. Second, each event has between 2 and 14 reflections recorded at 2 to 8 stations. Therefore the reflections for a given earthquake tend to sample a wide area of the magma body surface.

Overall dip to the north would give increasing large positive residuals to the north, and it is unlikely that the R value would remain below 1.0 in that case. This argument does not rule out possible undulations in the magma body surface however. Examination of reflection point residuals demonstrate an overall flatness for the magma body. Figure 5.3 shows the position of the 369 negative residuals associated with the reflected phases for the 84 events in my data set. Figure 5.4 presents the 251 positive residuals associated with the same data. Positive and negative residuals have about the same geographic distributions, a most unlikely observation if there was significant dip. The same patterns are observed for the negative and positive residuals which exceed assumed picking errors (Figures 5.5 and 5.6).

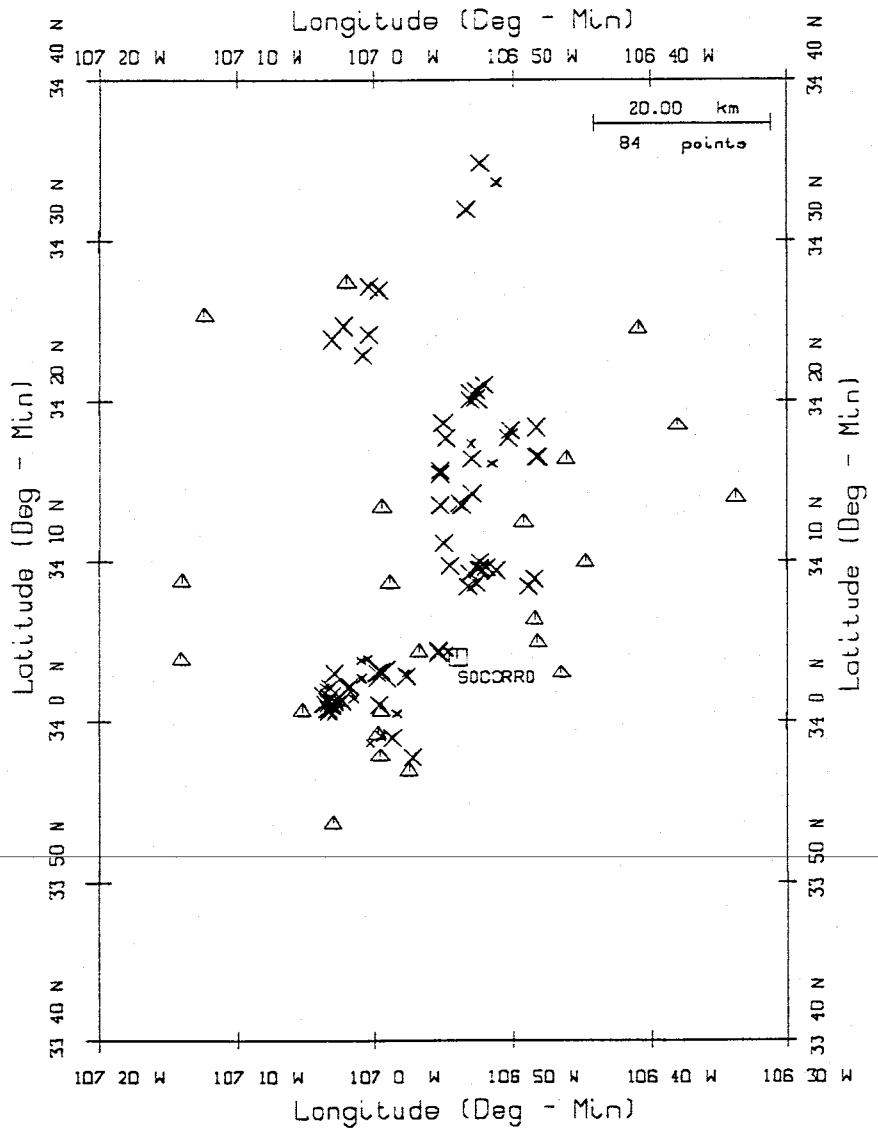

Figure 5.1. Epicenters (X's) of the 84 events used in my study. Also shown are the stations used to collect the data (Δ's).

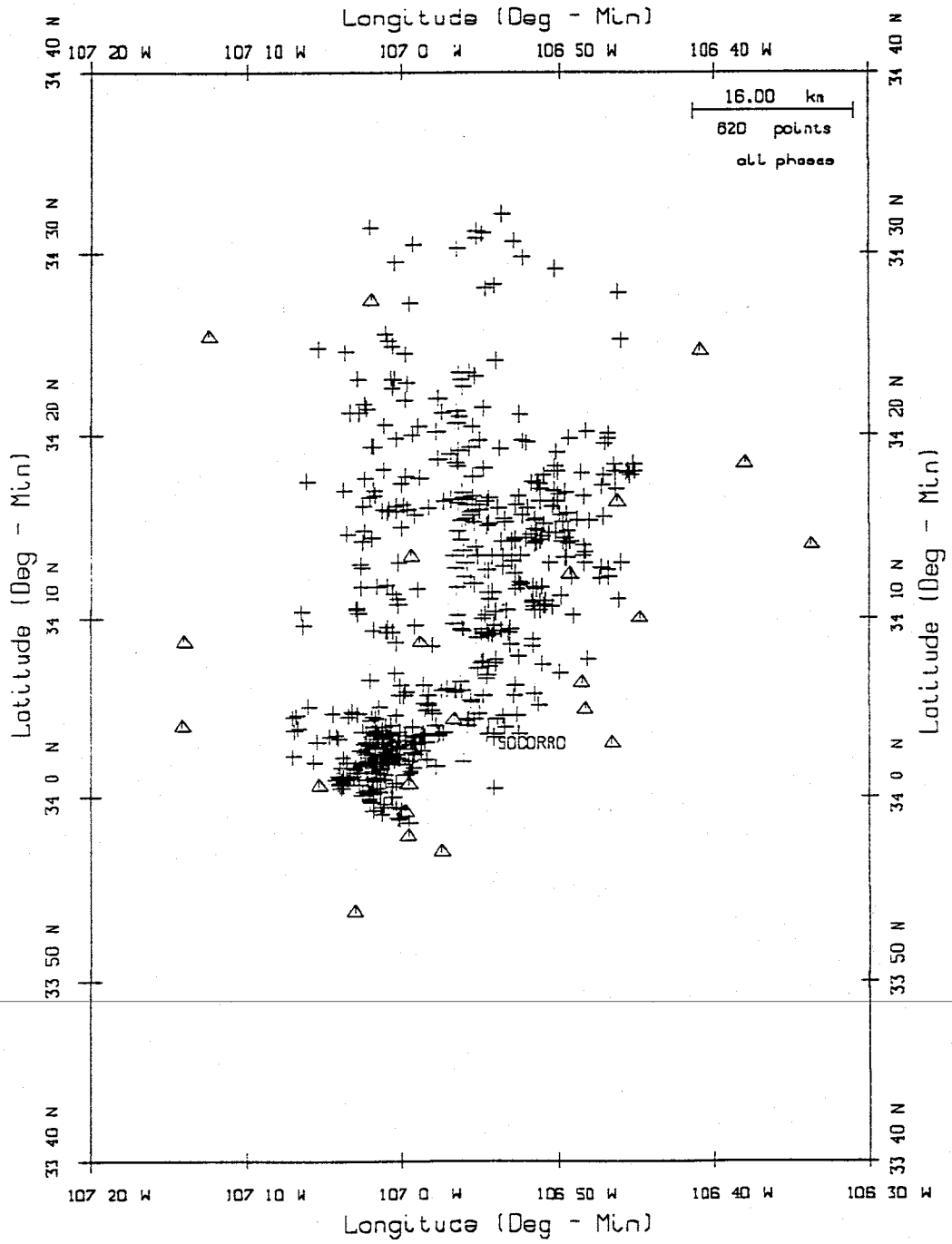

Figure 5.2. Observed reflection point map from the 84 events used in my study (+'s). Also shown are the stations used to collect the data (△'s).

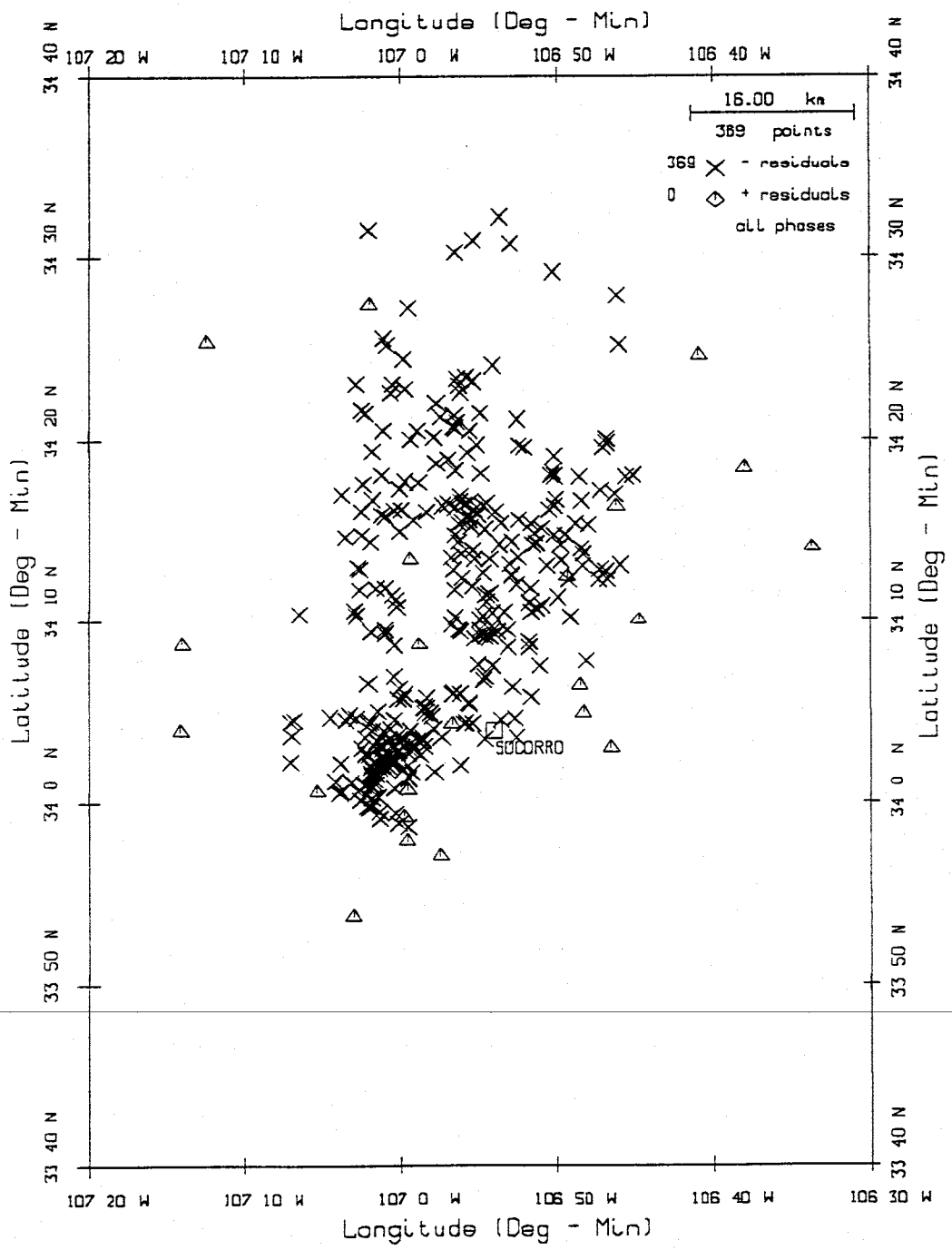

Figure 5.3. Observed reflections with negative residuals. Note the even distribution of residuals over the entire region. Also shown are th stations used to record the data (△'s).

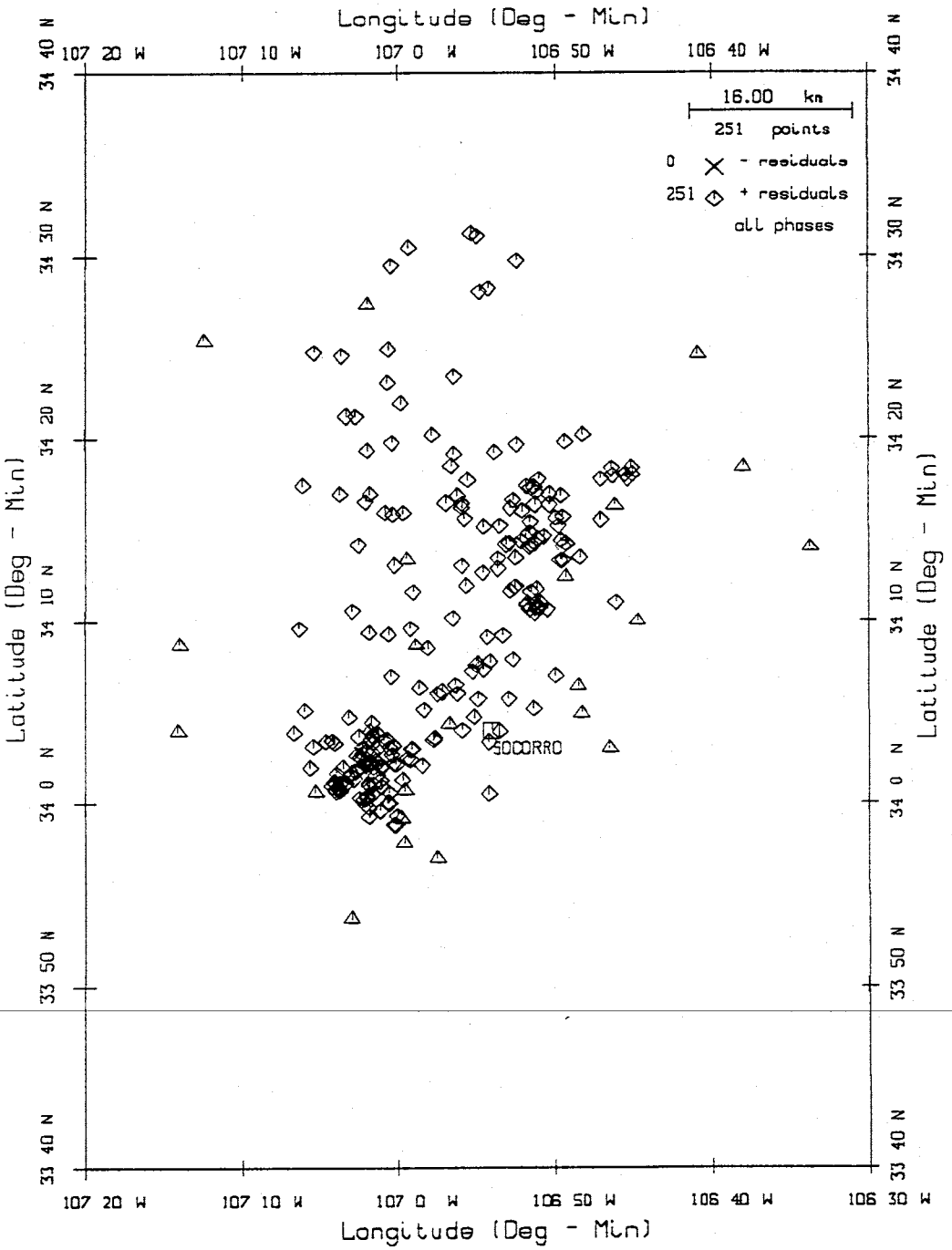

Figure 5.4. Observed reflections with positive residuals. Note the even distribution of residuals over the entire region. Also shown are the stations used to collect the data (Δ's).

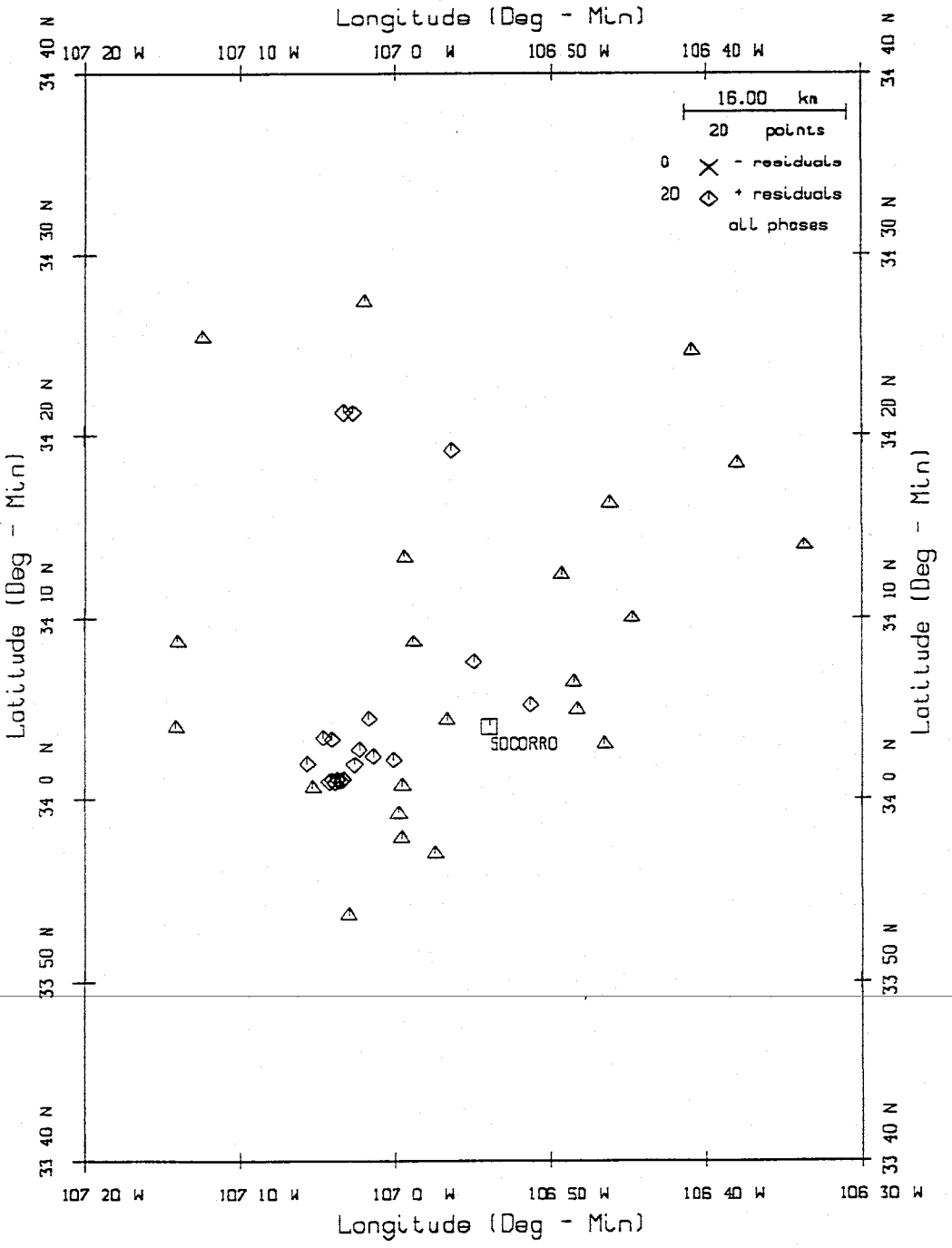

Figure 5.5. Observed reflections with positive residuals that exceed assumed timing error. The even distribution of these residuals is indicative of no progressive dip on the magma body surface. Also shown are the stations used to collect the data ($\triangle$'s).

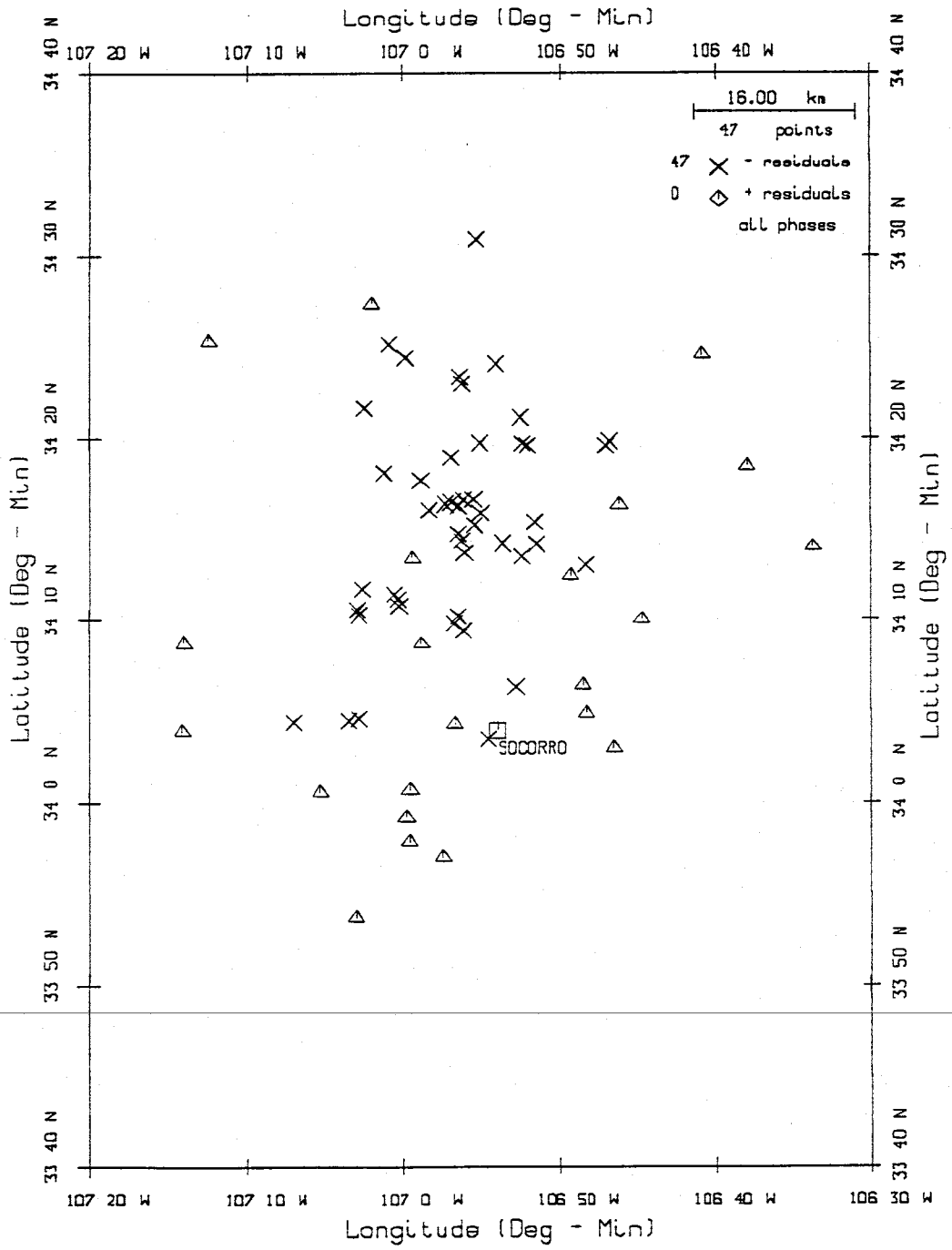

Figure 5.6. Observed reflections with negative residuals that exceed assumed timing error. The even distribution of these residuals is indicative of no progressive dip on the magma body surface. Also shown are the stations used to collect the data (Δ's).

Hypocenters

Table 5.4 lists the origin time and locations for the 84 hypocenters used in this study. Table 5.5 summarizes the statistical differences between the "all phase" and "direct only" hypocenters. Epicenter errors were approximately the same in both cases. Origin time errors were low with and without inclusion of reflections, but only about half as large with reflected phases. As expected the greatest reduction in error came in the focal depth when reflections were used. The average hypocenter depth error for the "all phase" hypocenters was 0.339, which is only about 25 percent of the average depth error using only direct phases.

Figure 5.7 shows the hypocenter depths with one standard deviation error bars for the case where all phases are used in the solution. Figure 5.8 gives the hypocenter depths with 1 standard deviation error bars, for the case where only direct arrivals are used. The average depth is nearly the same between the two sets, but the direct phase only solutions have many more extreme estimates (Figure 5.8). When only direct arrivals are used, the average error in hypocenter depth increases as depth decreases; with a "shallow" depth error average of 1.669 km, and a "deep event" depth error of 0.961 km. These averages are less than those found by *Hartse* [1991] in a similar analysis, primarily because of the tight array spacings for the data in my study. I nearly always had at least one near station, while Hartse seldom did. Hartse's average "deep event" depth error was 1.45 km, and the "shallow event" depth error was 2.40 km - for the case of direct arrivals only.

When reflected phases are used (Figure 5.7), the depth errors for deep and shallow hypocenters are similar because of the influence of the reflections on constraining focal depths. The errors obtained in my study were 0.291 km

Table 5.4 Hypocenters From Crustal Model Inversion

N event	Time YYMMDD HHMM SEC	Latitude deg min	Longitude deg min	Depth km	M_d
1	750724 1850 19.94	34 14.21	106 52.92	05.39	+0.81
2	750805 1419 22.46	34 01.29	107 02.50	09.48	-0.27
3	750813 0338 51.22	34 04.45	106 55.33	07.76	+0.83
4	750813 0739 18.56	34 04.33	106 55.44	07.83	+0.04
5	750813 1122 26.72	34 00.53	106 58.38	10.34	-0.12
6	750819 0811 46.82	34 03.00	106 57.75	09.57	-0.28
7	750820 1220 52.22	34 04.41	106 54.65	07.89	-0.07
8	750820 0344 48.80	34 01.36	107 02.33	08.79	+0.77
9	750821 1918 42.10	34 02.85	106 57.64	10.03	+0.27
10	751104 1630 11.90	34 02.19	107 03.63	08.71	-0.11
11	760122 1216 08.69	34 24.78	107 02.27	05.21	+0.50
12	760123 0253 33.03	34 02.07	107 01.92	09.07	+0.24
13	760127 0904 17.77	34 08.93	106 48.49	10.50	+0.29
14	760129 1506 40.13	33 59.05	106 58.68	07.84	+0.87
15	760206 0920 57.28	34 22.96	107 00.82	06.75	+0.05
16	760219 0008 36.95	34 01.07	107 03.15	09.23	+0.15
17	760220 1251 45.36	34 01.20	107 02.61	09.55	-0.44
18	760323 1253 19.93	34 18.14	106 50.19	05.89	+0.77
19	760413 0945 40.87	34 03.98	107 00.52	07.66	-0.36
20	760414 0150 28.79	33 58.72	107 00.30	10.58	-0.62
21	760415 1155 20.14	34 03.88	107 00.96	07.14	-0.62
22	760129 1506 40.13	33 59.05	106 58.68	07.84	+0.87
23	760421 1116 19.78	34 17.75	106 50.39	06.93	+0.65
24	760609 1742 21.53	34 27.02	106 59.67	07.43	+0.12

The hypocenter locations as solved for in the 1 layer inversion. These locations use the following crustal model: V_p = 5.86 km/s; ν = 0.243; and depth to the reflector Z = 19.26 km. Table 5.4 is continued on the next two pages.

Table 5.4 Continued

N event	Time YYMMDD HHMM SEC	Latitude deg min	Longitude deg min	Depth km	M_d
25	760715 1058 34.33	34 01.45	107 03.59	09.63	-0.40
26	760803 0710 16.33	34 27.24	107 00.45	05.36	+0.56
27	760810 1228 41.97	34 03.18	106 59.52	09.89	+0.20
28	760811 0315 19.39	34 08.47	106 53.23	05.11	+0.58
29	760812 0145 41.62	34 02.99	106 59.45	10.26	+1.13
30	760812 0456 05.36	34 03.08	106 59.80	09.30	+0.65
31	760823 2045 35.31	34 34.78	106 52.39	07.44	+0.36
32	760824 0131 13.83	34 02.73	107 00.94	06.88	-0.37
33	760827 0815 28.34	34 00.99	107 03.35	09.65	-0.15
34	760902 1315 05.91	34 08.64	106 52.64	08.25	+0.62
35	761007 2237 37.78	34 02.22	107 01.86	09.60	+0.31
36	770121 1638 11.45	34 01.32	107 02.95	09.30	+0.93
37	770121 1642 28.64	34 00.48	107 03.15	09.08	-0.44
38	770209 1100 01.14	34 01.09	106 59.65	07.49	+0.29
39	770211 1210 18.93	34 16.47	106 48.36	11.16	+0.65
40	770216 1444 49.56	34 00.79	107 02.92	09.41	-0.31
41	770217 1427 43.98	34 16.52	106 48.21	11.60	+0.41
42	770412 0321 36.10	34 17.66	106 54.83	07.88	+0.13
43	770427 0804 40.32	34 01.50	107 01.51	04.97	-0.12
44	770427 1215 56.39	34 01.06	107 03.23	08.98	+0.07
45	770428 1059 10.63	34 03.04	107 02.95	08.60	+0.27
46	770602 0650 24.40	34 01.24	107 03.38	08.98	+0.54
47	770603 2045 03.25	34 13.64	106 53.85	07.22	+0.78
48	770604 0618 51.53	34 13.52	106 53.63	08.42	+0.41
49	770714 1000 32.76	34 09.65	106 51.94	06.82	+0.41
50	770714 1131 51.09	34 09.53	106 52.47	07.09	+0.56
51	770727 1808 20.08	34 09.78	106 54.56	07.68	+0.90
52	770817 0603 20.03	34 10.01	106 52.45	06.66	+0.58
53	770817 1537 22.03	34 15.68	106 55.23	06.61	+0.81
54	770818 0930 13.47	34 09.68	106 52.04	05.99	-0.09

Table 5.4 Continued

N event	Time YYMMDD HHMM SEC	Latitude deg min	Longitude deg min	Depth km	M_d
55	770818 1038 14.91	34 01.43	107 03.48	08.81	+1.05
56	770819 0351 00.28	34 01.26	107 03.45	08.66	+0.28
57	770819 0928 22.98	34 01.16	107 03.71	09.33	+0.23
58	770824 1122 35.89	34 00.70	107 03.34	09.24	+0.17
59	770825 0452 32.95	33 57.81	106 57.19	07.45	+0.35
60	770825 0626 27.14	34 00.83	107 03.45	08.85	+0.29
61	770901 2230 41.99	34 08.48	106 48.91	04.87	+0.27
62	770902 0741 11.86	33 59.15	106 59.49	05.68	-0.13
63	770902 1329 31.60	34 18.35	106 48.33	10.62	+0.11
64	770914 1309 23.66	34 31.92	106 53.34	07.77	+0.64
65	770914 1741 16.38	34 20.23	106 52.71	07.07	+0.95
66	770915 0053 35.44	34 02.14	107 03.29	08.71	+0.53
67	770915 0101 34.35	34 15.47	106 55.20	06.70	+0.50
68	770915 0645 16.86	34 20.72	106 52.69	06.34	+0.53
69	770915 1143 34.32	34 18.61	106 55.03	06.96	+0.32
70	770920 0819 23.20	34 09.61	106 52.44	06.71	+0.40
71	770921 1921 55.03	34 24.25	107 00.44	05.38	+0.52
72	770922 0520 27.85	34 20.32	106 52.83	07.50	+1.19
73	770922 1919 16.78	34 20.08	106 53.10	08.93	+0.95
74	771004 2238 18.13	34 33.61	106 51.22	07.37	-0.10
75	771017 1935 35.08	34 11.17	106 55.02	07.06	+0.24
76	771018 0816 32.77	34 01.57	107 03.30	09.44	+0.76
77	771115 1902 41.50	34 09.24	106 53.07	07.07	+0.52
78	771118 0658 12.47	34 23.94	107 03.12	11.03	+0.86
79	771214 2057 28.11	34 17.36	106 53.05	06.59	-0.04
80	771221 0259 38.79	34 16.11	106 51.54	07.00	-0.41
81	780105 1203 23.29	34 16.41	106 53.01	07.07	+0.26
82	780105 1327 47.34	34 13.53	106 55.21	07.79	+0.21
83	780117 2314 21.27	34 21.05	106 52.11	07.55	+0.05
84	780118 1224 32.64	34 09.44	106 51.24	06.31	+0.87

Table 5.5 Statistical Comparison of Hypocenters With and Without Reflections

Parameter	With Reflections	Direct Phases Only
Average Longitude Error	0.321 ± 0.083	0.352 ± 0.099
Min / Max	0.188 / 0.550	0.196 / 0.619
Average Latitude Error	0.329 ± 0.080	0.381 ± 0.119
Min / Max	0.198 / 0.590	0.210 / 0.827
Average Depth Error	0.339 ± 0.083	1.277 ± 0.812
Min / Max	0.212 / 0.664	0.630 / 5.115
Average Origin Time Error	0.046 ± 0.009	0.100 ± 0.025
Min / Max	0.032 / 0.100	0.033 / 0.168
Average Depth Estimate	8.007 ± 1.577	8.001 ± 2.607
Min / Max	4.870 / 11.60	1.831 / 14.617

The measurements of latitude, longitude, and depth are in kilometers, while the measurements of origin time are in seconds.

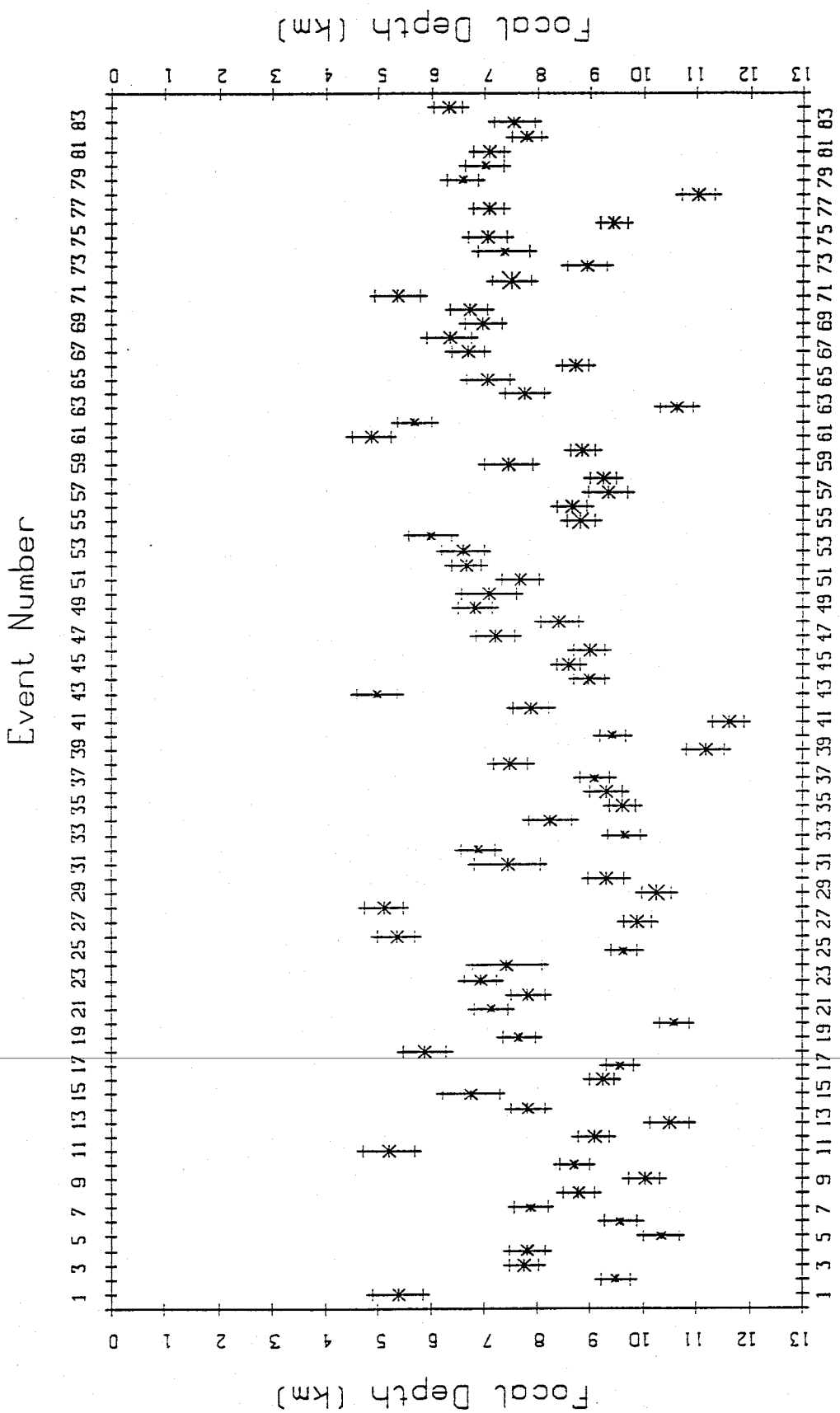

Figure 5.7. Focal depths with 1 std. error bars. Shown are focal depths based on direct and reflected phases.

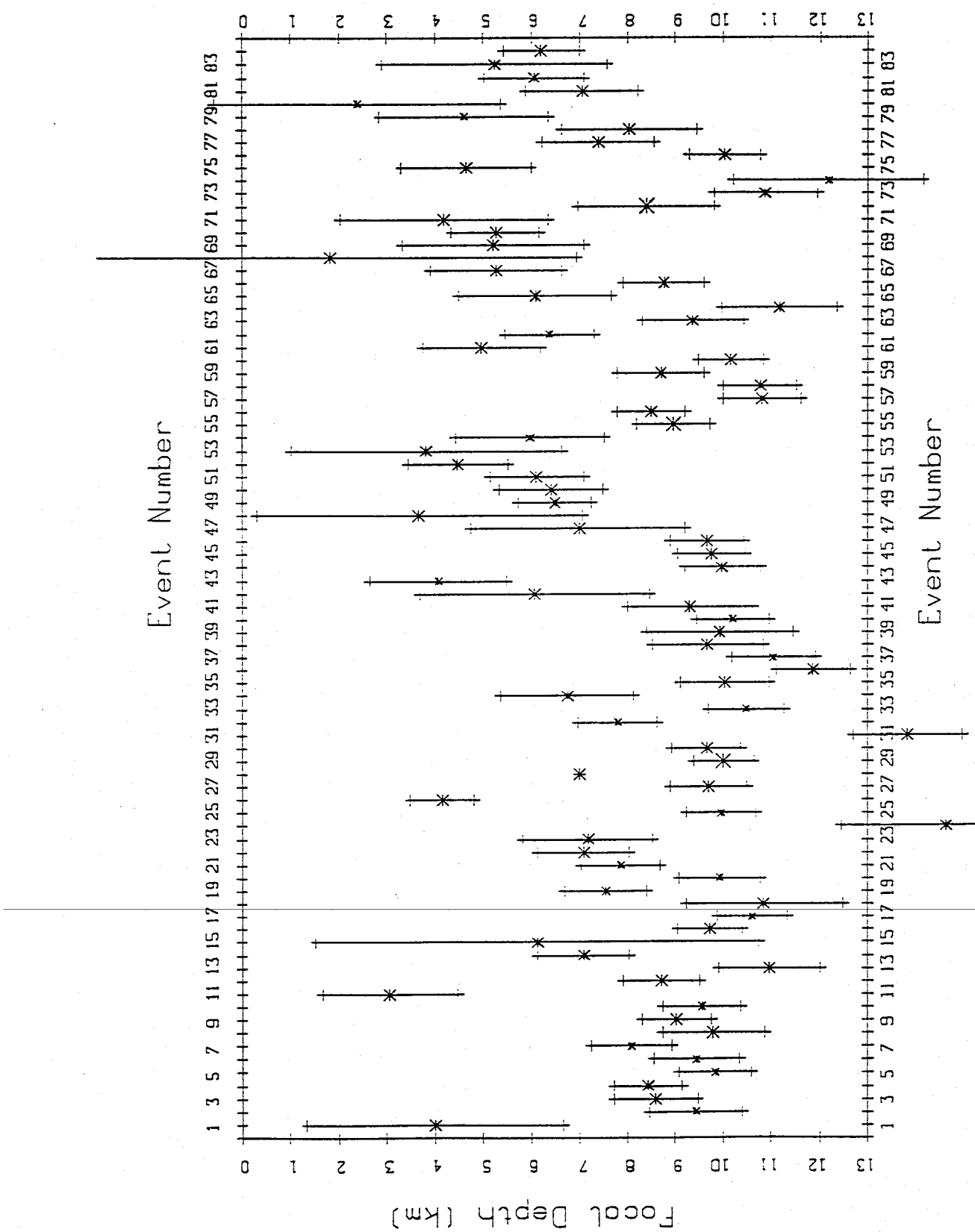

Figure 5.8. Focal depths with 1 std. error bars. Shown are focal depths based on direct phases only.

and 0.376 km for "deep" and "shallow" events, respectively. In his analysis *Hartse* [1991] found averages of 0.53 km and 0.64 km for the "deep" and "shallow" events. The use of the reflected phases also better constrains origin time simply by decreasing the trade off between focal depth and origin time estimates [*Hartse*, 1991].

The reflector depth in this study was 0.79 km deeper than that found by *Hartse* [1991] in his single layer inversion. The average hypocenters depth calculated using the model obtained in my study was 8.007 km ± 1.577 km, whereas the average hypocenter depth for the same data using Hartse's single layer model was 7.177 km ± 1.603 km, a difference of 0.83 km. A definite tradeoff exists between reflector depth and hypocenter depth estimates. It may be difficult to determine which model is actually more accurate. However, as expected, the model I found fits my data set better than the Hartse model. A close comparison of hypocenter depths found in the two studies may help determine how much of the difference can be attributed to varying the family of velocity models possible using the reflections.

6. Discussion

Overview

In this chapter I discuss the results of my study. In particular I discuss the validity of the calculated velocity model in comparison with previous work. I also discuss the lateral extent of the SMB with emphasis on new constraints of the northern boundary. Last I discuss the vertical extent of the seismogenic zone as determined from the 84 events used in this study and contrast it with previous work.

The Velocity Model

The crustal model determined in this study compares favorably with the results of *Rinehart and Sanford* [1981]. They determined that $V_s = 3.41 \pm 0.03$ km/s to the magma body at a depth of 19.2 km. Although the magma body depth was not inverted for, this depth represents the best fit model. My study solved for V_p and Poisson's ratio, from which V_s can be calculated using

$$V_s = \frac{V_p}{\sqrt{\frac{2(1-\nu)}{1-2\nu}}} \qquad 1)$$

Using equation (1), V_s was found to be 3.41 km/s.

A comparison of the results of my study with those of *Ward et al.* [1981] as well as those of *Rinehart and Sanford* [1981] are given in Table 6.1. The results of my inversion agree with the previous results of *Ward et al.* and *Rinehart and Sanford* very well. However, my model differs with the single layer crustal model proposed by *Hartse et al.* [1992]. Neither Poisson's ratio

Table 6.1 Comparison of Inversion Results

Parameter	Investigator	Value	This Study
Vp_1	Ward (1980)	5.85±0.02 km/s	5.86±0.03 km/s (to 19.26 km)
	Hartse (1992)	5.91±0.05 km/s	
V_s	Rinehart and Sanford (1981)	3.41±0.03 km/s	3.41 ± 0.03 km/s
	Hartse (1992)	3.39±0.04 km/s	
ν	Hartse (1992)	0.255±0.002	0.243 ± 0.002
z	Hartse (1992)	18.50±0.23 km	19.26 ± 0.11 km
	Rinehart and Sanford (1981)	19.2±0.6 km	

The measurement of Vp_1 for *Ward* [1980] is only for the seismogenic zone (to about 10 km depth), while for the study of *Hartse et al.* [1992] it is measured to the mid-crustal magma body. The measurements of V_s, ν, and z, are all from the surface to the reflector.

or depth to the magma body overlap even at 2 std, although the velocities easily overlap at 1 std. This highlights the non-uniqueness of these inversion results, and it may be necessary to use bootstrapping techniques in order to find a good average model, and better error estimates.

Lateral Extent of the Socorro Magma Body

A primary objective of this study was to evaluate the causes of differences between two maps of the lateral extent of the SMB; that of *Rinehart* [1979], and that of *Hartse* [1991]. Both studies used maps of reflection points to map the lateral extent, though Rinehart used only the S_zS reflections and Hartse used all available reflection data (P_zP, S_zP, and S_zS).

One possible explanation of the differences may be the use of the S_zP phase which reflects nearer to the hypocenter than does the S_zS and P_zP phases. In order to test this theory I produced a map comprised of only the S_zS reflections found in my data set (Figure 6.1), superimposed on the magma body outline as proposed by Rinehart. Figure 6.2 shows all of the theoretical S_zS reflection points for the 84 events used in this study. Based on a comparison of these two maps (Figures 6.1 and 6.2), Rinehart's map of the magma body can't be considered correct. The observed S_zS reflections outside of Rinehart's estimate may be due to three factors: (1) The data set I compiled uses the USGS stations MLM, ALQ, LPM, and LAD (Rinehart used LAD and LPM after mid-1977), and LPM allowed good quality hypocenters farther east than the stations used by Rinehart; (2) The use of reflections improves hypocenter estimates [*Hartse*, 1991], thus allowing me to use events that Rinehart may have deemed to be inaccurate; and (3) The data sets are

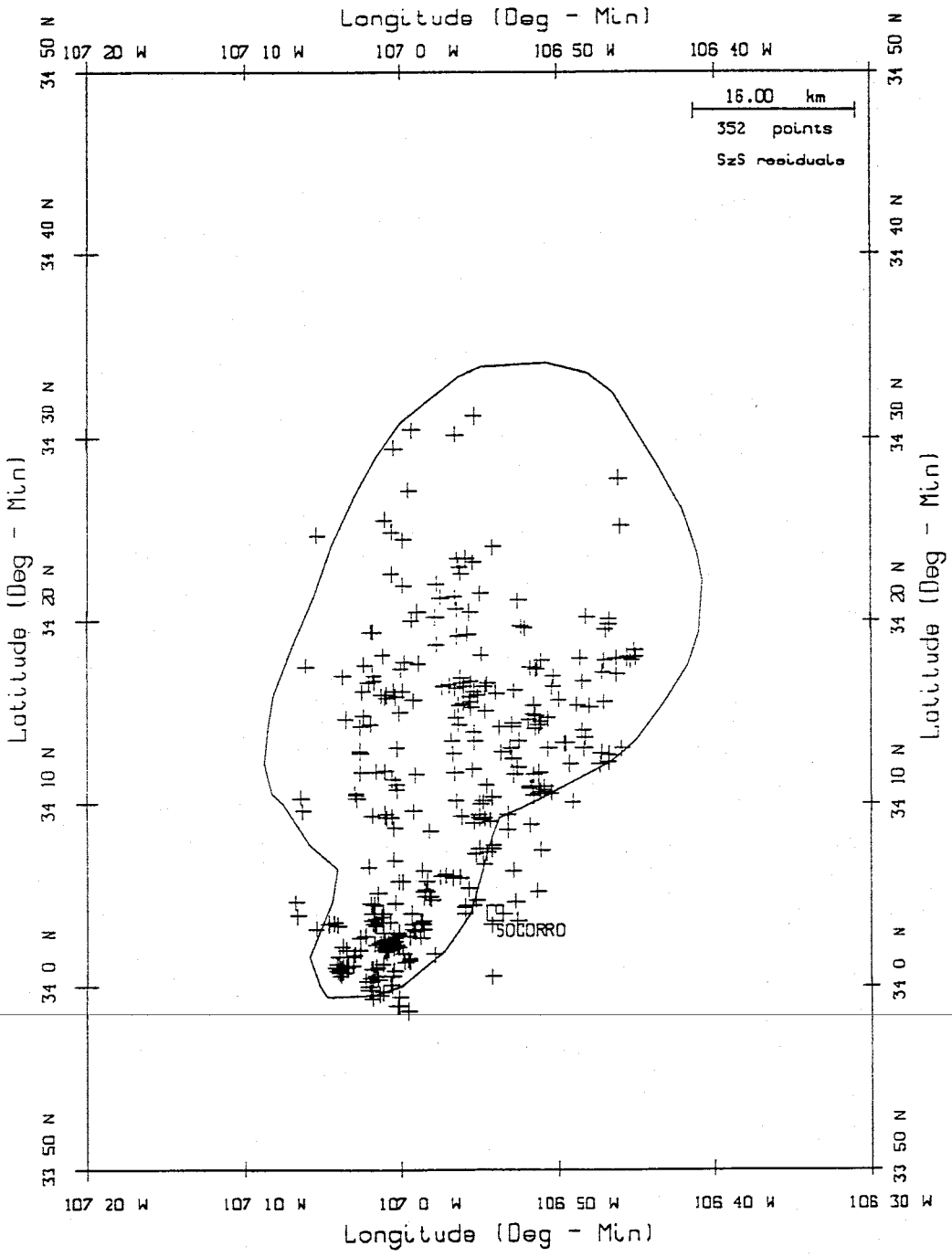

Figure 6.1. Observed S_zS reflections from the 84 epicenters used in my study. Also shown is the magma body outline as determined by *Rinehart et al.* [1979].

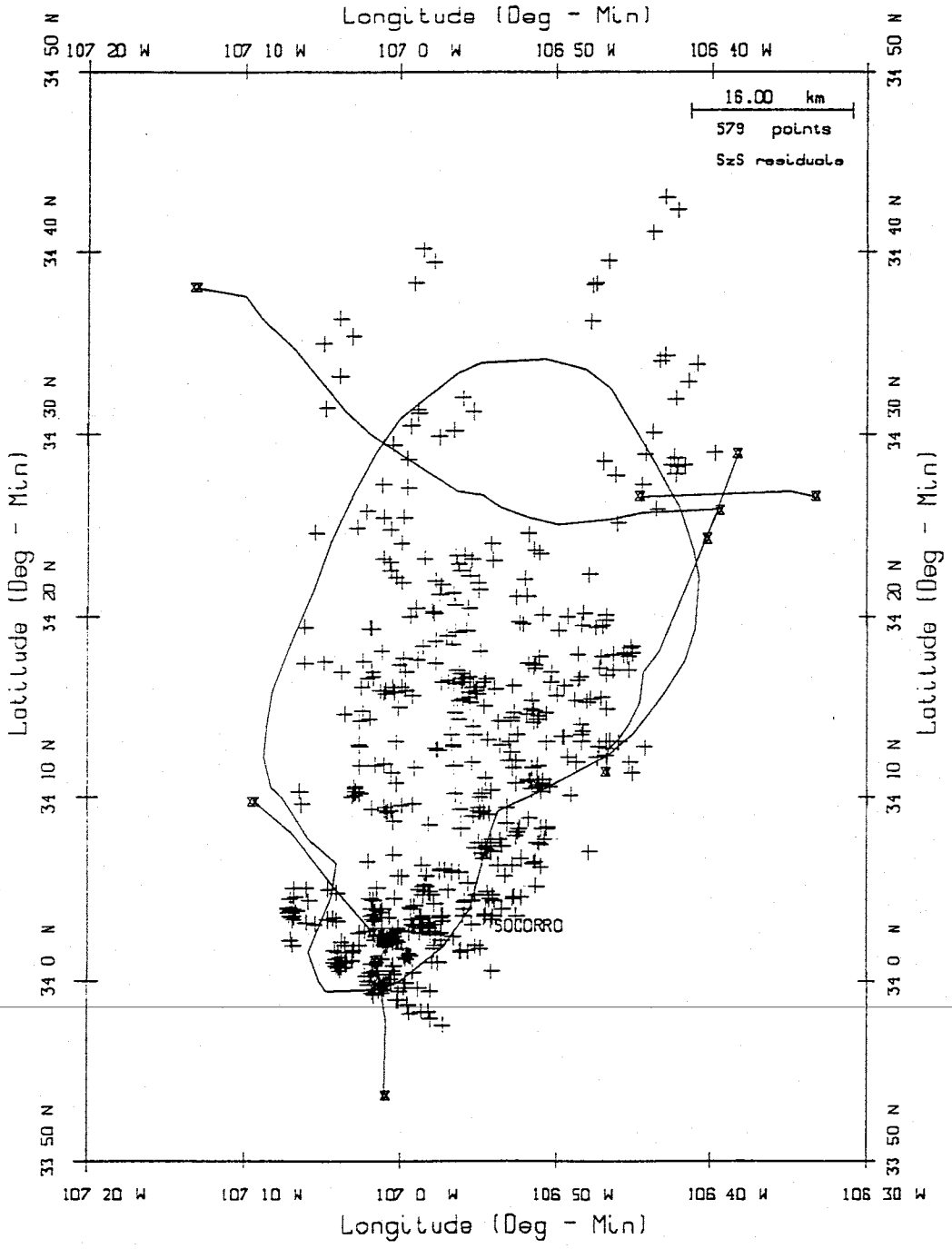

Figure 6.2. Theoretical S_zS reflections from the 84 events used in my study. Also shown are the COCORP lines and the magma body outline as determined by *Rinehart et al.* [1979].

not comprised of exactly the same earthquakes, thus I may have data Rinehart did not use.

To test possible cause number (3) above, I compiled a data subset from my 84 events which only contained events common with those used in Rinehart's study. The common event data set has 42 epicenters (Figure 6.3), with 179 observed S_zS reflection points (Figure 6.4) and 287 theoretical S_zS reflections (Figure 6.5) associated with the 42 events. A comparison of these two maps (Figures 6.4 and 6.5) demonstrates that Rineharts magma body map is appropriate for the 42 common events. It is clear that the observed S_zS reflections outside the magma body estimate in Figure 6.2 are from data not used by Rinehart.

The second primary objective of this study was to constrain the extent of the northern margin of the magma body. Figures 6.3 and 6.4 show the observed and theoretical reflection points, respectively, for the 84 events used in this study. Comparison of these two maps allows delineation of a boundary for the northern limit of the magma body.

Figures 6.6 and 6.7 also depict the magma body outline as determined from this data, except to the southeast, I use the boundaries of *Hartse* [1991]. My estimate for the margins of the magma body agree in general with Hartse's except along the northern end. Both this estimate and that of Hartse are superimposed on the observed reflection points found in this study (Figure 6.8).

Both *Hartse's* [1991] and my margin do not extend as far east as Rinehart's in the vicinity of station LPM. Rinehart constrained the magma body in this area using COCORP data. Neither Hartse or I have used COCORP data in establishing the outline of the magma body. My study has no observed or

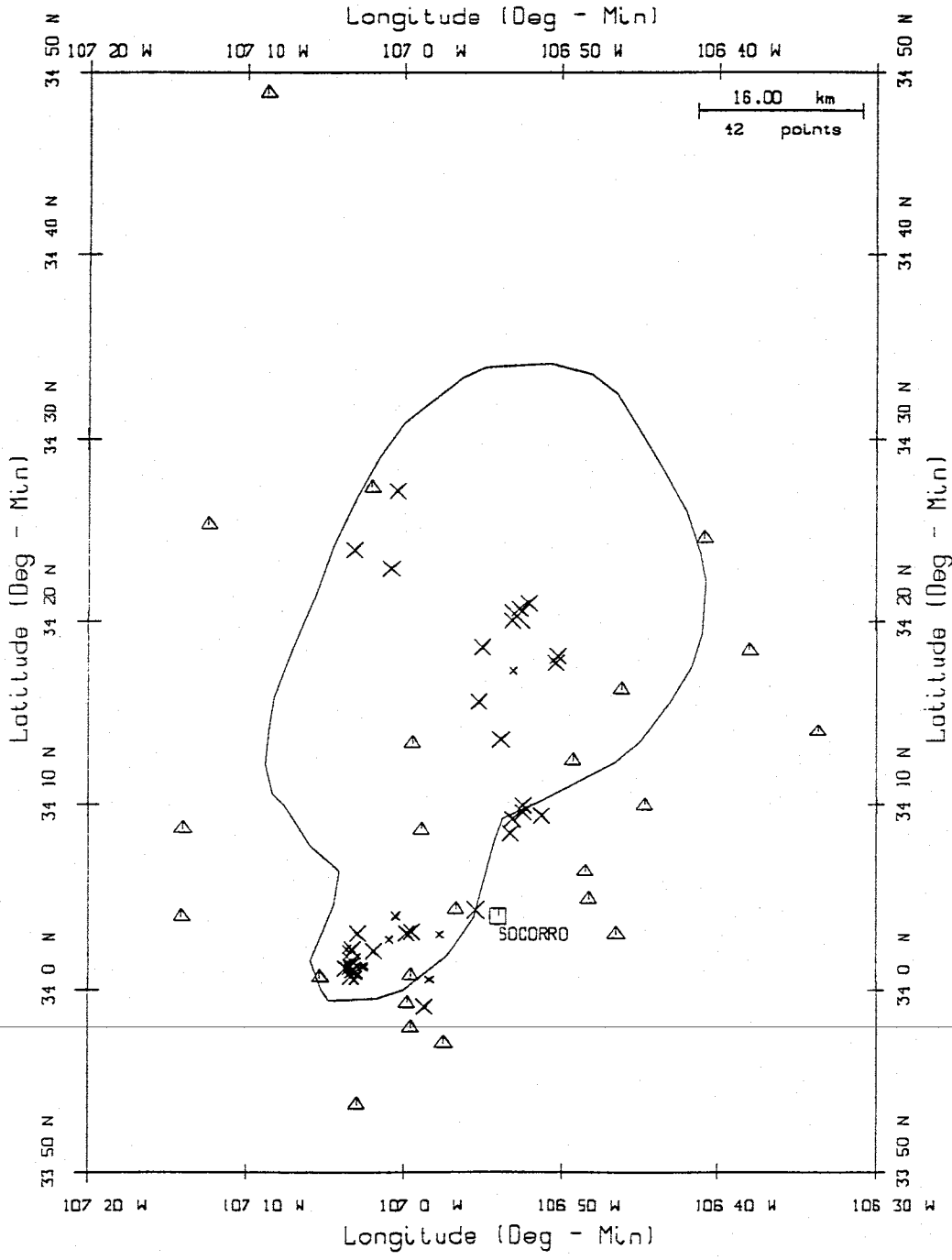

Figure 6.3. 42 epicenters common to *Rinehart's* [1979] study and this study. Also shown are the stations used to collect the data (△'s)

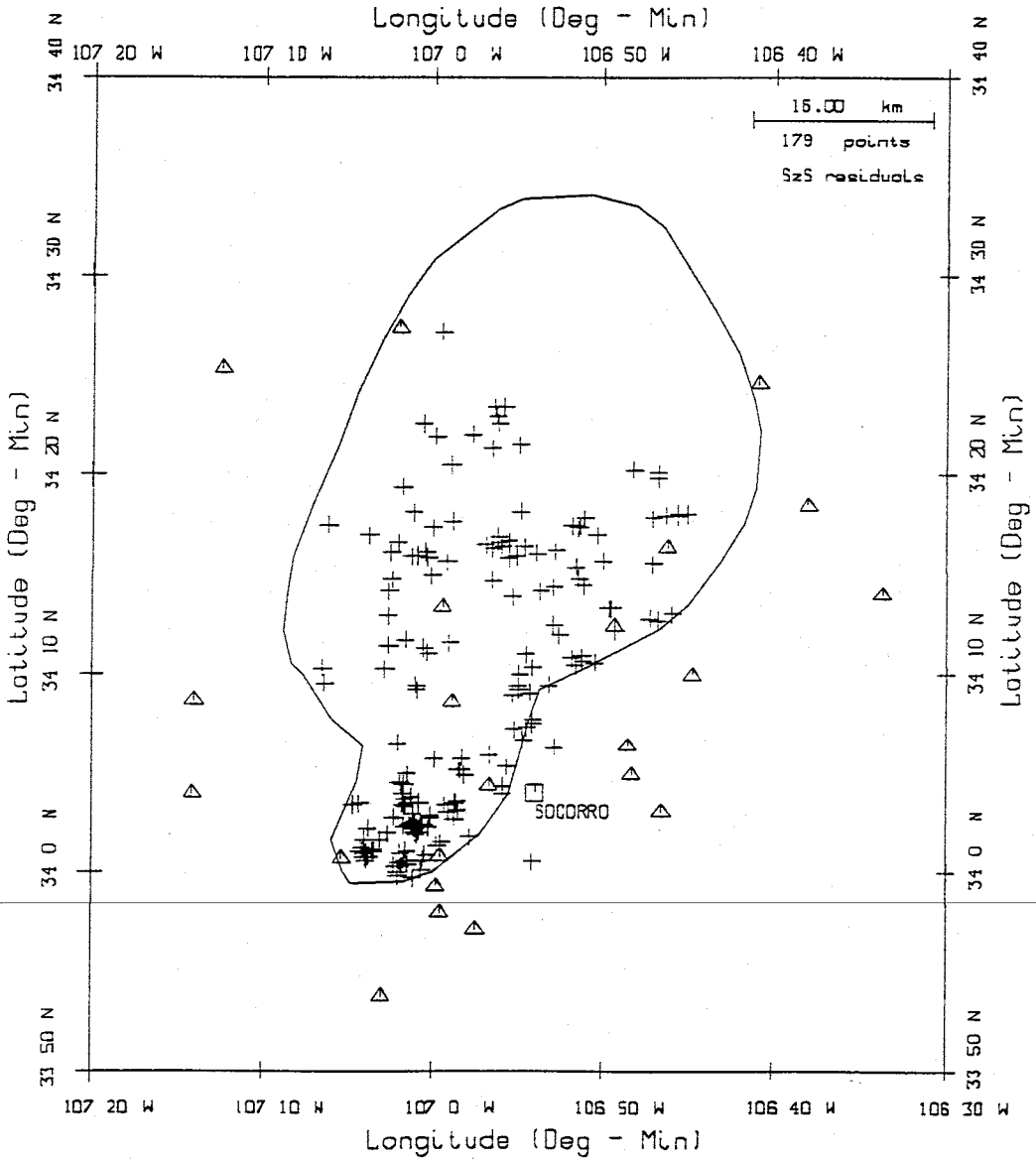

Figure 6.4. Observed S_zS reflections from the 42 common epicenters. Also shown is the magma body outline as determined by *Rinehart et al.* [1979].

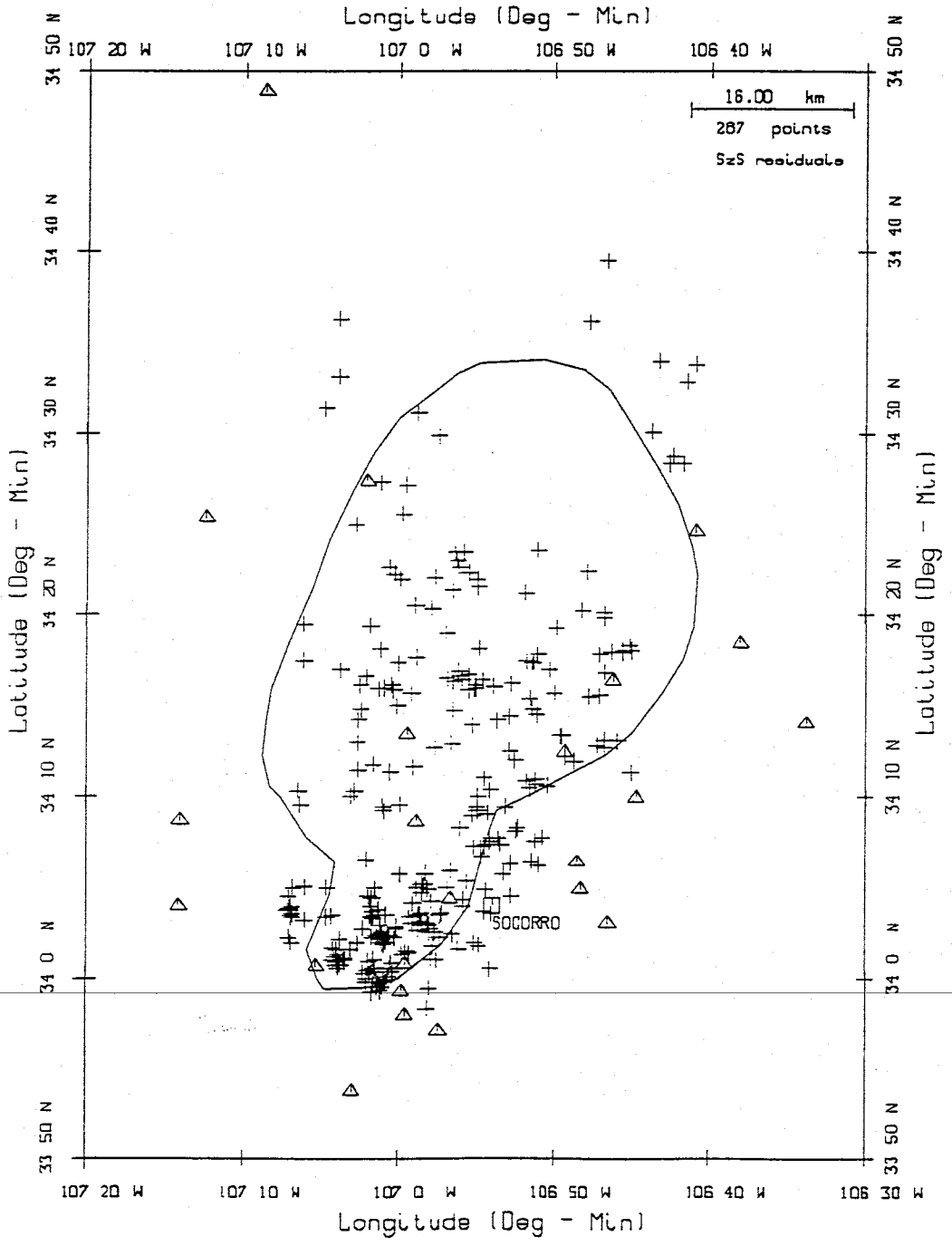

Figure 6.5. Theoretical S_zS reflections from the 42 common events. Also shown is the magma body outline as determined by *Rinehart et al.* [1979].

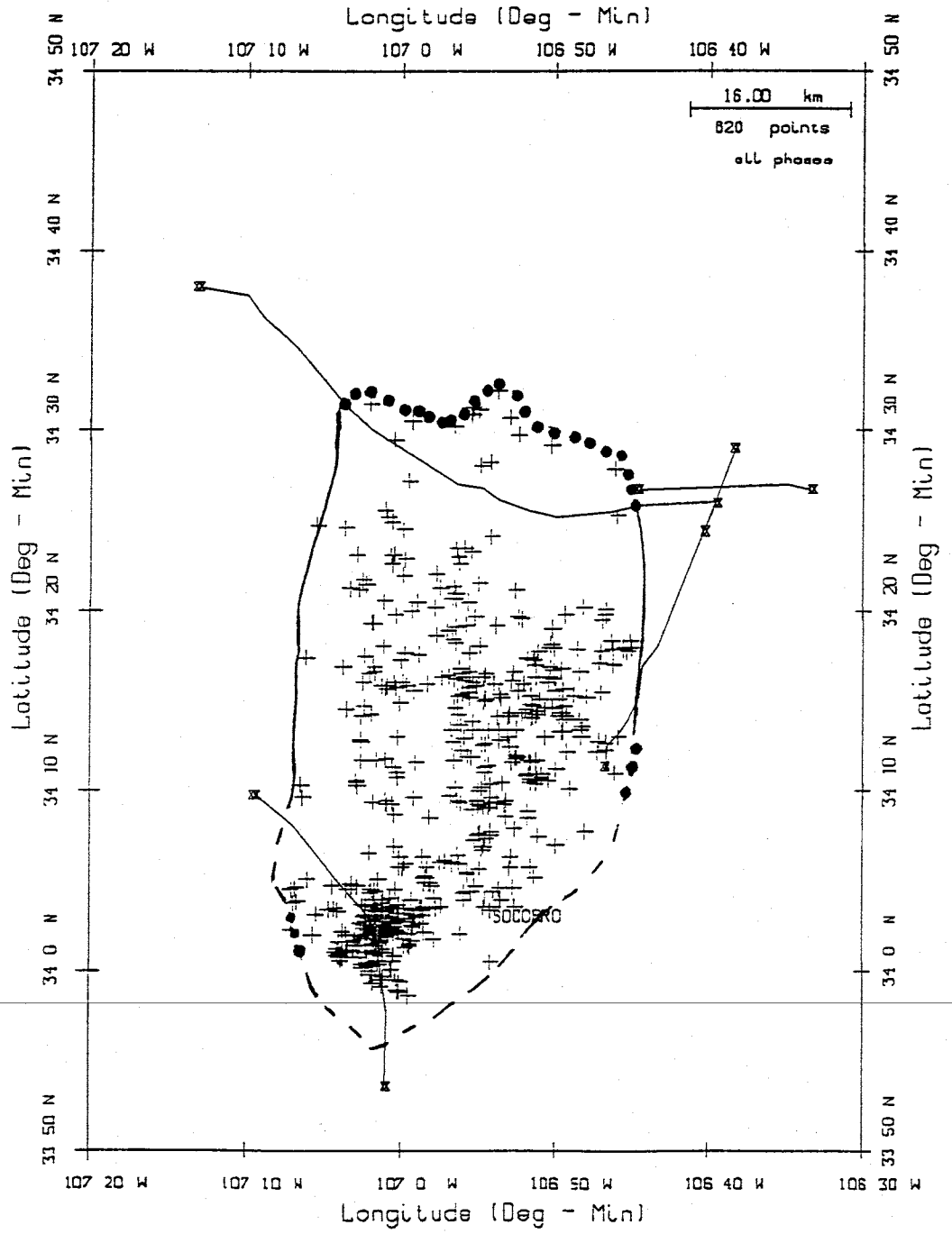

Figure 6.6. All observed reflected phases (+'s) from the 84 events used in my study. The dotted line represents the portions of the magma body outline constrained by this study. The dashed line represents portions of the magma body outline constrained by *Hartse* [1991]. Also shown are the COCORP lines.

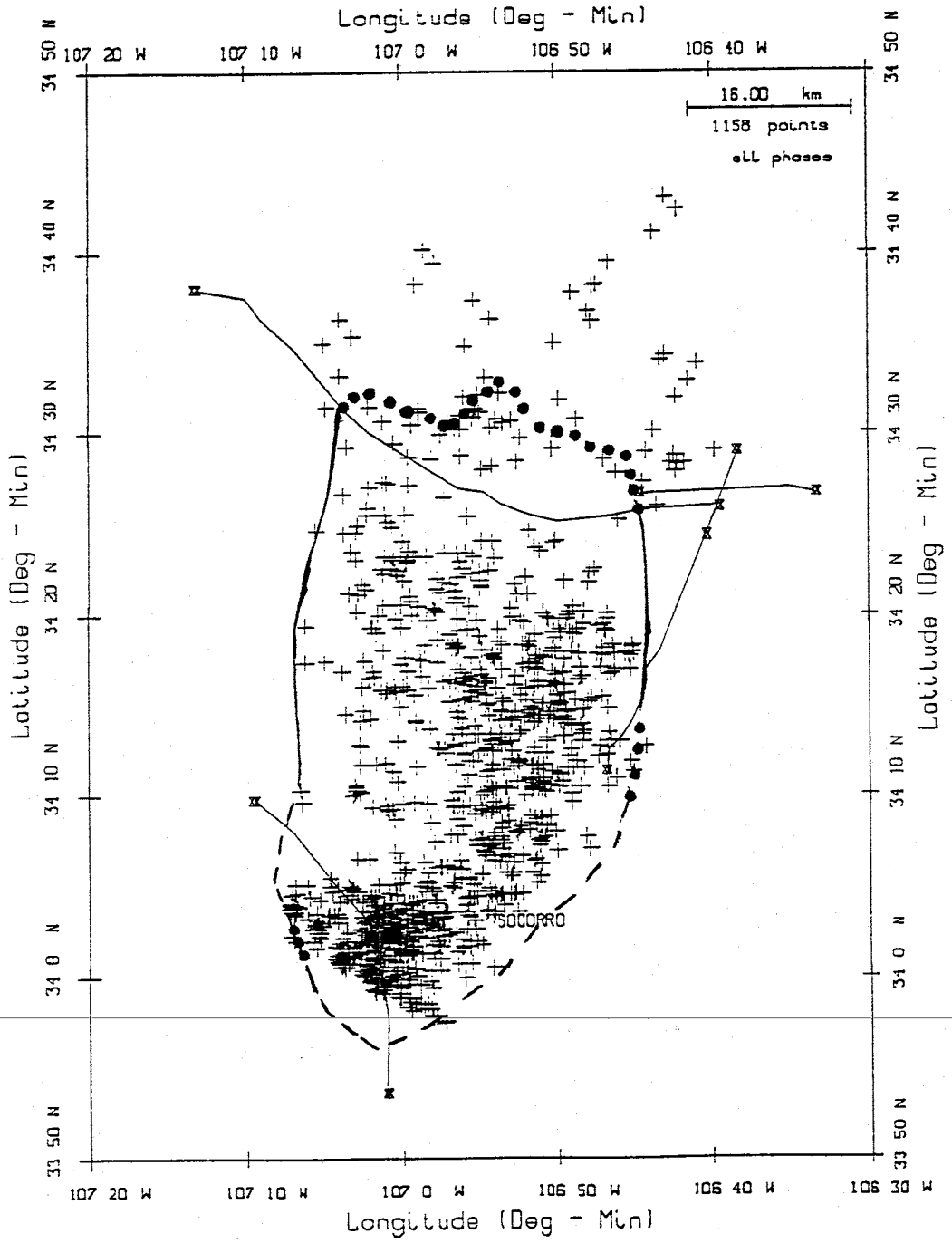

Figure 6.7. All theoretical reflected phases (+'s) from the 84 events used in my study. The dotted line represents the portions of the magma body outline constrained by this study. The dashed line represents portions of the magma body outline constrained by *Hartse* [1991]. Also shown are the COCORP lines.

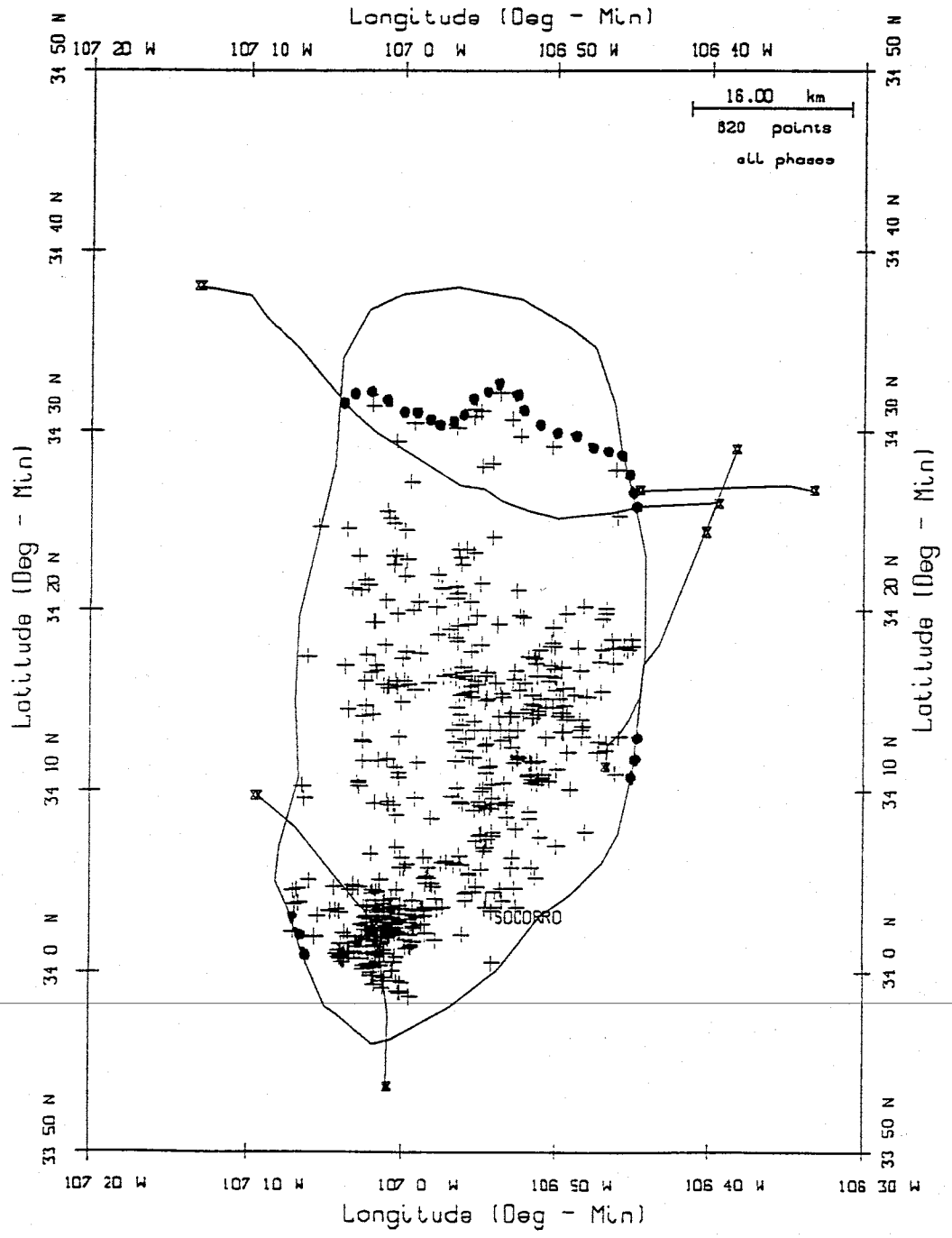

Figure 6.8. All observed reflected phases (+'s) from the 84 events used in my study. The magma body outline as determined by *Hartse* [1991] (solid line), is overlain by the outline determined in this study (dotted line). Also shown are the COCORP lines.

theoretical reflection points in the viscinity of LPM. The SMB could perhaps be extended in that region, because of the clear reflections on the COCORP profile 2A.

An observation which can be made from comparison of these theoretical vs. observed reflection point maps is that there are gaps on the observed reflection point maps that are filled in the theoretical reflection point maps - both in this study (Figures 6.6 and 6.7) and in Hartse's study (Figures 6.9 and 6.10). This may indicate that the magma is not continuous across this area of the SMB, or that the body is not uniformly liquid at its surface in that region. Alternatively, focal mechanisms may not favor downward transmission of energy from hypocenters over this portion of the magma body.

The Seismogenic Zone

The seismogenic zone in the Socorro area can be investigated using the hypocenter depths found in this study. Since only 84 hypocenters are used from low magnitude microearthquakes, this study probably doesn't completely define the seismogenic zone. Two other studies have examined the seismogenic zone in the Socorro area, *King* [1986], and *Hartse* [1991]. King used 513 hypocenters calculated using HYPO71 (Figure 6.11) his data set contained focal depth errors up to 2 km for some events. *Hartse* [1991] used only 75 hypocenters (Figure 4.11), but the errors in hypocenter depth averaged 0.6 km and no error was worse than 0.9 km. The average hypocenter depth error for the 84 events used in this study was 0.34 km with none greater than 0.66 km. This study has the lowest hypocenter depth errors of any seismogenic zone study to date, and a similar epicenter distribution to both previous studies.

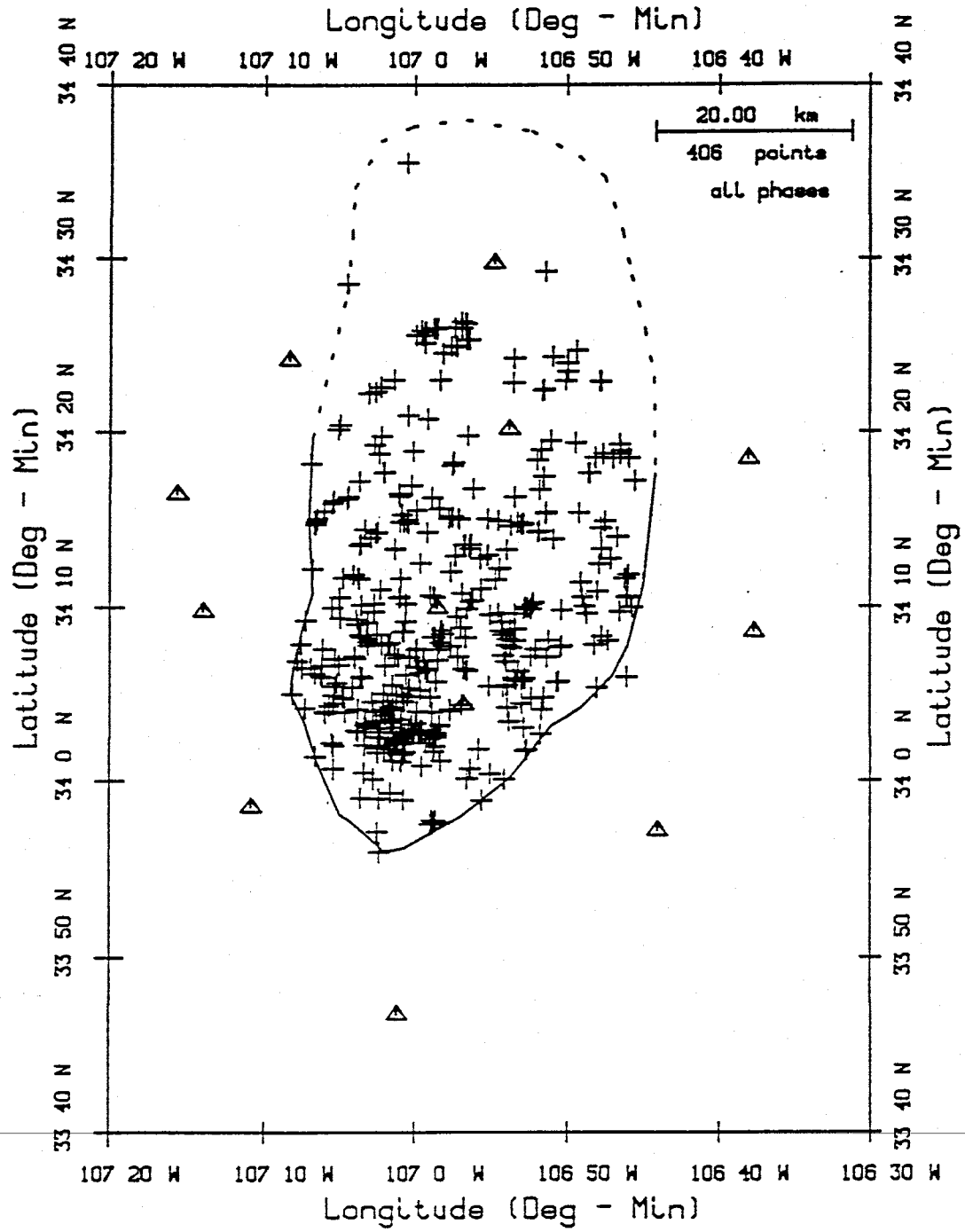

Figure 6.9. Observed reflected phases from the 75 events used by *Hartse* [1991] superimposed on his magma body map. All phases are used, stations are represented by Δ's.

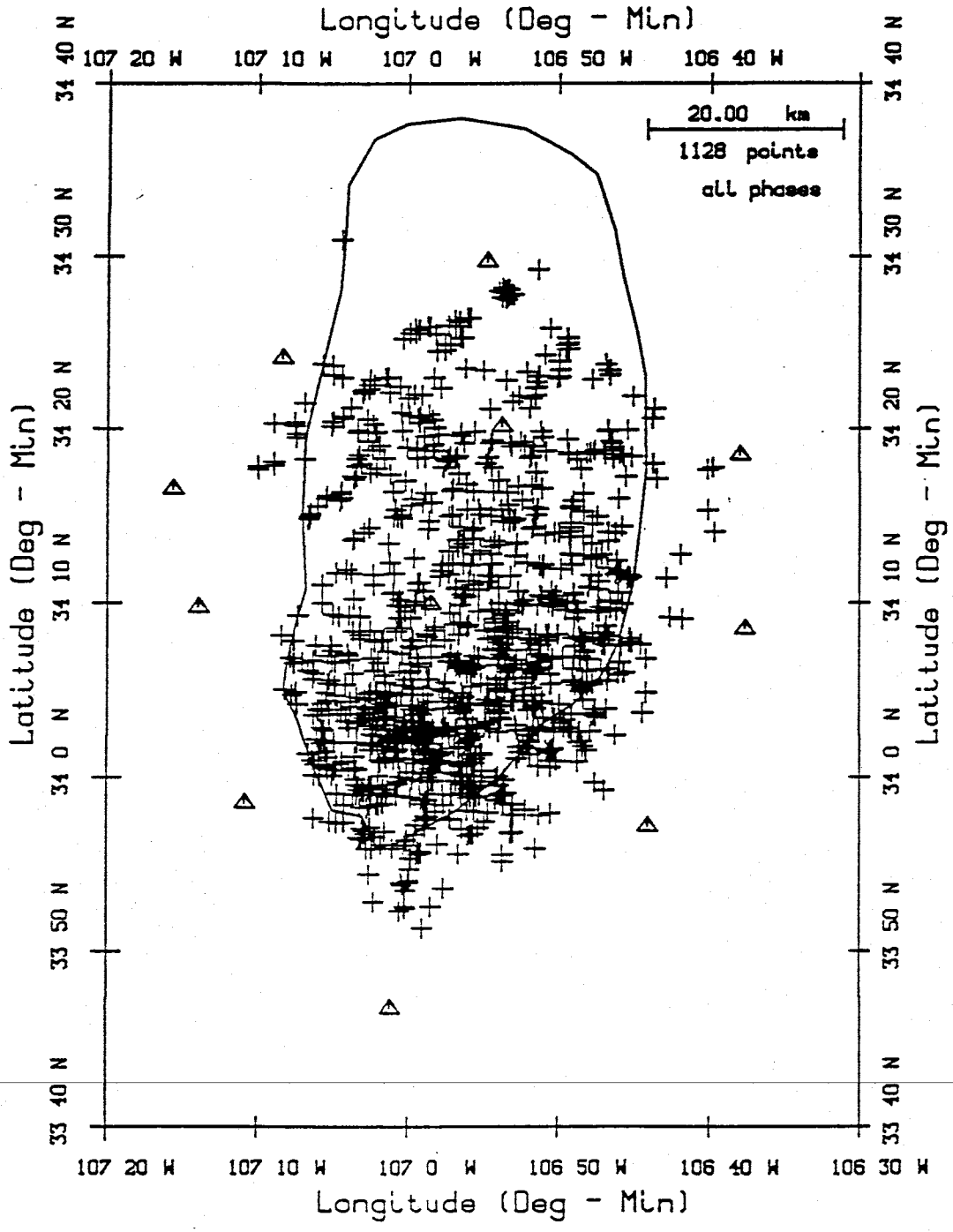

Figure 6.10.Theoretical reflected phases from the 75 events used by *Hartse* [1991] superimposed on his magma body map. All phases are used, stations are represented by △'s.

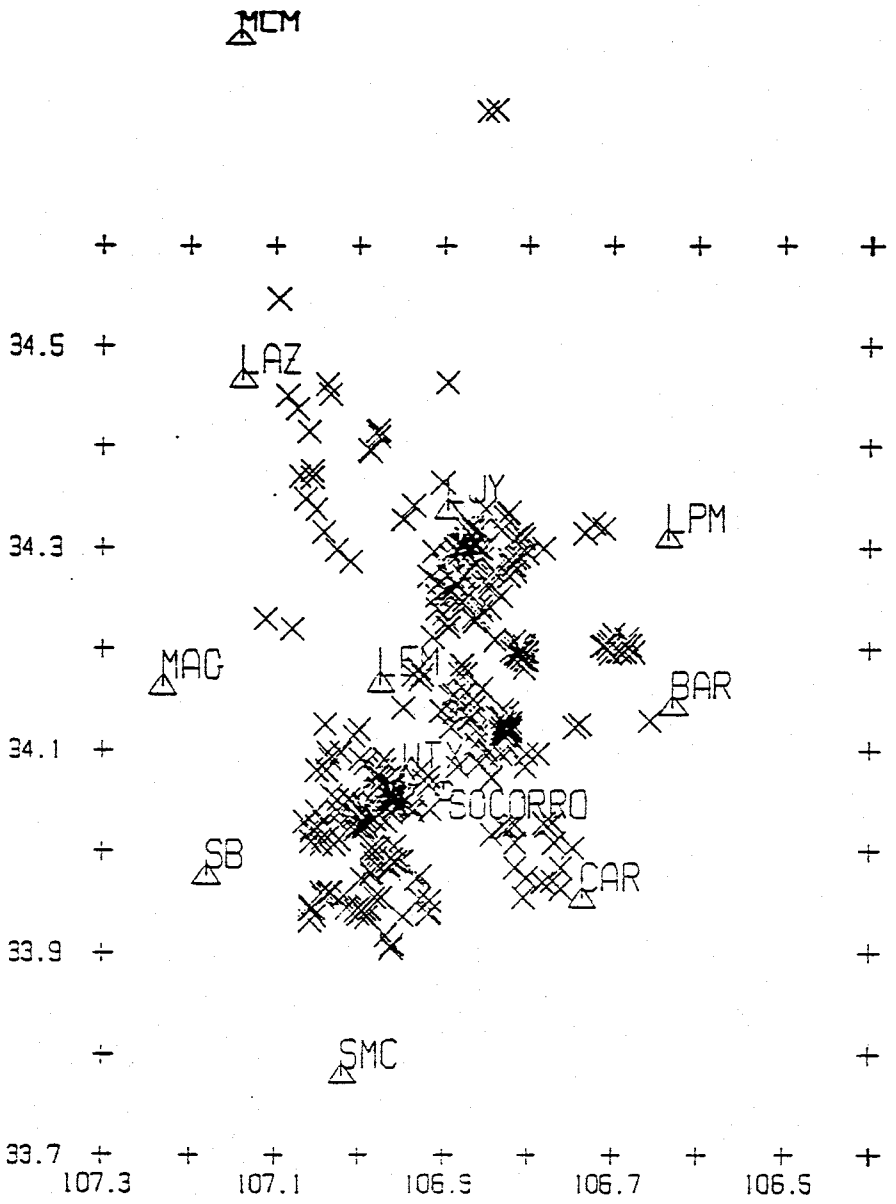

Figure 6.11. Epicenter distribution of events used by *King* [1986] to study the limits of the seismogenic zone in the Socorro area.

Figure 6.12 is a histogram of hypocenter depths for the 84 events used in this study. A possible cutoff in depth is observed at about 10 km, with only nine events being deeper. Of these nine events only five are deeper than 10.5 km, with three being deeper than 11.0 km. Figure 6.13 shows a histogram of the 513 events used in Kings study, and Figure 6.14 shows the histogram of the 75 events used by Hartse. Both Hartse and King have events shallower than 4.0 km in depth, of which I have none. In contrast to Hartse's result, I have three events deeper than 11.0 km depth, and my base to the seismogenic zone is not as sharp. In order to facilitate comparison of my events and those of Hartse which were calculated using a magma body depth of 18.75 km, I plotted a second histogram (Figure 6.15) which increments depth on the half km, rather than the integer km. In this figure only six percent of the events are deeper than 10.5 km and there is a fairly sharp breakoff in activity at the apparent upper limit of the seismogenic zone (4.5 km depth).

The possibility of lateral variation in the seismogenic zone is an important question. Figure 6.16 shows the 84 epicenters used in my study, with different symbols for different depth ranges. Examination of Figure 6.16 reveals the possibility that the average depth may be deeper for events in the southwest. Figure 6.17 has histograms for three geographic subsets of the 84 epicenters; area 1 is for all events south of $34°5'$ north; area 2 is for all events above $34°5'$ north and below $34°22.5'$ north; and area 3 is for all the hypocenters north of $34°22.5'$ north. Figure 6.17 shows that the average hypocenter depth is statistically different between area 1 (7.0 - 11.0 km depth range) and area 2 (5.0 - 9.0 km depth range). In area 2, the four deepest events are all located east of $106°50'$ west. There are not enough events in area 3 to determine the average hypocenteral depth range, though the distribution appears to better match that of area 2.

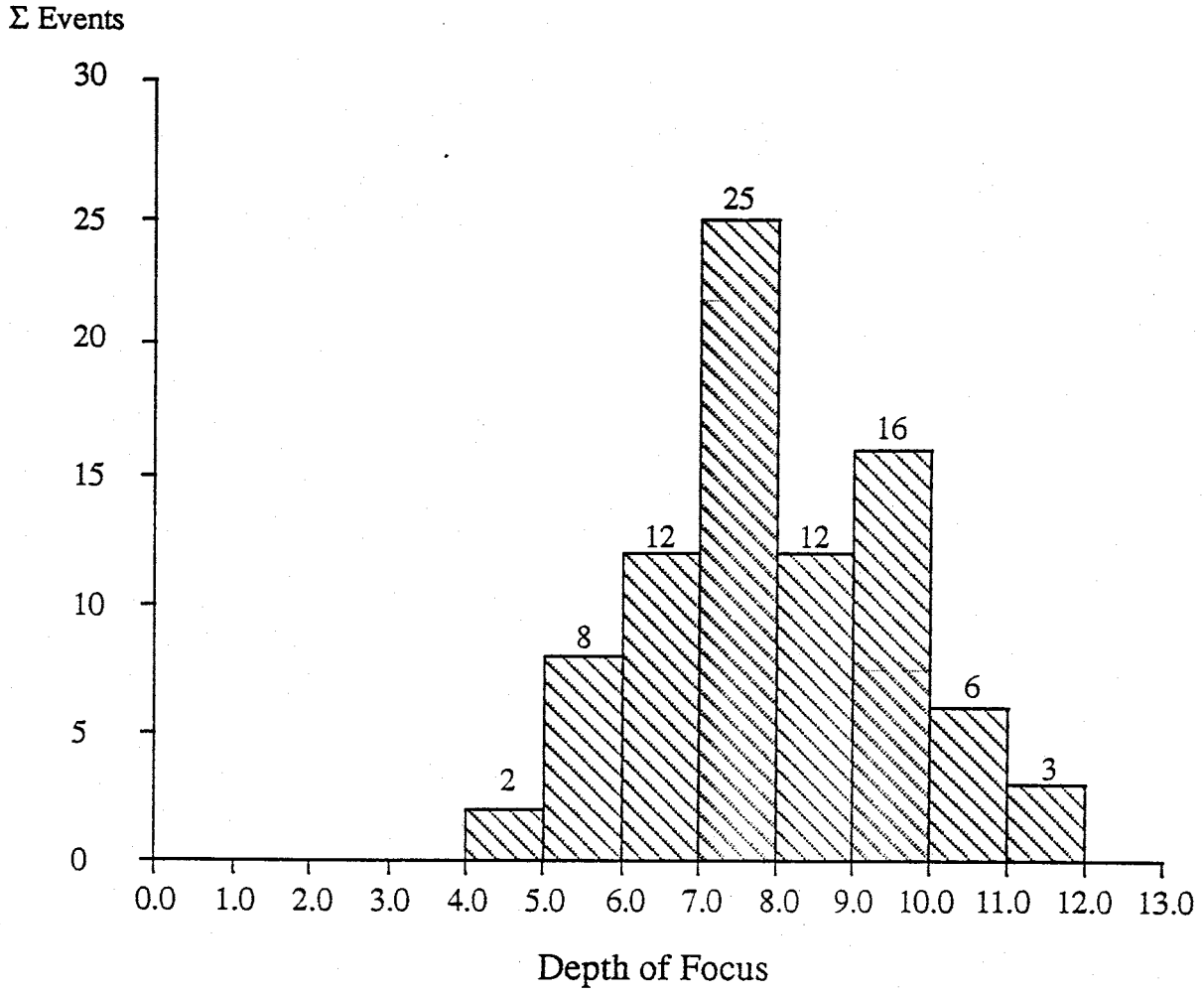

Figure 6.12. Histogram of hypocenter depth's for the 84 events used in my study.

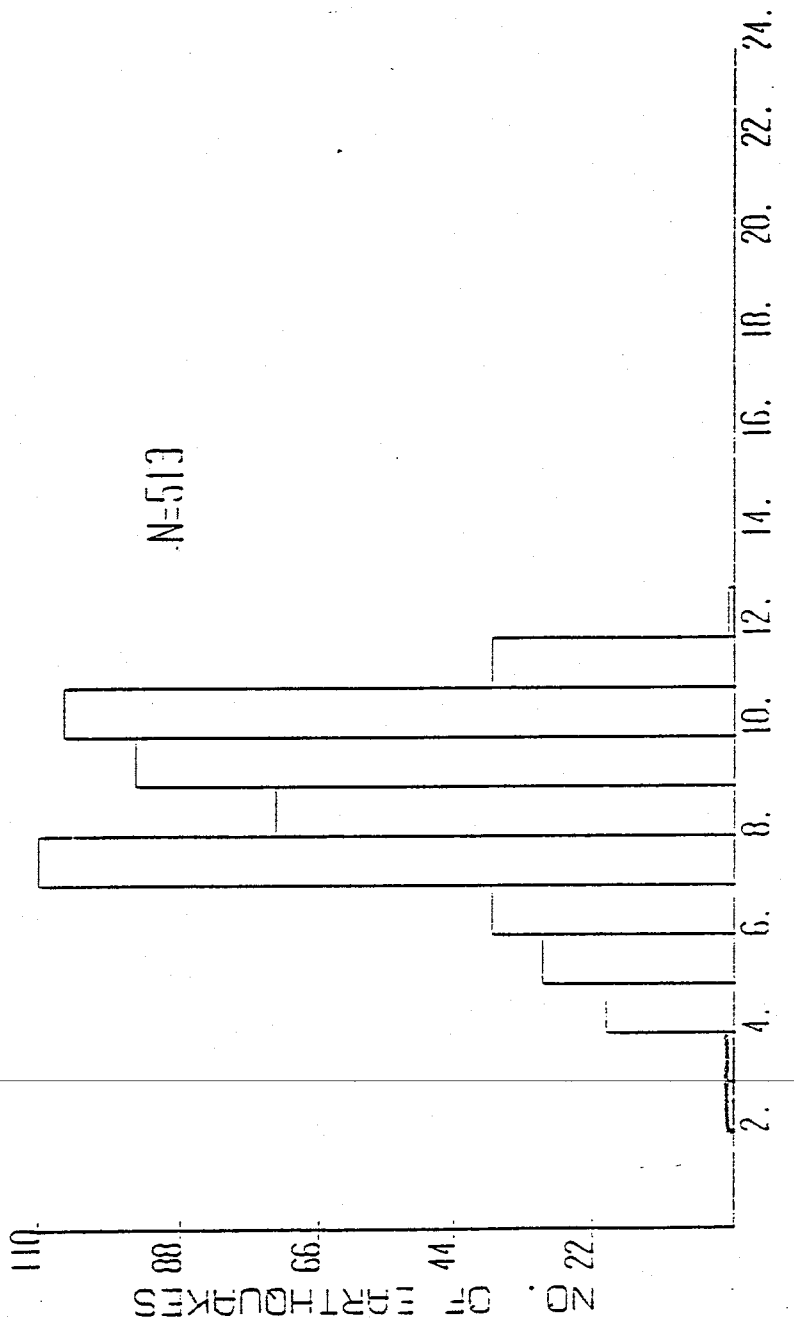

Figure 6.13. Focal depth histogram of the 513 events used by *King* [1986].

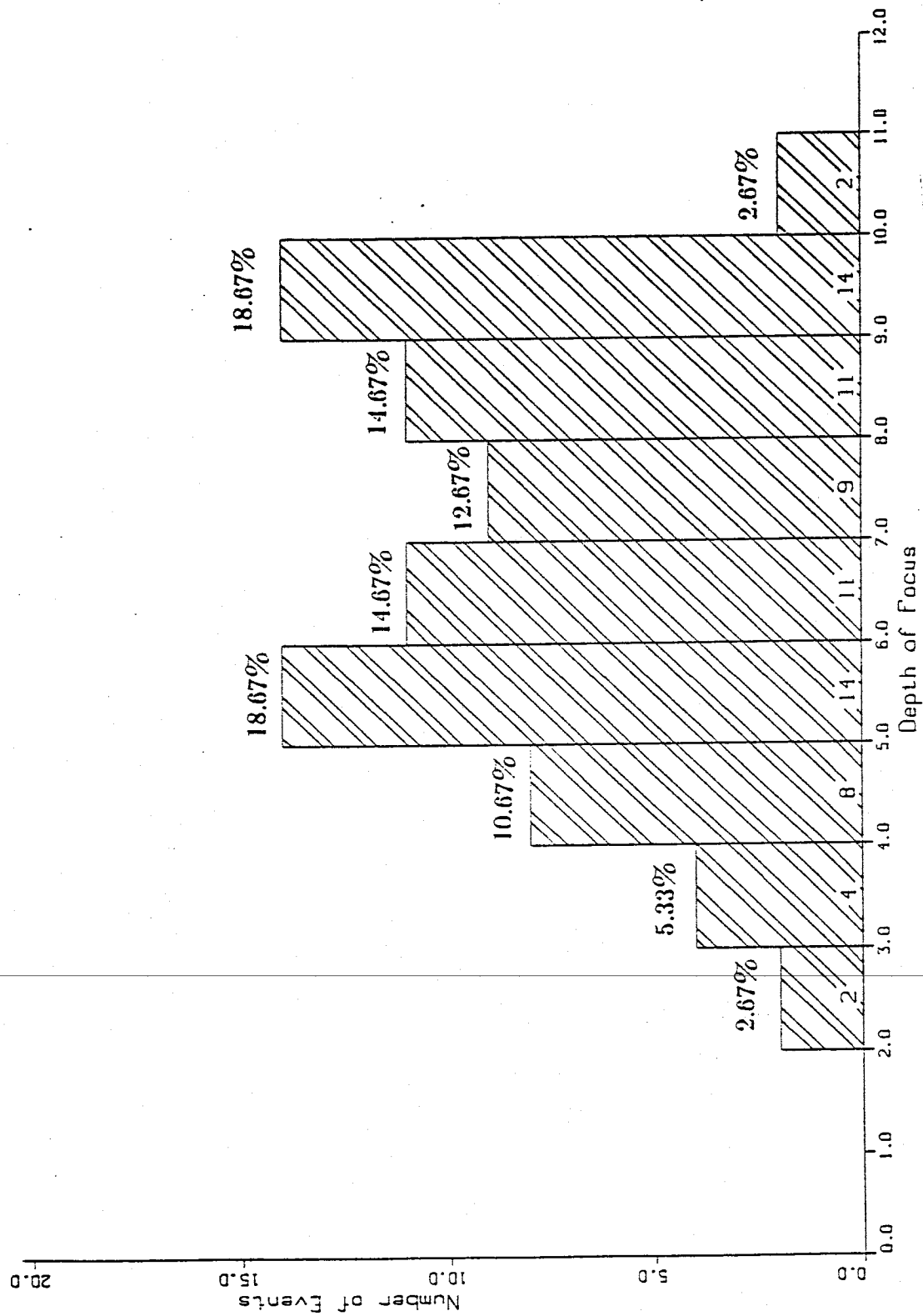

Figure 6.14. Focal depth histogram of the 75 events used by *Hartse* [1991].

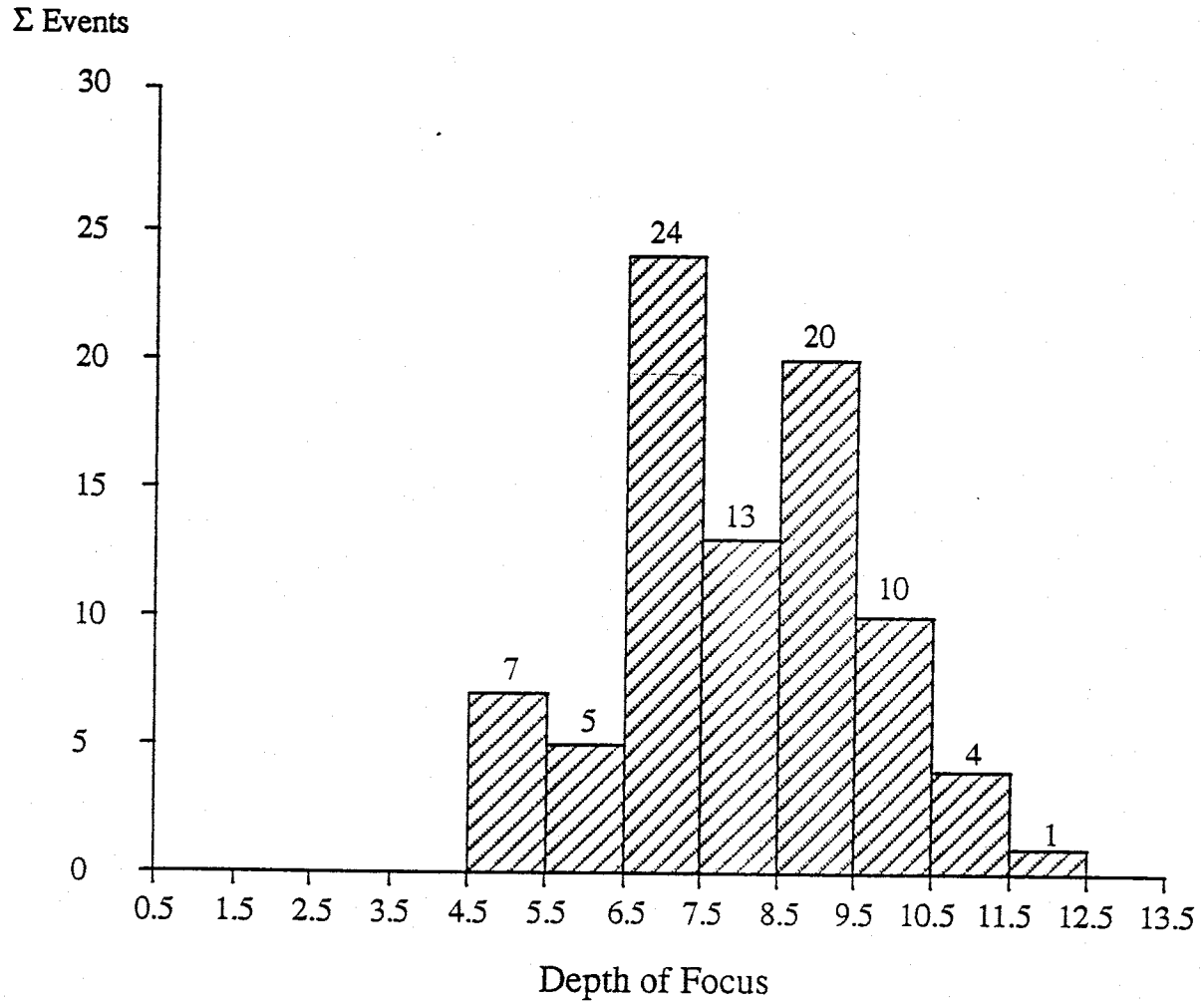

Figure 6.15. Histogram of hypocenter depth for the 84 events used in my study. The histogram has 1 km bins incremented on the half km.

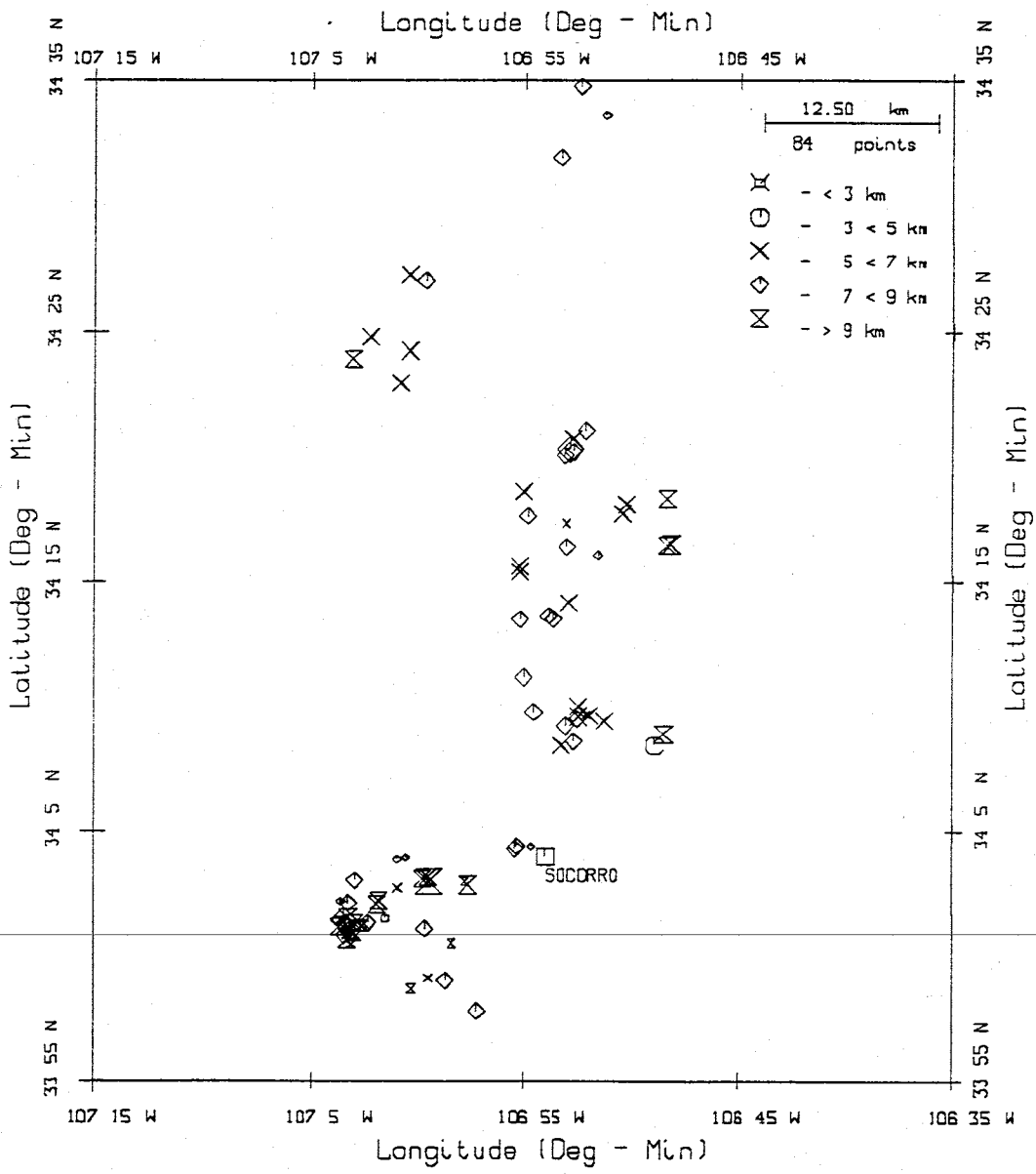

Figure 6.16. Distribution of the 84 epicenters used in my study showing variations in focal depth.

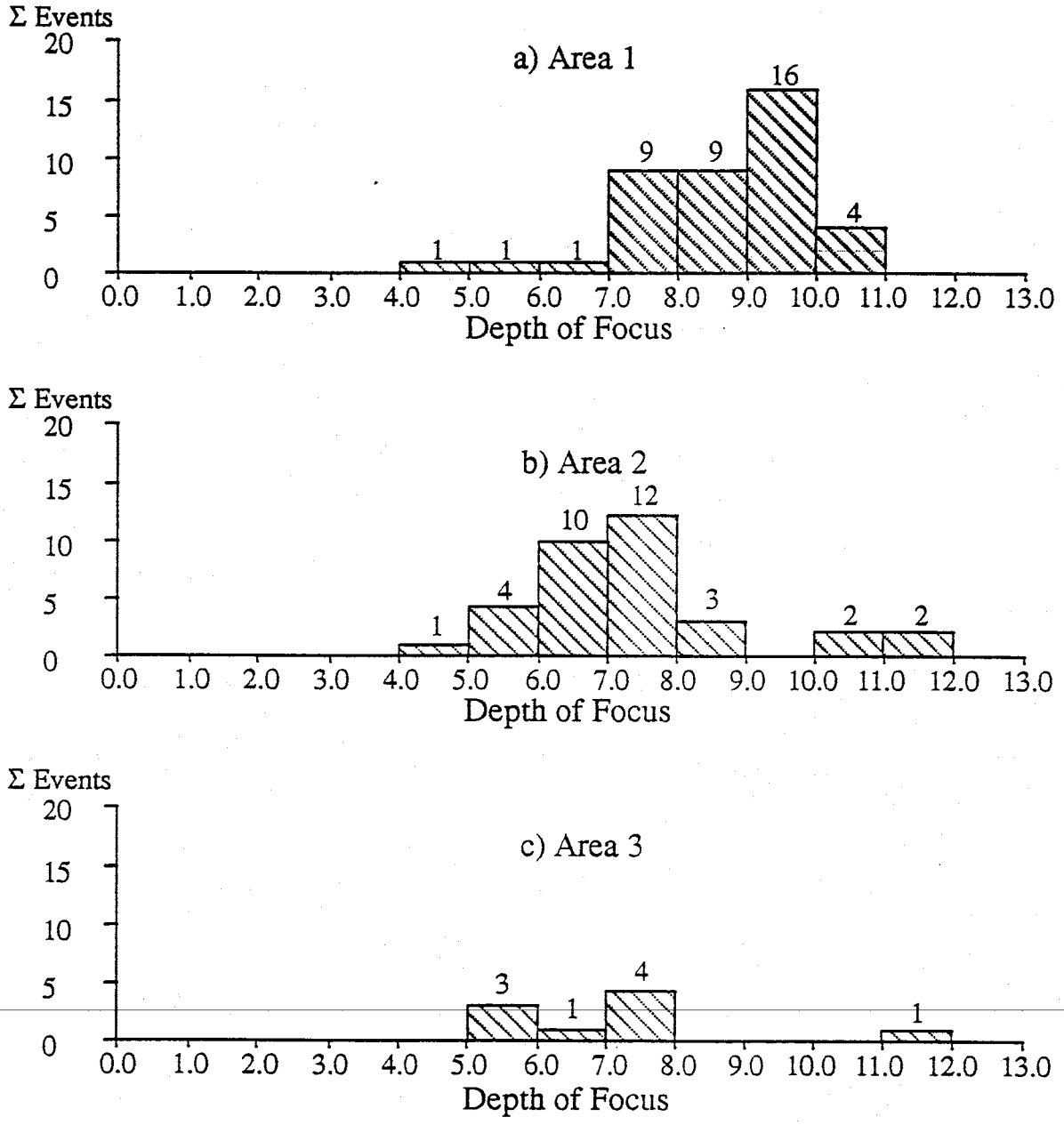

Figure 6.17. Histograms of hypocenter depth for the 84 events used in my study. (a) the 41 events south of 34° 5′ north latitude; (b) the 34 events above 34° 5′ and below 34° 22.5′ north latitudes; and (3) the 9 events above 34° 22.5′ north latitude.

In order to accurately define the seismogenic zone in the Socorro area, the crustal model needs to be more accurately constrained. The effect of increasing magma body depth is to increase hypocenter depth by double the amount, all other factors remaining the same. Therefore any estimate of the seismogenic zone using hypocenters calculated by **SEISMOS** is dependant on magma body depth. Thus, a comparison of depths from the two studies requires the use of the same crustal model. Bootstrapping using a combination of data from this study and Hartse's data set could resolve the reflector depth in a more statistically significant manner and allow comparisons.

7. Conclusion

The primary objectives of this study were to address the differences between two estimates of the lateral extent of the SMB, and to constrain the northern boundary of the magma body. Secondary objectives were; 1) to calculate a crustal model which best fit the data collected for the study, and 2) examine the seismogenic zone above the SMB.

The northern limit of the SMB was constrained using data from the Socorro portable network and four stations of the Albuquerque Seismological Laboratory network. The northern limit was reduced several km with respect to the estimate of *Hartse* [1991].

Theoretical vs. observed reflection maps using only the S_zS phase were used in order to determine if the use of the S_zP phase improved *Hartse's* [1991] estimate over that of *Rinehart* [1979]. Using only the S_zS phase from the 42 events common to both Rinehart's and my data set, the earlier map is supported. When all 84 events with all direct and reflected phases are used the results are close to the margins of Hartse which were also determined using all phases. An additional observation to be made in comparing theoretical vs. observed reflection point maps is that theoretical points are found in areas within the margins where there are no observed points. This observation is true for my study, as well as the study of *Hartse* [1991] - and may imply that the magma body is discontinuous.

A crustal model was found using generalized least square inversion of all observed Socorro area phases. The inversion algorithm **SEISMOS** of *Hartse* [1991] was employed to produce a one-layer crustal model for the Socorro area down to the sill-like magma body. P-wave velocity was determined to be

5.86 ± 0.03 km/s, Poisson's ratio was found to be 0.243 ± 0.002, and depth to the magma body was estimated to be 19.26 ± 0.11 km. These results correspond well with earlier results from *Rinehart and Sanford* [1981], who employed data from a subset of the network I used in my study. *Rinehart and Sanford* [1981] found an S-wave velocity of 3.41 ± 0.03 km/s for a best fit depth of 19.2 ± 0.6 km. Poisson's ratio (ν) and V_p from my study were used to calculate $V_s = 3.41$ km/s.

The results of my inversion do not fit the single layer crustal model of *Hartse* [1991] within 2 std for depth or Poisson's ratio. however the P-wave velocity is within 1 std of that found by *Hartse*.

The seismogenic zone in the Socorro area was examined using the 84 hypocenter depths found in this study. A moderately sharp cutoff in event occurrence was found at 10 to 10.5 km depth, and this may correlate to the 10 km depth cutoff observed by *Hartse* [1991] for his 75 event data set. In addition, a fairly sharp cutoff was observed at 4.5 km depth which may correspond to the upper limit of the seismogenic zone. Average hypocenter depths varied noticeably over the magma body with deeper average hypocenters in the southwest.

Relative hypocenter depths are affected by the estimate of the magma body depth when reflections are used in hypocenter location. Thus it is difficult to directly compare this study and the study of Hartse. Shifting my depths 0.5 km shallower may bring my results more in line with those of Hartse although I would still observe no events shallower than 4.0 km and Hartse's study has 8 percent (6 events) above that depth.

Suggestions for Further Study

In order to portray the seismogenic zone accurately, a more precise determination of a crustal model needs to be found for the Socorro area. The statistical bootstrapping technique could be used with a large data set (perhaps a combination of this and Hartse's) to more accurately compute an average model and the associated errors.

A large data set utilizing reflected phases in hypocenter estimates would be useful for examining the limits of the seismogenic zone in the Socorro area, particularily lateral variations.

A more detailed study of the observed vs. theoretical reflection point maps is warranted, particularly in the southern half of the magma body. Numerous theoretical reflection points appear in regions within the margins of the magma body where there are no observed reflection points, perhaps implying a fine scale segmentation of the magma body.

8. References

Ake, J. P. and A. R. Sanford (1988). New evidence for the existence and internal structure of a thin layer of magma at mid-crustal depths near Socorro, New Mexico, *Bull. Seism. Soc. Am.* **78**, 1335-1359.

Bachman, G. O. and H. H. Mehnert (1978). New K-Ar dates and late Pliocene to Holocene geomorphic history of the Central Rio Grande region, *Geol. Soc. Am. Bull.* **89**, 283-293.

Bagg, R.M (1904). Earthquakes in Socorro, New Mexico, *Am. Geologist* **34**, 102-104.

Brocher, T. M. (1981). Geometry and physical properties of the Socorro, New Mexico, magma bodies, *J. Geophys. Res.* **86**, 9420-9432.

Bryan, K. (1938). Geology and ground-water conditions of the Rio Grande depression in Colorado and New Mexico, *Regional planning, Part 4; Rio Grande joint investigation in the upper Rio Grande Basin: Washington D.C., National Resource Committee* **1**, 197-225.

Brown, L. D., C. E. Chapin, A. R. Sanford, S. Kaufman, and J. Oliver (1980). Deep structure of the Rio Grande rift from seismic reflection profiling, *J. Geophys. Res.* **85**, 4773-4800.

Caravella, F. J. (1976). A study of Poisson's ratio in the upper crust of the Socorro, New Mexico area, *M.S. Indep. Study*, New Mexico Institute of Mining and Technology, Socorro, New Mexico, 80 pp.

Carlson, D. (1983). A crustal structure study in the Socorro area using the time-term method, *M.S. Indep. Study*, New Mexico Institute of Mining and Technology, Socorro, New Mexico, 30 pp.

Chapin. C. E. (1971). The Rio Grande rift; modifications and additions, *New Mexico Geol. Soc. 22nd Annual Field Conference Guidebook*, 191-201.

Chapin, C. E., R. M. Chamberlin, et al. (1978). Exploration framework of the Socorro geothermal area, New Mexico, *New Mexico Geol. soc. Spec. Pub.* **7**, 114-129.

Chapin, C. E. (1979). Evolution of the Rio Grande rift - a summary, *Rio Grande Rift: Tectonics and Magmatism*, edited by R. E. Reicker, 1-5.

de Voogd, B., L. Serpa, and L. Brown (1988). Crustal extension and magmatic processes: COCORP profiles from Death Valley and the Rio Grande rift, *Geol. Soc. Am. Bull.* **100**, 1550-1567.

Fender, J. J. (1978). A study of Poisson's ratio in the upper crust in the Socorro, New Mexico, area, *M.S. Indep. Study*, New Mexico Institute of Mining and Technology, Socorro, New Mexico, 30 pp.

Gomberg, J. S., K. M. Shedlock, and S. T. Roecker (1990). The effect of S-wave arrival times on the accuracy of hypocenter estimation, *Bull. Seism. Soc. Am.* **80**, 1605-1628.

Gridley, J. (1989). Microearthquake reflection phases of a mid-crustal magma body in the Socorro area, *M.S. Indep. Study*, New Mexico Institute of Mining and Technology, Socorro, New Mexico, 25 pp.

Hammond, J. F. (1966). *A Surgeon's Report on Socorro, New Mexico, 1852*, Sante Fe, New Mexico, Stagecoach Press.

Hartse, H. E. (1991). Simultaneous hypocenter and velocity model estimation using direct and reflected phases from microearthquakes recorded within the central Rio Grande rift, New Mexico, *Ph.D. Dissertation*, New Mexico Insti-

tute of Mining and Technology, Socorro, New Mexico, 251 pp.

Hartse, H. E., A. R. Sanford, and J. S. Knapp (1992). Incorporating Socorro Magma Body reflections into the earthquake location process, *Bull. Seism. Soc. Am.* **82**, 2511-2532.

Kelly, V. C. (1952). Tectonics of the Rio Grande depression of central New Mexico, *New Mexico Geol. Soc. 3d Annual Field Conference Guidebook*, 93-105.

King, K. M. (1986). Investigation of the seismogenic zone in the viscinity of Socorro, New Mexico, from the analysis of focal depth distributions, *M.S. Indep. Study*, New Mexico Institute of Mining and Technology, Socorro, New Mexico, 124 pp.

Kluth, C. F. and P. J. Coney (1981). Plate tectonics of the Ancestral Rocky Mountains, *Geology* **9**, 10-15.

Larsen, S., R. Reilenger, and L. Brown (1986). Evidence of ongoing crustal deformation related to magmatic activity near Socorro, New Mexico, *J. Geophys. Res.* **91**, 6283-6292.

Lee, W. H. K. and J. C. Lahr (1975). HYPO71 (revised): A computer program for determining hypocenter, magnitude, and first motion pattern of local earthquakes, *U.S. Geological Survey Open File Report 75-311.*

Northrop, S. A. (1945). Earthquake history of central New Mexico [abstract], *Geol. Soc. Am. Bull.* **56**, 1185.

Northrop, S. A. (1947). Seismology in New Mexico [abstract], *Geol. Soc. Am. Bull.* **58**, 1268.

Ouichi, S. (1983). Effects of uplift on the Rio Grande over the Socorro Magma

Body, New Mexico, *Field Conference Guidebook N. M. Geol. Soc.* **34**, 54-56.

Reid, H. F. (1911). Remarkable earthquakes in central New Mexico in 1906 and 1907, *Bull. Seism. Soc. Am.* **1**, 10-16.

Rinehart, E. J. (1979). Upper crustal model for the Rio Grande rift, *Ph.D. Dissertation*, New Mexico Institute of Mining and Technology, Socorro, New Mexico, 91 pp.

Rinehart, E. J. and A. R. Sanford (1981). Upper crustal structure of the Rio Grande rift near Socorro, New Mexico, from inversion of microearthquake S-wave reflections, *Bull. Seism. Soc. Am.* **71**, 437-450.

Rinehart, E. J., A. R. Sanford, and R. M. Ward, 1979. Geographic Extent and Shape of an Extensive Magma Body at Mid-Crustal Depths in the Rio Grande Rift Near Socorro, New Mexico, *Rio Grande Rift: Tectonics and Magmatism*, edited by R. E. Reicker, 237-251.

Sanford, A. R. (1992). The Bernardo, New Mexico earthquake swarm (1989-1990), *Personal communication*, New Mexico Institute of Mining and Technology, Socorro, New Mexico.

Sanford, A. R., Ö. Alptekin, and T. R. Toppozada (1973). Use of reflection phases on microearthquake seismograms to map an unusual discontinuity beneath the Rio Grande rift, *Bull. Seism. Soc. Am.* **63**, 2021-2034.

Sanford A. R. and P. Einarsson, 1982. Magma chambers in rifts, *Continental and Oceanic Rifts, A.G.U. Geodynamics Series* **8**, 147-168.

Sanford, A. R. and C. R. Holmes (1961). Note on the July 1960 earthquakes in central New Mexico, *Bull. Seism. Soc. Am.* **51**, 311-314.

Sanford, A. R., L. H. Jaksha, and D. J. Cash (1991). Seismicity of the Rio Grande

Rift in New Mexico, *The Geology of North America Decade Map* **1**, 229-244.

Sanford. A. R. and L. T. Long (1965). Microearthquake crustal reflections, Socorro, New Mexico, *Bull. Seism. Soc. Am.* **55**, 579-586.

Sanford, A. R., R. P. Mott, P. J. Shuleski, E. J. Rinehart, F. J. Caravella, R. M. Ward, and T. C. Wallace (1977). Geophysical evidence for a magma body in the crust in the viscinity of Socorro, New Mexico, *The Earth's Crust: It's Nature and Physical Properties, Geophysical Monograph Series* **20**, 385-403.

Singer. P. J. (1989). Crustal structure in the Socorro area of the Rio Grande rift from time-term analysis, *Ph.D. Dissertation*, New Mexico Institute of Mining and Technology, Socorro, New Mexico, 206 pp.

Ward, R. M. (1980). Determination of a three-dimensional velocity anomalies in the upper crust near Socorro, New Mexico, using P arrival times from local microearthquakes, *Ph.D. Dissertation*, New Mexico Institute of Mining and Technology, Socorro, New Mexico, 146 pp.

Ward, R. M., J. W. Schlue, and A. R. Sanford (1981). Three-dimensional velocity anomalies in the upper crust near Socorro, New Mexico, *Geophys. Res. Letters* **8**, 553-556.

Weider, D. P. (1981). Tectonic significance of microearthquake activity from composite fault-plane solutions in the Rio Grande rift near Socorro, New Mexico, *M.S. Indep. Study*, New Mexico Institute of Mining and Technology, Socorro, New Mexico, 159 pp.

Appendix 1: Digital Seismograms

Digital seismograms are presented for some of the events used in this study. Each seismogram represents one station site.

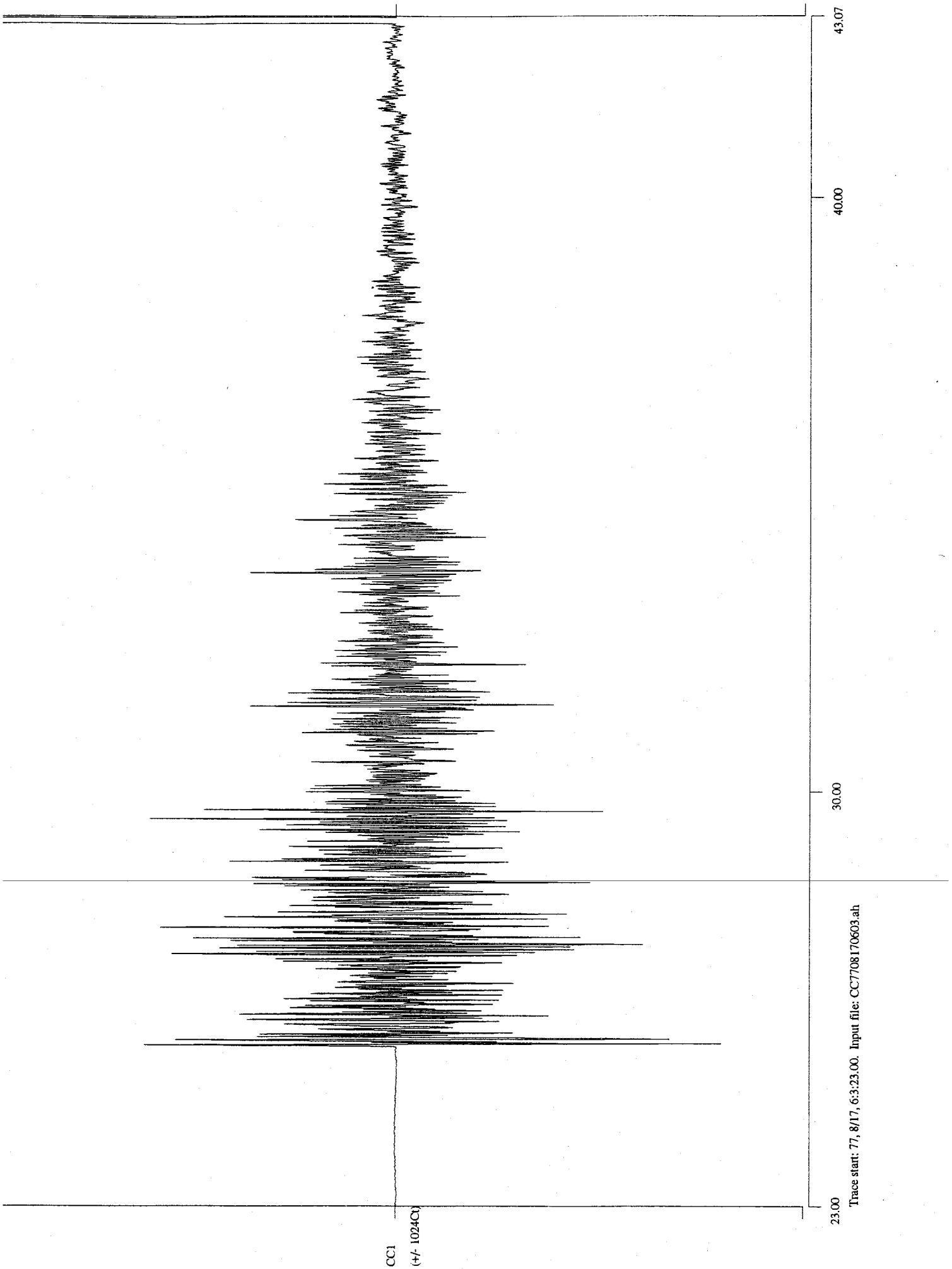
43.07
40.00
30.00
23.00
CC1
(+/- 1024Ct)
Trace start: 77, 8/17, 6:3:23.00. Input file: CC7708170603.ah

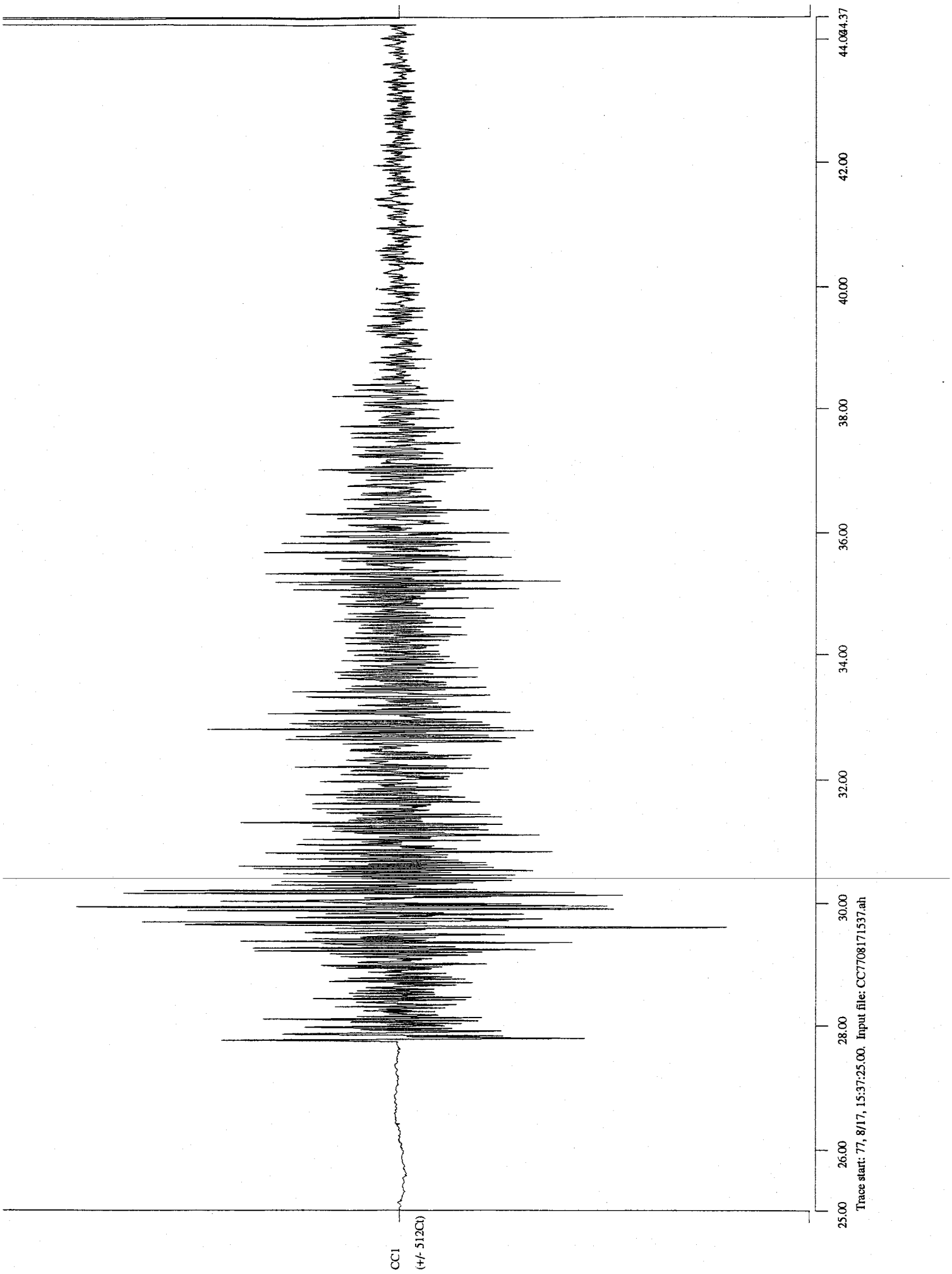
CC1
(+/- 512Ct)
25.00
26.00
28.00
30.00
32.00
34.00
36.00
38.00
40.00
42.00
44.00
44.37
Trace start: 77, 8/17, 15:37:25.00. Input file: CC7708171537.ah

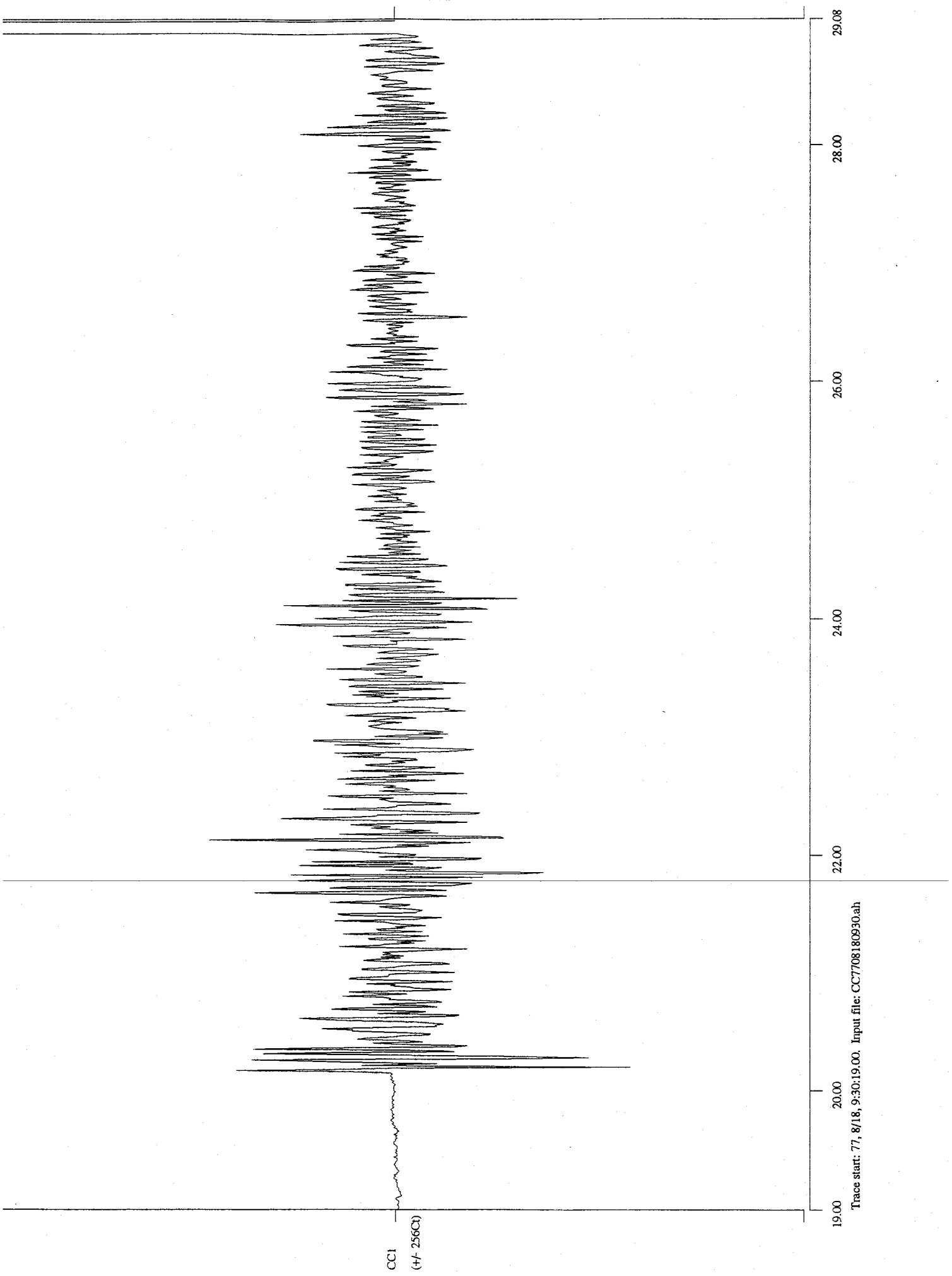
29.08
28.00
26.00
24.00
22.00
20.00
19.00
CC1
(+/- 256Ct)
Trace start: 77, 8/18, 9:30:19.00. Input file: CC7708180930.ah

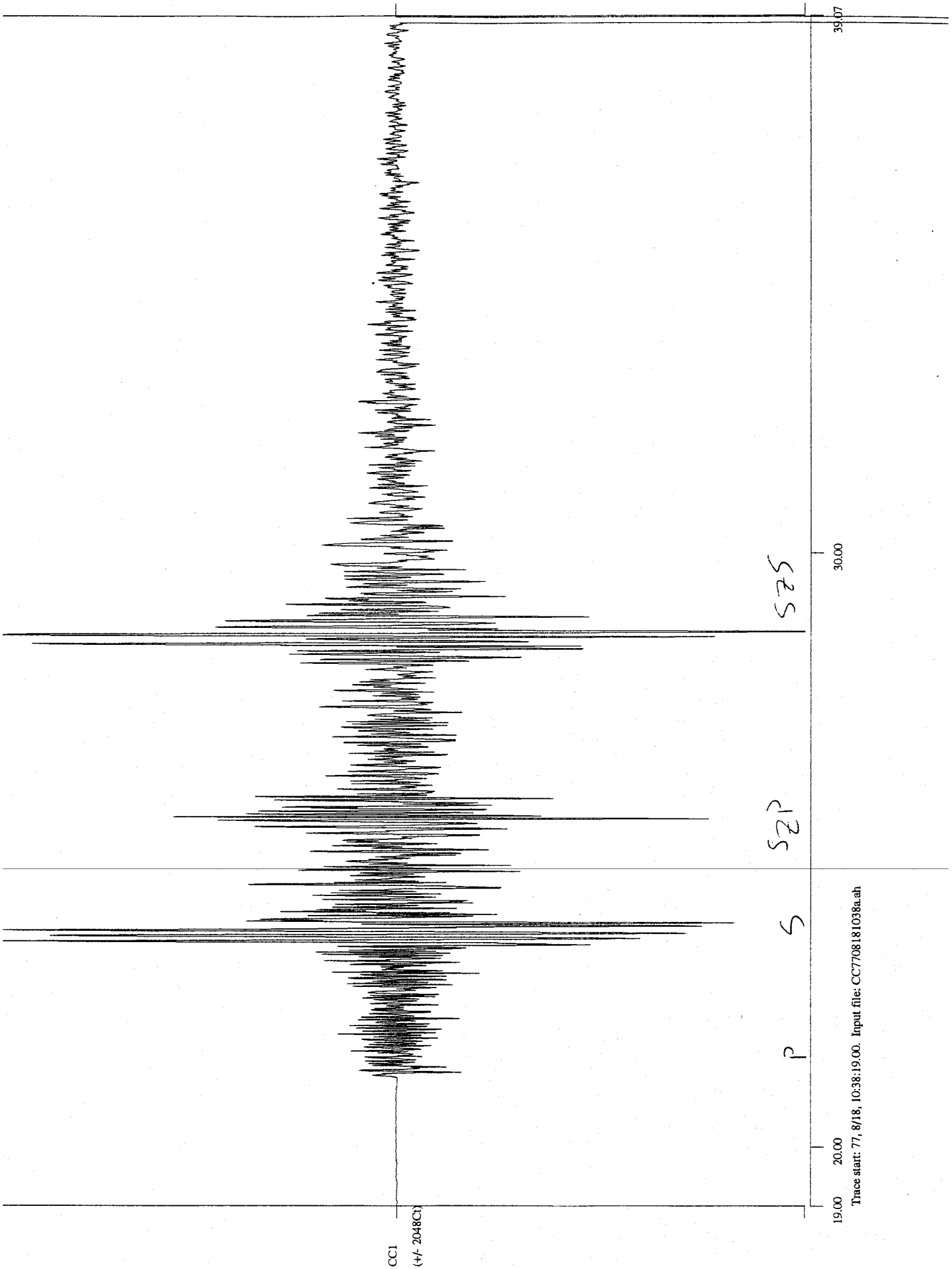
CC1
(+/- 2048Ct)
19.00
20.00
30.00
39.07
P
S
S2?
S2S
Trace start: 77, 8/18, 10:38:19.00. Input file: CC7708181038a.ah

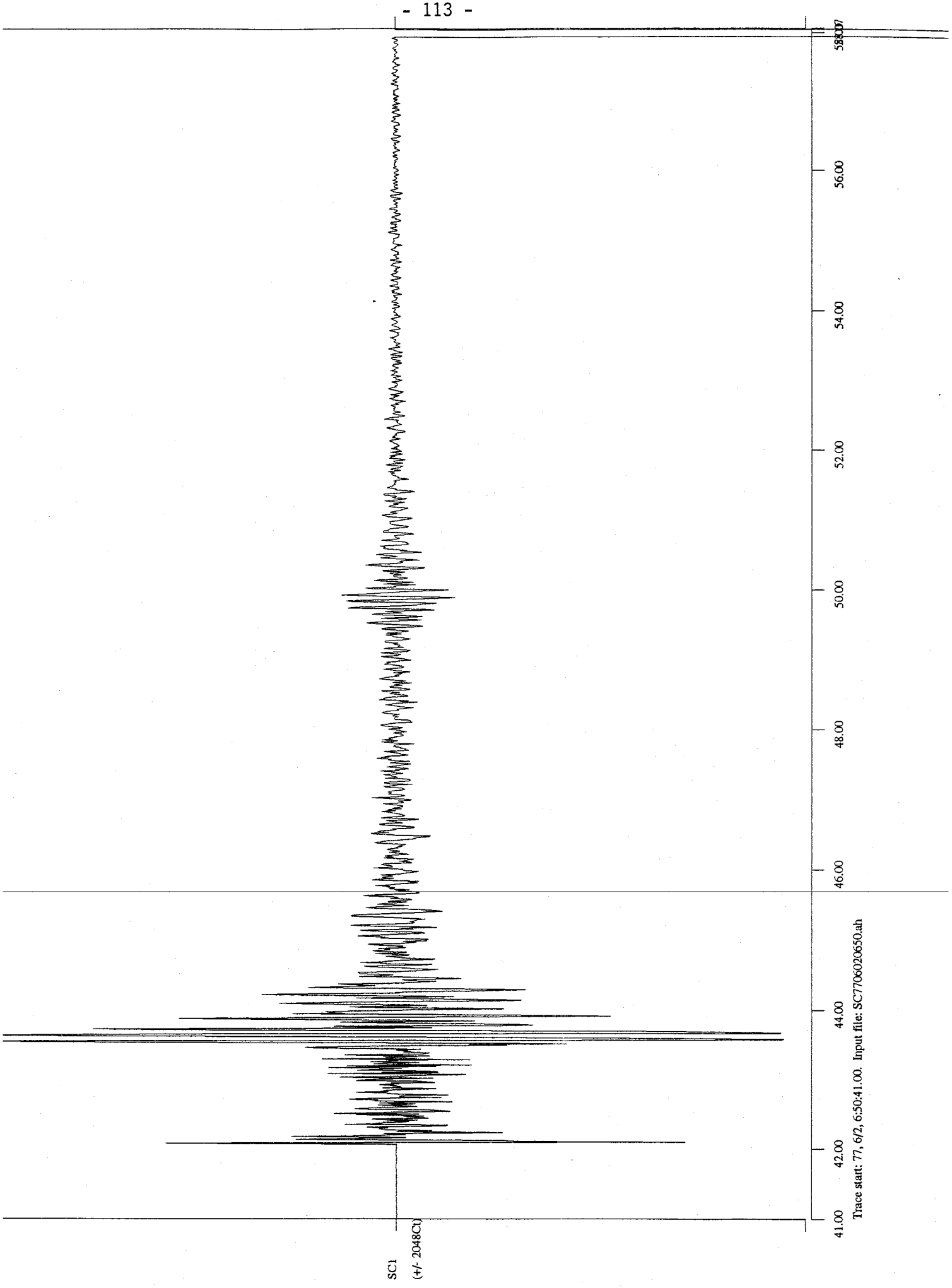
SC1
(+/- 2048Ct)
41.00
42.00
44.00
46.00
48.00
50.00
52.00
54.00
56.00
58.00
Trace start: 77, 6/2, 6:50:41.00. Input file: SC7706020650.ah

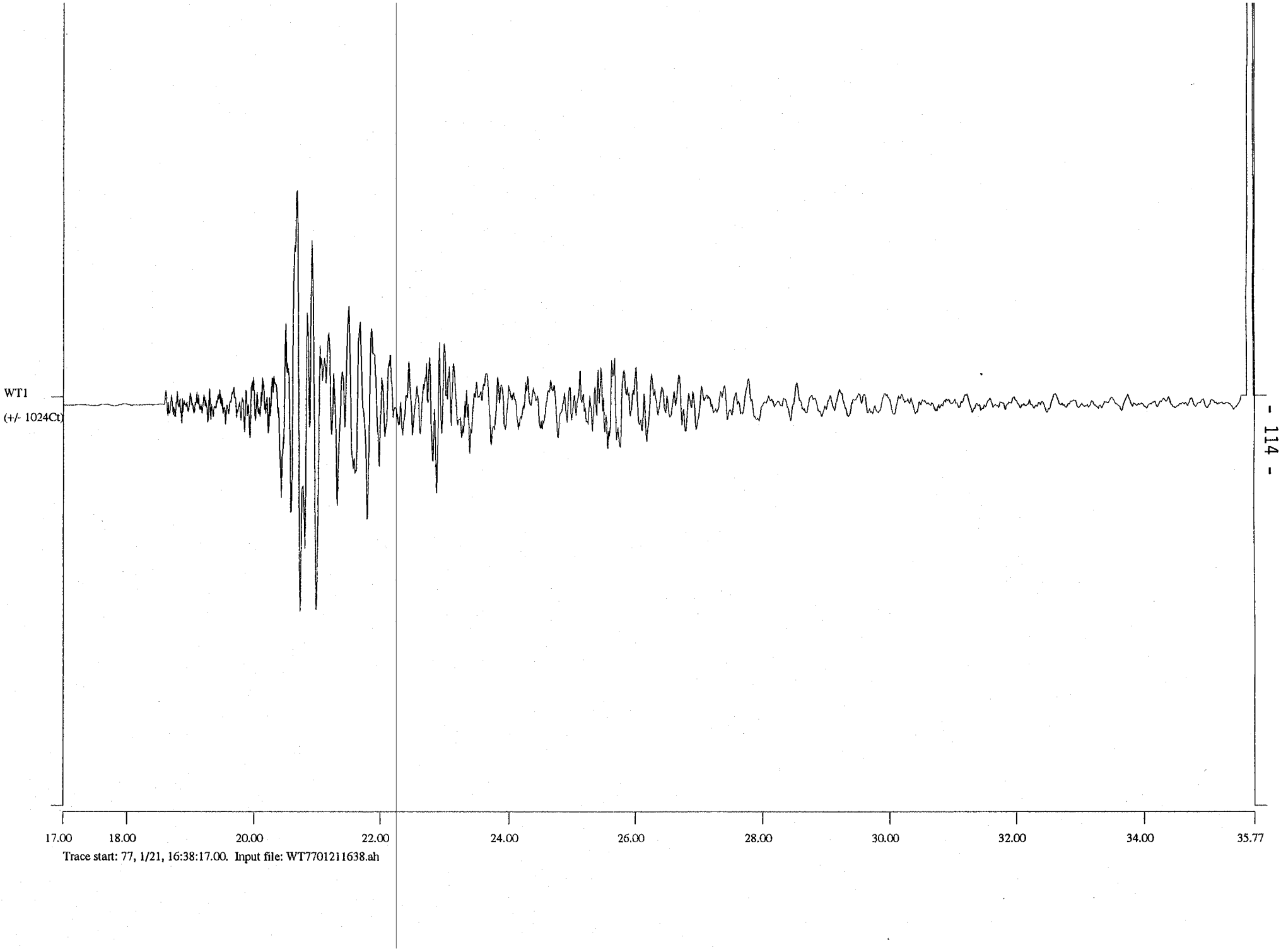
WT1
(+/- 1024Ct)
17.00
18.00
20.00
22.00
24.00
26.00
28.00
30.00
32.00
34.00
35.77
Trace start: 77, 1/21, 16:38:17.00. Input file: WT7701211638.ah

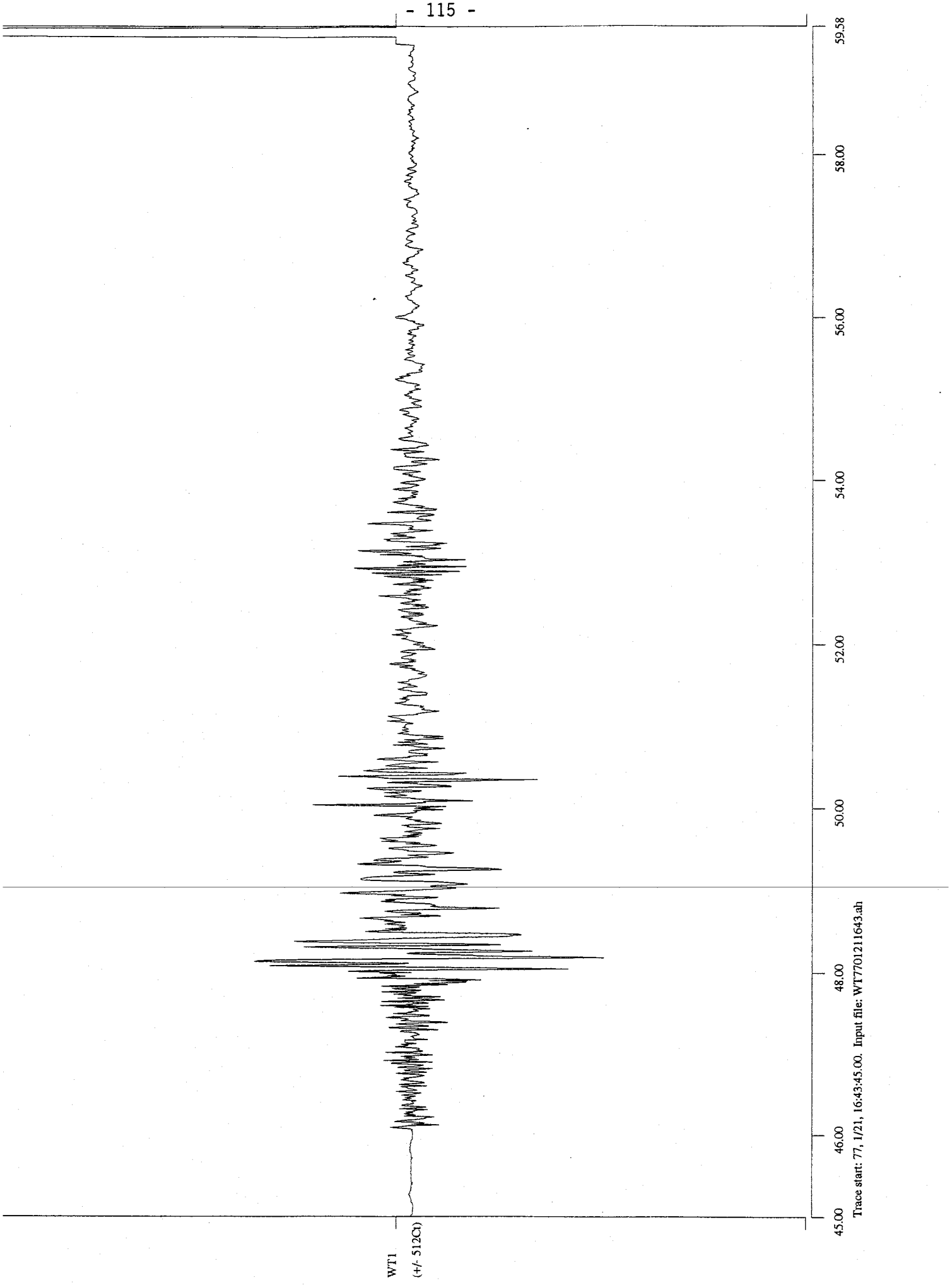
WT1
(+/- 512Ct)
45.00
46.00
48.00
50.00
52.00
54.00
56.00
58.00
59.58
Trace start: 77, 1/21, 16:43:45.00. Input file: WT7701211643.ah

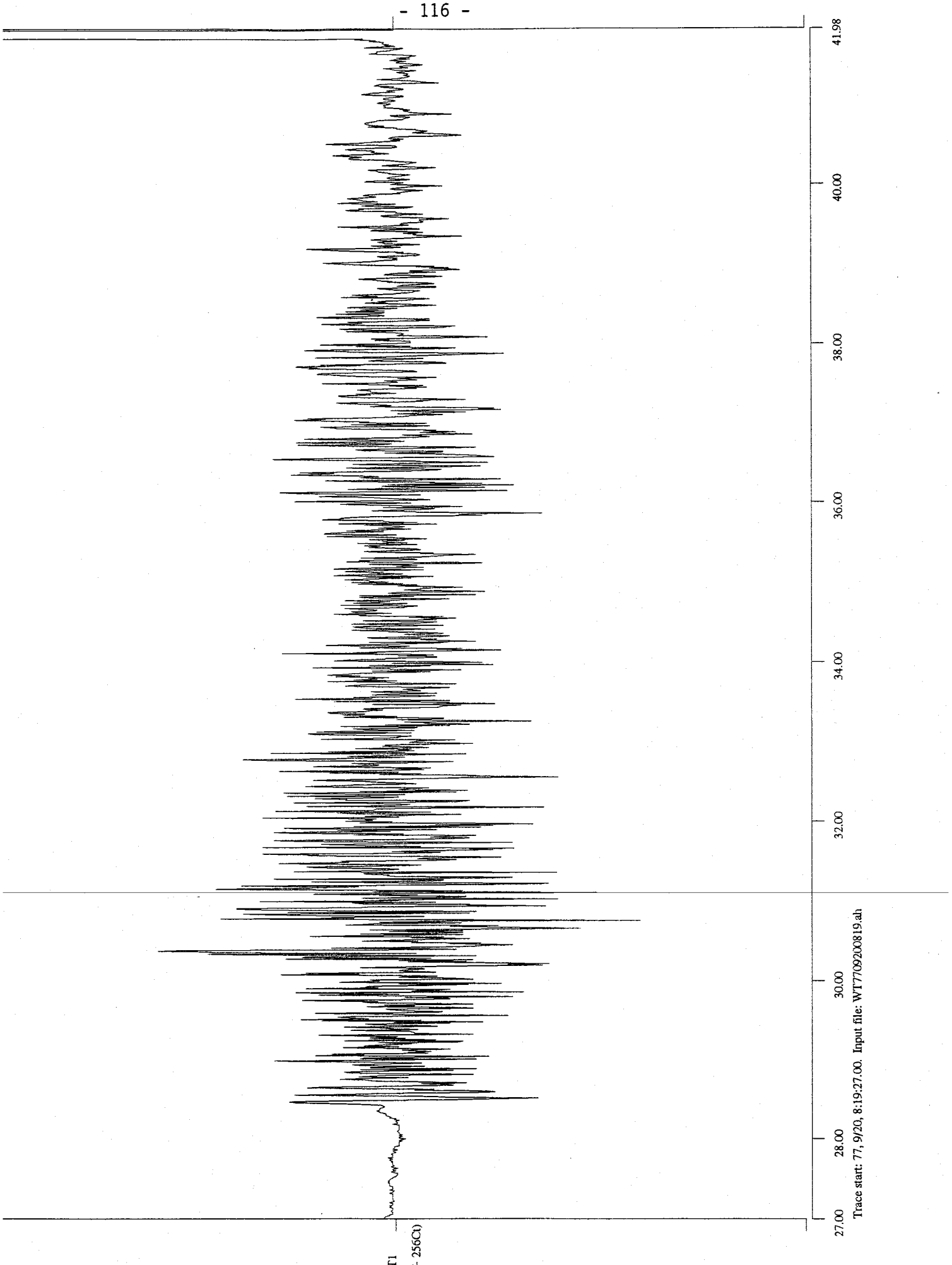
41.98
40.00
38.00
36.00
34.00
32.00
30.00
28.00
27.00
WT1
(+/- 256Ct)
Trace start: 77, 9/20, 8:19:27.00. Input file: WT7709200819.ah

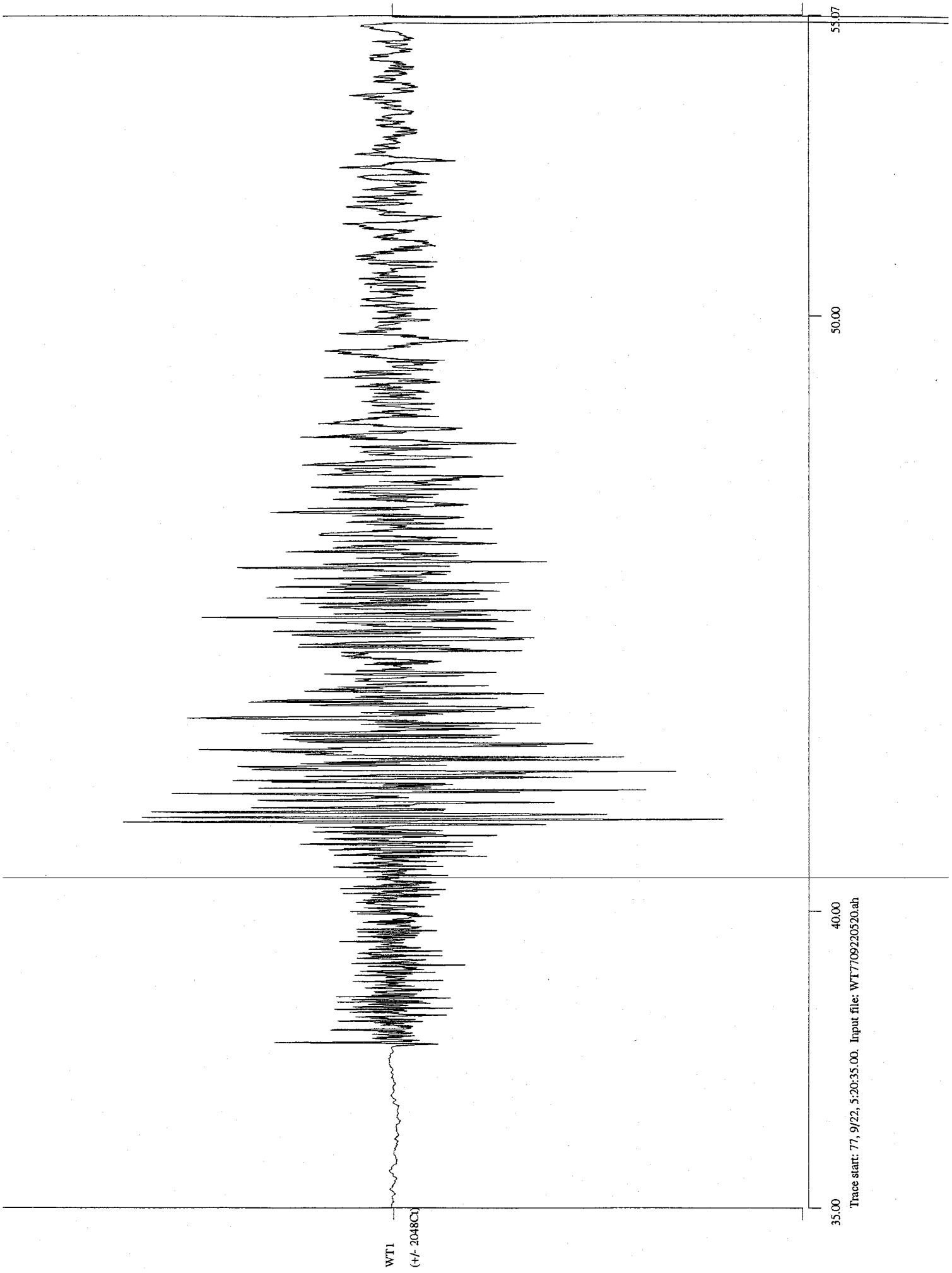
55.07
50.00
40.00
35.00
WT1
(+/- 2048Ct)
Trace start: 77, 9/22, 5:20:35.00. Input file: WT7709220520.ah

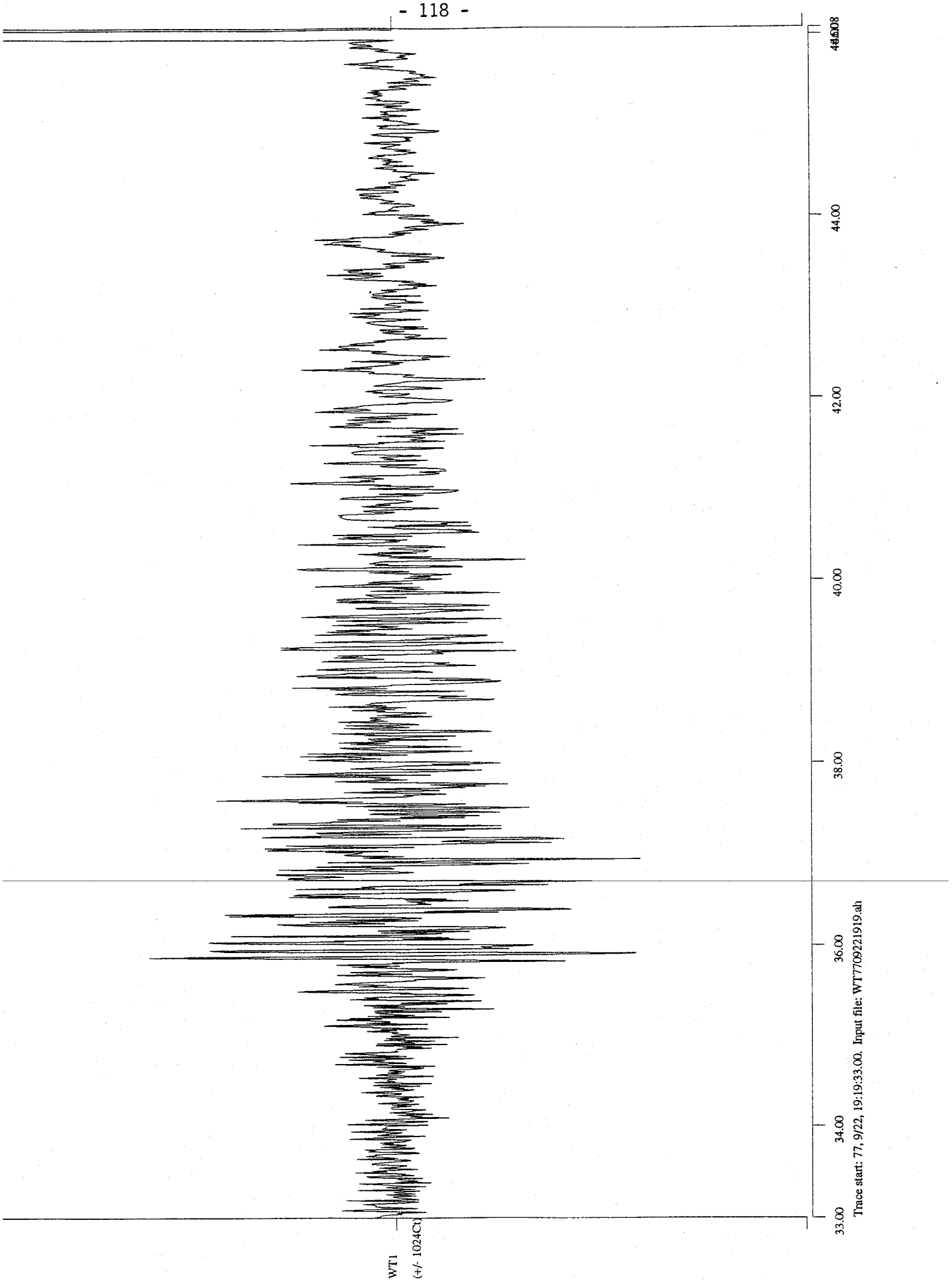
WT1
(+/- 1024Ct)
33.00
34.00
36.00
38.00
40.00
42.00
44.00
Trace start: 77, 9/22, 19:19:33.00. Input file: WT7709221919.ah